Sapienza University of Rome
Department of Physics

Ph.D. degree in Physics, XVI Ciclo

Diffusive processes in systems with geometrical constraints: from lattice models to continuous channels

Candidate:
Giuseppe Forte
Matricola 1138380

Thesis Advisors:
Prof. A. Vulpiani
Dott. F. Cecconi

A thesis submitted in partial fulfillment of the requirements for the degree of Doctor of Philosophy in Physics
October 2013

Coordinator:
Prof. M. Testa
External Referee:
Prof. F. Marchesoni
Examination Committee:
Prof. L. Biferale
Prof. C. Pierleoni
Prof. A. Polimeni

"Go, wondrous creature! mount where science guides,
Go, measure earth, weigh air, and state the tides;
Instruct the planets in what orbs to run,
Correct old time, and regulate the sun;
Go, soar with Plato to th' empyreal sphere,
To the first good, first perfect, and first fair;
Or tread the mazy round his followers trod,
And quitting sense call imitating God;
As Eastern priests in giddy circles run,
And turn their heads to imitate the sun.
Go, teach Eternal Wisdom how to rule—
Then drop into thyself, and be a fool!"

———

Pope [1734]

Alla mia Famiglia.

RINGRAZIAMENTI

Voglio ringraziare Mamma, Papà e mio Fratello, che hanno sempre saputo sopportarmi. Rigrazio i miei supervisori: Angelo e Fabio, insieme a tutto il gruppo TNT. Grazie a Gaia ed i bellissimi giri in Francia; grazie a Marco, Simone, Mariano e tutti i colleghi di bivacco :-) (dimenticavo gli espatriati Rosso e l'Arrampicatore) .... grazie per l'aiuto, il sostegno e la comprensione. Grazie a LiL per avermi accompagnato (quasi :-)) fino alla fine.

Un ringraziamento particolare va al professore Fabio Marchesoni, i cui suggerimenti e le cui critiche hanno contribuito a migliorare il mio lavoro.

Rigrazio tutti voi, vi saluto e vado avanti, ciao a tutti !!!

Roma, october 2013 G. F.

INTRODUCTION

Diffusion is a passive transport process resulting in a net movement of mass from higher to lower concentration, without requiring bulk motion. It occurs in all the states of the matter, on several orders of time and length scales, thus characterizing a lot of physical, chemical and biological phenomena [Berg, 1983; Kärger and Ruthven, 1992; Frey and Kroy, 2005; Roque-Malherbe, 2005; Bressloff and Newby, 2013], especially when the viscosity of the background environment is high and the diffusion process becomes the predominant one.

Diffusive motion can either be described by using a continuum (macroscopic) approach, based on the Fick's laws [Fick, 1855; Crank, 1975], or by taking into account a microscopic point of view in terms of the erratic motion of the suspended particles [Einstein, 1905; Smoluchowski, 1906; Langevin, 1908]. Such random motion was firstly observed by R. Brown [Brown, 1827] in 1827 while he was studying pollen grains suspend in an aqueous solution and represents one of the most fundamental works for the contemporary development of Statistical Physics [Hänggi and Marchesoni, 2005]. The link between the macroscopic and microscopic description of Diffusion was studied by Einstein [1905]. He described the erratic motion observed by Brown as the emergence of the random displacements experienced by the macroscopically sized particles (pollen grains) in terms of the collisions with the molecules composing the background environment, which naturally tend to scatter because their thermal energy. As a consequence, the continuum macroscopic description is strictly related to the probability density to observe a suspended particle in a certain volume element at a given time. In the same work, Einstein derived also an expression between a fundamental transport quantity, the diffusion coefficient, which is a macroscopic quantity, and the microstructural features of the environment, thus suggesting the first example of a Fluctuation–Dissipation Relation (FDR) [Kubo, 1957; Kubo et al., 1991; Marconi et al., 2008] and, at the same time, a way to probe the atomic hypothesis. The definitive experimental proof of the Einstein's theory was done by J. B. Perrin [Perrin, 1913], who was awarded with the Nobel Prize for his experiments.

In the recent days, the increasing technology enabled scientists to perform experiments on systems showing diffusion up to the meso–scale ($\sim 10^{-6}$ m), thus suggesting to investigate diffusive phenomena in confined systems. Explicit examples of diffusive processes occurring in a complex geometrical environment are provided by the diffusion in dendrites [Santamaria et al., 2006; Bressloff and Earnshaw, 2007], extracellular transport in brain tissue [Hrabe et al., 2004; Sen, 2004], diffusion in fractal environment [ben Avraham and

Havlin, 2000], like the chromatin structure [Lebedev et al., 2008; Lieberman-Aiden et al., 2009; Bancaud et al., 2009] or on comb–like structures, as for example the biological polyelectrolytes [Papagiannopoulos et al., 2006; Waigh and Papagiannopoulos, 2010].

In the present work, we will focus on the case of diffusion in channels with varying cross–section as well as on the diffusion on branched structures.

With regard to the random walk process on branched structures, our work was focused on both the asymptotic (e.g. the effective diffusion coefficient) and the pre–asymptotic properties, for example the transient Mean Square Displacement (MSD) or the Fluctuation Dissipation relation (FDR) [Einstein, 1905; Kubo, 1957; Kubo et al., 1991; Marconi et al., 2008]. In particular, many of the analyzed systems show a regime of anomalous transport [Metzler and Klafter, 2000; Klages et al., 2008] and one of our main result is related to the Einstein FDR, indeed we found that the FDR can be extended, in some cases, also to the anomalous regime [Forte et al., 2013a], at least within the linear response approximation. On the other hand, we pointed out how the FDR can be broken by choosing properly the branching of the analyzed structure, as a consequence of the emergence of an "entropic" drift due to the high ramifications introduced. This result suggests that FDRs are more sensitive to the geometrical structure rather than to the details of the dynamics. We analyzed, in contrast to those examples showing anomalous diffusion, also a series of situations characterized by a standard scaling of the mean square displacement (and/or of the higher order moments), however with a non Gaussian probability density, thus showing how standard diffusion is not always Gaussian [Forte et al., 2013b].

In our work on two dimensional continuous channels, we propose a method to estimate the effective diffusion coefficient, which is one of the main quantity of interest for a diffusive process. We will compare our results with the already known approximations, such as the Fick–Jacobs (FJ) approximation [Burada et al., 2009]. Moreover we studied the transient diffusion, in particular the transient MSD. We found that a strong perturbation of the channel from the simple cylindrical structure introduces a time scales separation between the transversal and the longitudinal motion. We used a phenomenological model to emphasize the influence of such time scales separation on the transient MSD along the transport direction, showing how the pre–asymptotic regime can be controlled by choosing properly the initial particle distribution within the channel.

The present work is organized as follow.

FIRST CHAPTER We introduce the phenomenological Fick's equation [Fick, 1855], which describes the diffusion process on the macroscopic scale, that is, on the length scale greater than the atomic one ($\sim 10^{-8}$ m). In particular we will discuss some examples of diffusion in confined systems.

SECOND CHAPTER We review some of the most important results on diffusion in non homogeneous channels. In particular we will take into account symmetric channels with respect to some given space direction, referred to as the longitudinal direction, whose boundaries are periodic functions of the longitudinal coordinate. We discuss the Fick–Jacobs (FJ) approximation [Jacobs, 1967; Burada et al., 2009], which can be viewed as the Fokker–Planck equation [Risken, 1989] associated to a one–dimensional Langevin equation whose external potential is a function of the boundary profile only.

THIRD CHAPTER We review some of the mathematical results related to the diffusion theory [Crank, 1975]. In particular we will discuss the Central Limit Theorem (CLT) [Feller, 1945, 1968] and its violations, thus introducing the concept of anomalous transport [Klages et al., 2008].

FOURTH CHAPTER We present our analytical and numerical results about the random walk process on branched structures. We will discuss, using an approach based on simple scaling arguments [Forte et al., 2013a], the random walk on the comb–lattice [Goldhirsch and Gefen, 1986; Weiss and Havlin, 1986], emphasizing the emergence of an anomalous transport regime, however pointing out that the Einstein [1905] FDR still holds true, both in the anomalous regime and in the standard diffusive one. We will show that it is possible to "destroy" the FDR by considering particular ramified geometries. Such structures introduce an "entropic" bias, that is, a non vanishing drift related only to the particular geometry of the lattice considered. Further discussions, taking as examples generalized comb structures and fractal trees, will be discussed [Forte et al., 2013a,b].

FIFTH CHAPTER We present an analytical and numerical study on diffusion in periodic channels. Such channels are characterized by the fact that on large time and length scales, the longitudinal diffusion process will be standard , with a renormalized diffusion coefficient D_{eff}. We will construct a simple one–dimensional model to work out an expression for D_{eff}, showing how our approach can be applied also when the usual FJ approximation fails. We will also discuss the importance of the pre–asymptotic regime, showing how it is possible to control it by choosing properly the initial particle distribution within the channel.

SIXTH CHAPTER We discuss our main conclusions.

CONTENTS

1 MOTIVATION

"If the movement discussed here can actually be observed (together with the laws relating to it that one would expect to find), then classical thermodynamics can no longer be looked upon as applicable with precision to bodies even of dimensions distinguishable in a microscope: an exact determination of actual atomic dimensions is then possible"

Einstein [1905]

1.1 INTRODUCTION: DIFFUSION AND BROWNIAN MOTION

Diffusion is a mass transport process arising in Nature, which results in molecular or particle mixing without requiring bulk motion. The physical laws that explain this phenomenon are called Fick's laws [Fick, 1855]

$$\mathbf{J}(\mathbf{r},t) = -D_0 \boldsymbol{\nabla} \mathscr{C}(\mathbf{r},t) \tag{1.1}$$

$$\frac{\partial \mathscr{C}(\mathbf{r},t)}{\partial t} = -\boldsymbol{\nabla} \cdot \mathbf{J}(\mathbf{r},t) \tag{1.2}$$

where $\mathbf{J}(\mathbf{r},t)$ is the net particle flux at time t and space point $\mathbf{r}$, $\mathscr{C}(\mathbf{r},t)$ is the particle concentration, and the constant of proportionality, D_0, is called the diffusion coefficient. Unlike the flux vector or the concentration, the diffusion coefficient is an intrinsic property of the medium [Einstein, 1905; Berg, 1983; Hänggi and Marchesoni, 2005; Frey and Kroy, 2005], and its value is determined by the size of the diffusing molecules and the temperature and microstructural features of the environment (see also Sec. 2.1). The sensitivity of the diffusion coefficient on the local microstructure enables its use, for example, as a probe of physical properties of biological tissue [Berg and Behrens, 2009]. Clearly there are no ways to relate the diffusion coefficient

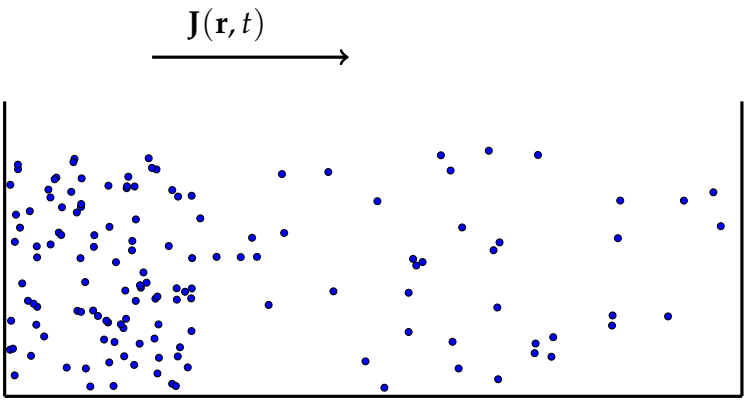

Figure 1.1: *Illustration of the Eq. (1.1); particles flow from regions of high concentration to regions of low concentration.*

with the microstructural features of the environment simply using the Fick macroscopic description.

A microscopic model for the diffusion process was suggested for the first time by Einstein [1905] and it is related on an apparently different motion, called Brownian movement.

Robert Brown [Brown, 1827] is credited to be the first one who report the random motions of pollen grains suspended in a water solution while studying them under his microscope (see Fig. 1.2), for this reason the erratic motion observed by Brown was called Brownian motion. Sometimes particles which show this type of erratic motion are also called Brownian particles.

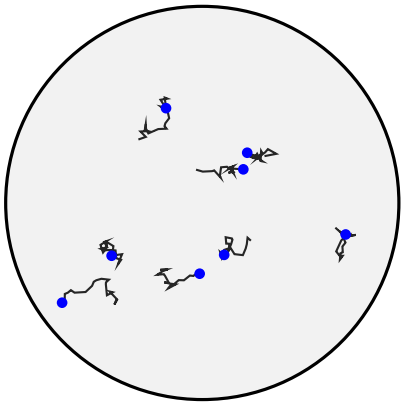

Figure 1.2: *Botanist Robert Brown is known as the first scientist who has reported the apparent erratic motion of pollen grains suspended in aqueous solution.*

In the early part of the 20th century, Albert Einstein, who was seeking evidence that would undoubtedly imply the existence of atoms, came to the conclusion that [Einstein, 1905] " $[\cdots]$ *bodies of microscopically visible size suspended in a liquid will perform movements of such magnitude that they can be easily observed in a microscope*".

Substance	*Molecular Weight*	$\mathbf{D_0 \times 10^{-7}\ cm^2 s^{-1}}$
Glucose	192	660
Insulin	5734	210
cytochrome c	13370	11.4
myoglobin	16900	11.3
β–lacroglobulin	37100	7.5
serum albumin	68500	6.1
hemoglobin	64500	6.9
catalase	247500	4.1
urease	482700	3.46
fibrinogen	339700	1.98
myosin	524800	1.10
tobacco mosaic virus	40590000	0.46

Table 1.1: *Molecular weight and diffusion coefficients of some biochemical substances in aqueous solution at standard temperature and pressure conditions.*

Einstein has used a probabilistic framework to describe the motion of an ensemble of particles undergoing Brownian motion, reconciling the Fick's laws with Brown's observations and thus leading to a coherent description of the diffusion process (see Chap. 3). He introduced the displacement distribution for this purpose, which quantifies the fraction of particles that will traverse a certain distance within a particular time–frame, in particular Eq. (1.2) is showed to be (up to a dimensional factor) the equation describing the time and space evolution of the probability density $\mathscr{P}(\mathbf{r}, t)$ to find a Brownian particle in a small volume element $d\mathbf{r}$ around $\mathbf{r}$ at time t. Einstein pointed out also the relation between the diffusion coefficient D_0, which is a macroscopic quantity, with the intrinsic properties of the bulk material within which particles can diffuse, thus suggesting at the same time a first example of Fluctuation–Dissipation Relation [Kubo et al., 1991; Marconi et al., 2008] (see also Chap. 4 and Chap. 5).

A brief review of the diffusion theory and Brownian motion is reported in Chap. 3. In the following we will refer to the phenomenological Fick's laws, which can be reasonably derived by requiring mass conservation, as we show in the next section.

1.2 MASS CONSERVATION AND CONSTITUTIVE LAWS

The time evolution of the concentration in Eq. (1.2) can be explained by using a balance equation. More specifically, let be $M(t)$ the total mass contained in a fixed space volume $\mathcal{V}$, enclosed by the surface $\mathcal{S}$; moreover, $\mathscr{C}(\mathbf{r},t)$ is the volume density associated to the mass $M(t)$, that is

$$M(t) = \int_{\mathcal{V}} d\mathbf{r}\, \mathscr{C}(\mathbf{r},t)$$

The variation of $M(t)$ within $\mathcal{V}$ during an assigned observation time, assuming absence of sources and sinks in $\mathcal{V}$, is given by

$$\frac{\partial}{\partial t}\int_{\mathcal{V}} d\mathbf{r}\, \mathscr{C}(\mathbf{r},t) = -\int_{\mathcal{S}} dS\hat{\mathbf{n}}\cdot\mathbf{J}(\mathbf{r},t)$$

where dS is the surface element on $\mathcal{V}$ and $\hat{\mathbf{n}}$ is the outgoing local versor from the closed surface $\mathcal{S}$. The flux $\mathbf{J}$ of the quantity $M(t)$ across $\mathcal{S}$ balances the variation of $M(t)$ in time; using the divergence theorem and noting that $\mathcal{V}$ is an arbitrary volume, we get the continuity equation

$$\frac{\partial\mathscr{C}(\mathbf{r},t)}{\partial t} + \boldsymbol{\nabla}\cdot\mathbf{J}(\mathbf{r},t) = 0 \tag{1.3}$$

which is exactly Eq. (1.2).

The generalization to the more general case characterized by the presence of sources and sinks is straightforward; indeed the above equation retains the same structure once on the right hand side a source term $f(\mathbf{r},t)$ is added to the problem.

To solve Eq. (1.3) it is necessary to introduce a connection between the concentration $\mathscr{C}(\mathbf{r},t)$ and its flux $\mathbf{J}(\mathbf{r},t)$ which is, for example, the content of the Fick's first law (1.1). Relations between the state quantity $\mathscr{C}(\mathbf{r},t)$ and the flow quantity $\mathbf{J}(\mathbf{r},t)$ are usually based on the generalization of experimental observations and depend on the properties of the particular medium or material. They are usually called constitutive laws or material relations. In Chap. 3 we will review how it is possible to derive the constitutive laws which relate the flux $\mathbf{J}(\mathbf{r},t)$ to the concentration $\mathscr{C}(\mathbf{r},t)$ for the case of a diffusive process, starting from the microscopic interpretation of diffusion.

The fundamental solution of the diffusion equation [Einstein, 1905; Crank, 1975; Berg, 1983; Gardiner, 2009] defined by Fick's first and second laws can be obtained by looking at the simple boundary value problem:

$$\begin{cases} \frac{\partial\mathscr{C}(x,t)}{\partial t} = D_0\frac{\partial^2\mathscr{C}(x,t)}{\partial x^2}, & -\infty < x < \infty \\ \mathscr{C}(x,0) = \mathscr{C}_0\delta(x) \end{cases} \tag{1.4}$$

where, for simplicity, we focus on a problem defined in one spatial dimension. The solution of the Eq. (1.4) can be found, for example, by using the Fourier

transform method. In particular, if we take the Fourier transform on both sides of the first equation in (1.4) we get

$$\frac{\partial \hat{\mathscr{C}}(k,t)}{\partial t} = -D_0 k^2 \hat{\mathscr{C}}(k,t)$$

with $\hat{\mathscr{C}}(k,t)$ given by

$$\hat{\mathscr{C}}(k,t) = \int_{-\infty}^{+\infty} dx\ \mathrm{e}^{ikx} \mathscr{C}(x,t)$$

The solution of the transformed equation can be expressed as

$$\hat{\mathscr{C}}(k,t) = \hat{\mathscr{C}}(k,0)\ \mathrm{e}^{-D_0 k^2 t}$$

where $\hat{\mathscr{C}}(k,0) = \mathscr{C}_0$ is the Fourier transform of the initial condition $\mathscr{C}(x,0)$. By applying the inverse Fourier transform we find the final result

$$\mathscr{C}(x,t) = \frac{\mathscr{C}_0}{\sqrt{4\pi D_0 t}}\ \mathrm{e}^{-x^2/4D_0 t} \tag{1.5}$$

The Eq. (1.5) defines naturally a probability density, indeed by observing that the quantity $\mathscr{P}(x,t) = \mathscr{C}/\mathscr{C}_0$ is normalized to the unity at every instant of time, we can read $\mathscr{P}(x,t)$ as the probability density to find a particle in a length interval dx around x at the time t. This interpretation leads directly to the property which "labels" (almost) every diffusive processes, that is

$$\langle x^2(t) \rangle = \int_{-\infty}^{+\infty} x^2 \mathscr{P}(x,t) = 2D_0 t \tag{1.6}$$

In the following sections we will show a series of practical examples in which diffusion plays a central role, in particular we will focus on those situations characterized by non trivial geometries, showing how these situations naturally come into play in a lot of physical problems.

1.3 DIFFUSION IN DENDRITES

Dendrites are extensions of the cell body of the neuron specialized for receiving and processing the vast majority of excitatory synaptic inputs [Yuste and Denk, 1995; Stuart and Spruston, 1999; O'Reilly and Munakata, 2000; Fall, 2002]. Dendrites exhibit enormously diverse forms, resulting in a various types of branched structures [Ramón-Moliner, 1968; Ramón y Cajal, 1995; Fiala and Harris, 1999; Scott and Luo, 2001; Jan and Jan, 2010]. The density of dendritic ramifications lies on a continuum of values, reflecting differences in connectivity. At one extreme there are selective branched structures in which each dendrite connects the cell body to a single remote target, as shown on the left of Fig. 1.3. Typically an olfactory sensory cell provides an example

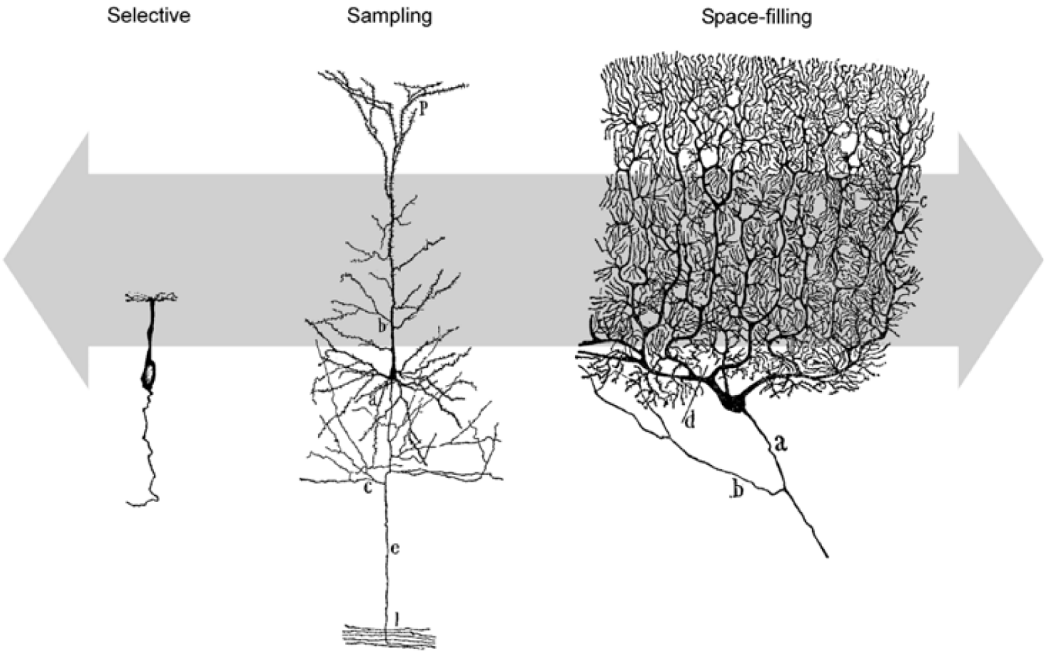

Figure 1.3: *Usual types of dendritic structure:* ***(left)*** *selective structure;* ***(middle)*** *sampling arborization ;* ***(rught)*** *space–filling dendrite. Adapted from Ramón y Cajal [1995].*

of this type of structure. At the other extreme lies the so called space–filling structure in which the dendrites cover a region, as with the cerebellar Purkinje cell illustrated in the right part of Fig. 1.3. Intermediate branching densities are referred to as sampling arborizations, as demonstrated by a pyramidal cell from cerebral cortex. An example of a sampling structure is shown in the middle part of Fig. 1.3.

Every dendrite's branch is covered typically by hundreds to thousands of spines, which are synaptic protuberances along a given ramification. Dendritic spines serve as a storage site for synaptic strength and help transmit electrical signals to the neuron's cell body. Most spines have a bulbous head, the spine head, and a thin neck that connects the head of the spine to the shaft of the dendrite. Dendritic spines may also serve to increase the number of possible contacts between neurons [Stuart and Spruston, 1999].

Most of the input coming into a neuron enters in the dendrites, whereas the axon, which originates at the cell body, sends the output signal to other neurons. To enable different neurons to communicate with each other despite being encased in membranes, there are little openings in the membrane called channels (see Sec. 1.4). The basic mechanisms of information processing in a neuron are based on the movement of charged atoms (ions) in and out of these channels, and within the neuron itself. These ions move according to basic principles of electrodynamics and diffusion.

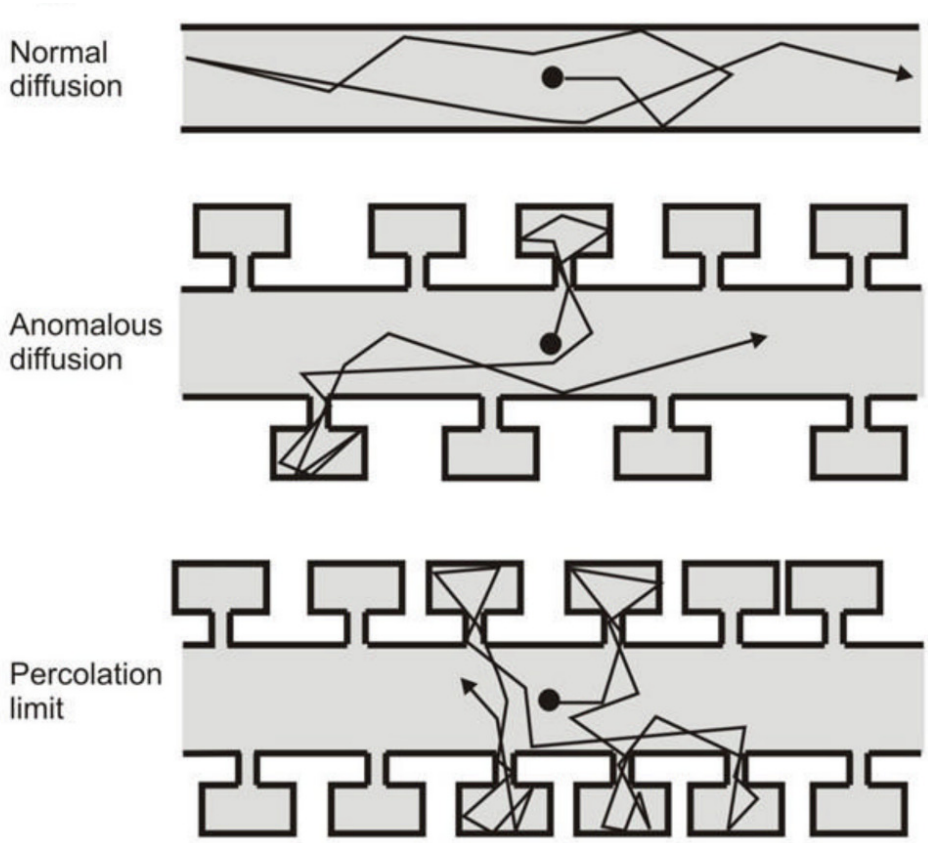

Figure 1.4: *Schematic representation of a dendrite with different densities of spines:* ***(top panel)*** *a dendrite with zero spines;* ***(middle and bottom panel)*** *spiny dendrites with an increasing density of spines. Adapted from Santamaria et al. [2006]*

An idealized geometrical model of a single dendrite along with its spines, for two different spine density, is shown in the middle and bottom panels of Fig. 1.4. Such structures are used to study the diffusion problem within spiny dendrites [De Schutter and Smolen, 1998; Santamaria et al., 2006]. More specifically, in the picture 1.4 it is well distinguished a main transport direction, the shaft of the dendrite, along with transversal dead–ends, each one composed by narrow channels, i.e. the spine neck, with squared compartments, introduced to model the spine head.

The dendrites of cerebellar Purkinje cells contain both sections without spines as well as branches with high densities of spines [Fiala and Harris, 1999], thus representing a good template to study the diffusion process in the limiting case of a smooth channel (see the up panel of Fig. 1.4) as long as the case of channels characterized by a varying cross–section (see the middle and bottom panel of Fig. 1.4).

Combining local photolysis of caged compounds with fluorescence imaging, Santamaria et al. [2006] have observed diffusion in the spiny dendrites

of cerebellar Purkinje cells. They found that the mean square displacement in the case of a dendrite with high density of spines is slower than the typical linear growth in time expected from a diffusion process, as explained in Eq. (1.6). This retardation is due to a transient trapping of molecules within dendritic spines.

When the behaviour in time of the mean square displacement is not linear:

$$\langle x^2 \rangle \sim t^{2\nu}$$

with $\nu \neq 1/2$, the resulting diffusion process is called anomalous [Bouchaud and Georges, 1990; Metzler and Klafter, 2000]. We will discuss in more details the standard and anomalous diffusion in Chap. 3 and Chap. 4, while in Chap. 5 we will present our work on diffusion in non homogeneous channels. In particular, we will also take into account structures like those shown in Fig. 1.4.

Recent experimental observations strongly suggest that there are voltage–dependent sodium [Araya et al., 2007], potassium [Ngo-Anh et al., 2005] and calcium [Yuste and Denk, 1995] channels in the spine heads (see the next section for a general discussion on ionic channels), so implying that the transport along a spiny dendrite could be characterized by the presence of local mass sources or sinks.

Dendrites provide an example of complex environment within which diffusion can take place. While a single dendrite along with its spines can be modeled as a non homogeneous channel, the typical fractal–like structure of an ensemble of dendrites can be modeled with an appropriate branched structure, as can be done by building a model in terms of the comb–lattice [Goldhirsch and Gefen, 1986] or its generalizations [Forte et al., 2013a], as well as using an appropriate fractal tree [Forte et al., 2013b]. We will discuss these types of discrete branched structures and the properties of diffusion on such graphs in Chap. 4.

1.4 DIFFUSION IN IONIC CHANNELS

Generally speaking, ionic channels, are macromolecular pores on the membrane of living cells [Hodgkin and Huxley, 1939, 1952; Hille, 1978, 1992; Doyle et al., 1998]; they regulate the flow of charged ions across the cell membrane, indeed ionic channels can be thought to have gates that regulate the permeability of the pore to ions. These gates can be controlled by membrane potential, producing voltage gated channels.

Diffusion in ionic channels [De Schutter and Smolen, 1998] represents another example in which geometrical limitations, due to the boundaries of the channel, constraint the "normal" evolution of the particles, whose behaviour is expected to be dominated asymptotically by a Gaussian probability density, as described in Sec. 1.2 for the case of simple diffusion in one dimension.

Before to discuss a crude example of diffusion in ionic channels, we recall briefly the usual way to describe a ionic channel.

The simplest description of a ionic channel can be done by using a kinetic model [Fall, 2002]. In particular a ionic channel is thought as composed by two states, respectively closed (C) and open (O). Transitions between these states are allowed with two transition rates, k^+ ($C \to O$ transitions) and k^- ($O \to C$ transitions) which can be defined through the (constitutive) "law" of mass action, namely

$$\begin{aligned} J_+ &= k^+[C] \\ J_- &= k^-[O] \end{aligned}$$

where $J_\pm$ are the net flux across the channel and $[C]$ ($[O]$) the concentration of molecules in the channel state C (O); typically the concentration can be expressed as a frequency, that is if there are N channels on the membrane and $N_O \leq N$ channels are in the open state, then $[O] = N_O/N$. Ionic channels are composed by lateral chains of charged amino–acid proteins, inducing a difference potential ΔV across the membrane, which has an influence on the transition rates, so in agreement with the Arrhenius [Laidler, 1987] law, the rate transitions will be of the form

$$k^\pm \propto \mathrm{e}^{-\Delta V^\pm / RT}$$

with R the fundamental gas constant an T the absolute temperature. The influence of the difference potential on the transition rates explains why ionic channels are also called voltage gated ionic channels. More realistic models can be found for example in [Hille, 1992; Fall, 2002], in particular the gating process can be described itself with a diffusive model, see for example Sansom et al. [1989]; Oswald et al. [1991]; Goychuk and Hänggi [2003].

Once a channel is in the Open state, material can flow from one side to the other side of a ionic channel. A simple abstraction of the diffusion process in ionic channels is sketched in Fig. 1.5. Looking to a stationary state and taking into account only the longitudinal direction (transport direction), i.e. assuming that the transversal motion equilibrates much more faster than the longitudinal one, we can write the following problem

$$\begin{cases} \frac{\partial^2 \mathscr{C}(x)}{\partial x^2} = 0 \\ \mathscr{C}(0) = c_1; \quad \mathscr{C}(L) = c_2 \end{cases}$$

whose solution is given by

$$\mathscr{C}(x) = c_1 \left(1 - \frac{x}{L}\right) + c_2 \frac{x}{L}$$

from which we can extract the flux using the constitutive law (1.1) (Fick's first law) $J(x) = -D_0 \partial \mathscr{C}(x)/\partial x$:

$$J(x) = \frac{D_0}{L}(c_1 - c_2)$$

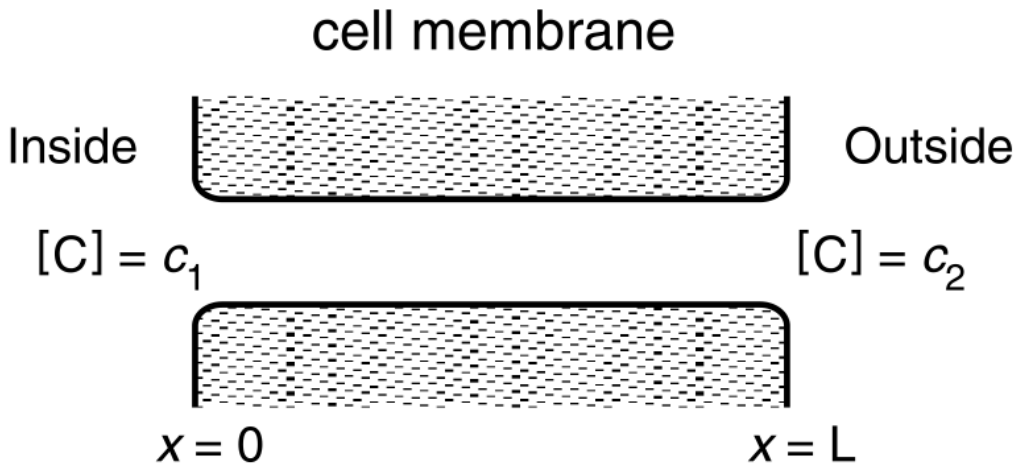

Figure 1.5: *A simple picture of Ionic channel. Adapted from Fall [2002]*

The simple picture of diffusion in ionic channels described above has a series of limitations:

- the geometrical shape of the boundaries is obviously too much idealized; indeed in nature it is reasonable to expect a non homogeneous boundary (i.e. with a position–dependent cross section), rather than a perfectly cylindrical tube (constant cross section), see Chap. 2 and Chap. 5 for a discussion on this point;

- the typical diffusive time across a space region Δ_x along the longitudinal direction is of the order $\tau \approx \Delta_x^2/2D_0$, that is, the grater is the free diffusion coefficient D_0, the slower is the process, thus the stationarity of the observed process, on a given length and time scale, depends on the diffusing materials (see Tab. 1.1) as well as, for example, by the temperature of the background environment, being $D_0 \propto T$ (see Chap. 2); ;

- the assumption of equilibration along the transversal direction is essentially correct when we look at the asymptotic properties. However during the pre–asymptotic regime (strongly non stationary), the diffusion can be modified by the transverse motion, as we will show in Chap. 5, treating the case a of a non homogeneous channel (see also Chap. 2);

- another limitation is due to the particle–wall interaction, such as sticky walls, randomized boundary conditions, etc...however we will not discuss such situations in this Thesis. In the following sections we will always consider (perfect) reflecting boundaries.

The above discussion reinforces the idea of diffusive features controlled by the geometrical constraints; in order to better describe processes like the diffusion in ionic channels or, as we explained in Sec. 1.3, the diffusion in a spiny dendrite, different types of complex geometric environments must be taken into account, such as channels with a non homogeneous boundary or complicated branched structures. Further improvements can be done by analyzing a "moving geometry", that is all those situations characterized by a dynamical boundary.

Diffusion in ionic channels and spiny dendrites is clearly not the only examples inspired by the biology and important from the point of view of the diffusion occurring in complex geometries. In the following sections we will describe other situations, such as the implications in studying Brownian motors [Astumian and Hänggi, 2002; Hänggi et al., 2005; Hänggi and Marchesoni, 2009] or DNA separation.

1.5 OTHER EXAMPLES: BROWNIAN RATCHETS AND DNA SEPARATION

In 1969 Huxley and Simmons [1971] proposed a theory for how the cross-bridges in muscle generate the force that drives muscle contraction. Their model was built around the idea of capturing Brownian fluctuations in an elastic element to generate a unidirectional force; it was the first application of the Brownian ratchet [Feynmann et al., 1977] idea to a protein motor.

Roughly speaking, a ratchet is a motor in which the motion is driven directly by thermal fluctuations and rectified, or biased, by chemical reactions. Brownian ratchets also defines a large class of problems linked, at least in some aspects, to the problem of diffusion in non homogeneous channels.

In 2003 Matthias and Müller [2003] showed how a series of one dimensional pores of a macroporous silicon membrane, etched to obtain a periodically asymmetric space modulation in their diameters (see left panel of Fig. 1.6), can work as parallel and multiply stacked Brownian ratchets.

In this type of processes another relevant aspect of diffusion comes into play, namely the dependence of drift or diffusion from the particle size. As a consequence, this type of nano–devices can be potentially used for large–scale particle separations. Microscopic calculations based on the Langevin equation on ratchets devices [Astumian and Hänggi, 2002; Hänggi et al., 2005; Hänggi and Marchesoni, 2009] show that there is a closely dependence of the observed motion on the particle size (at constant pressure), as well as on the pressure amplitude (at constant particle size). This effect was observed by Matthias and Müller, so confirming the emergence of non trivial effects when diffusion properties are controlled by the external geometry.

The same effect due to the diffusing material size is used for example by Han and Craighead [2000] to obtain DNA separation, see right panel of Fig. 1.6. In particular the experiment was performed by engineering a

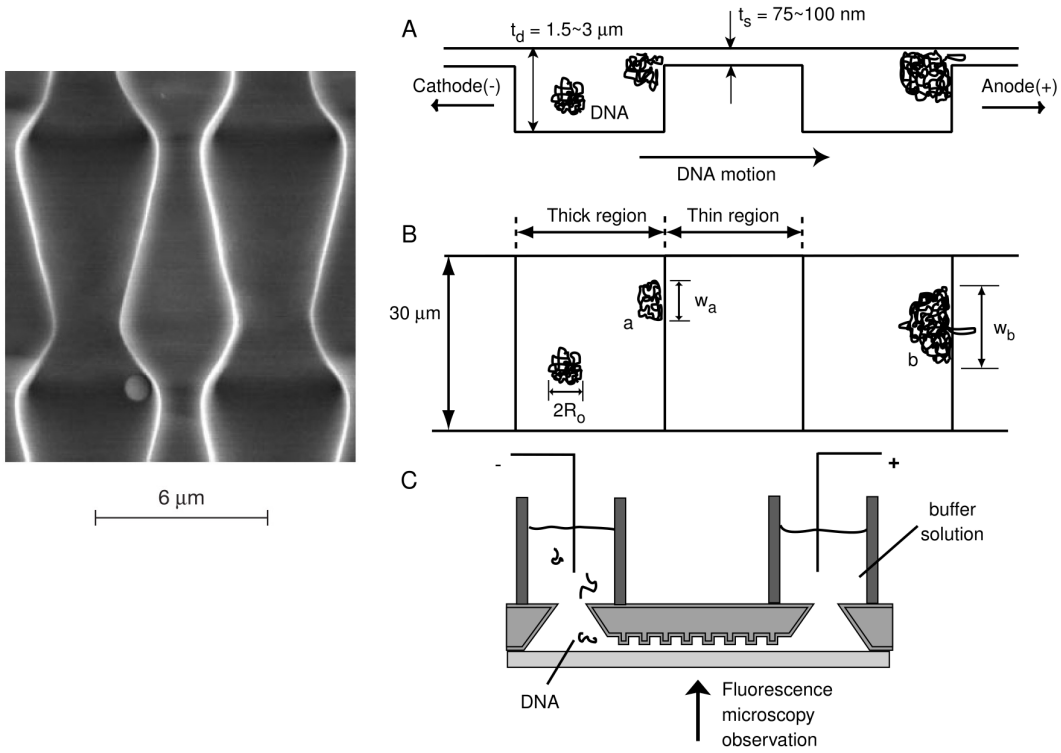

Figure 1.6: ***(left)*** *stacked nano channels obtained by etching a series of one dimensional pores of a macroporous silicon membrane. Adapted from Matthias and Müller [2003]; **(right)** engineered nano–channel in order to obtain DNA separation. Adapted from Han and Craighead [2000]*

"square–like" non homogeneous nano–channel, whose narrow and wider regions cause the size–dependent trapping of DNA diffusing within the channel at the onset of a constriction.

1.6 SUMMARY AND REMARKS

The mutual link between all the examples treated in the previous sections is the "geometrical frustration" of the diffusion process due to physical restrictions on moving particles. Such restrictions are able to produce astonishing effects in the diffusion properties.

From the one hand, the engineered ratchets and the square–like channel described in the last section (see Fig. 1.6), or the geometrical model of spiny dendrite discussed in Sec. 1.3 (see Fig. 1.4), suggest to study diffusive processes within non homogeneous channels.

On the other hand, the geometrical complexity of the Nature emerges also in a series of thin and highly ramified structures, which can be frequently described using fractal (or random fractal) geometries [Stanley and Meakin, 1988]. An example of fractal environment is provided by the chromatin structure, which can be investigated by neutron scattering [Lebedev et al., 2008], rheology techniques [Bancaud et al., 2009] and more recently the Hi–C method [Lieberman-Aiden et al., 2009]. Independently by the used technique the chromatin revealed a fractal structure characterized by a fractal dimension which was found in the range 2.2–3. A theoretical model of diffusion in chromatin which takes into account such fractal structure was worked out by Bénichou et al. [2011].

Driven by these complementary aspects of the geometrical complexity, we will present in this thesis a work on the geometric constraints acting on diffusive processes, analyzing both branched structures and continuous channels with a non homogeneous cross–section.

2

DIFFUSION IN CONFINED GEOMETRIES

" We therefore conclude that the principles of geometry are only conventions; but these conventions are not arbitrary..."

Poincaré [1952]

In the previous chapter we analyzed some physical situations well described by diffusion, in particular we emphasized the role of the geometric constraints on such processes.

In this chapter we will take into account the diffusion process within periodic channels, describing in a more detailed way the mathematical background.

We consider the Fick–Jacobs description [Jacobs, 1967; Burada et al., 2009] and its generalizations, based on a one–dimensional effective description strictly related to a Langevin equation with a non vanishing external potential. Such potential can be expressed as a function of the boundary profile [Reguera et al., 2006; Kalinay and Percus, 2006a; Burada et al., 2009, 2010], establishing the real astonishing idea of an effective transport influenced by an external potential which is only a function of the possible available position–states along the longitudinal direction.

The idea of the entropic particle transport is complementary to another phenomenological approach, the boundary homogenization [Berezhkovskii et al., 2004; Makhnovskii et al., 2006; Berezhkovskii et al., 2006, 2009], being it still characterized by an effective one–dimensional description, however replacing the non homogeneous boundary with an uniform one, keeping a radiation–type condition at the boundary with an appropriately chosen trapping rate.

2.1 THE LANGEVIN EQUATION

Consider the dynamical problem defined by two ensemble of particles, one composed by particles of mass M (water solution) and the other one composed by particles of mass m, with $M \ll m$ (colloidal particles). In principle

the equations of motion of the whole system have to be written taking into account all the canonical variables [Gantmakher, 1970; Goldstein et al., 1950], however, due to the large numbers of degrees of freedom ($N \sim 10^{23}$) in the problem, a dynamical approach looking at the solution of, generally coupled, evolution equations is clearly not a feasible way.

Part of the explanation resides in the idea, due to Einstein [1905], that the random thermal motion of the components on the microscopic level (i.e. water constituents) are manifested macroscopically as a pressure. In other words, the averaged tendency of components to scatter because of their thermal motions (microscopic description) is also manifested as a pressure, being it the pressure of an ideal gas or the partial pressure of a gas in a mixture or the osmotic pressure of a solute in solution (macroscopic description). This idea is at the heart of the explanation of the random motion observed by Brown [Brown, 1827] with his microscope, once the pollen grains in the Brown's experiment are identified with the suspended particles of mass m.

Introducing the random noise experienced by the colloidal particles of mass m due to the surrounding environment, the Newton's second law applied to the suspended particles takes the form [Langevin, 1908; Chandrasekhar, 1943]

$$m\frac{dv}{dt} = -6\pi\mu a v + \xi(t) \tag{2.1}$$

with a the radius of the grain (assumed spherically symmetric) and $v = dx/dt$ its instantaneous velocity; μ is the fluid viscosity, for example the viscosity of the water in the case of Brown's experiment. The first term on the right hand of Eq. (2.1) is called Stokes' force while the second one is the random force exerted on the pollen grain by the fluctuating environment. If we do not take care of the random term in Eq. (2.1), then it is possible to integrate the above equation, giving

$$v(t) = v(0)\exp\left(-t/\tau_c\right)$$

where $\tau_c = m/6\pi\mu a$ is a characteristic relaxation time, that is, when $t \gg \tau_c$, $v(t)$ is practically zero and the grain should appear at rest in the laboratory reference frame; for the case of a grain of $a \sim 1\ \mu$m suspended in water at room temperature we have $\tau_c \sim 10^{-7}s$, which is smaller than the typical reaction time ($\sim 10^{-1}s$) of a good experimentalist, so clearly not appreciable by human eyes, also with the aim of a microscope, implying that we should see the suspended grains immediately at rest, contrary to the Brown's observations. The Stokes' law alone is not sufficient to describes the Brownian motion; the stochastic term $\xi(t)$, which summarizes the pressure exerted by the environment on m, is a reasonable source that can be able to support the motion. However it is necessary to assume that the typical time scale on which m is scattered by the molecules contained into the environment, is smaller than τ_c. This is a quiet assumption in the Einstein's work on Brownian motion, however is not less important; indeed the separation of the two

time scales enables us to treat the random force as a time uncorrelated noise, independent by the grain position and isotropic, that is, the average $\langle x\xi \rangle$ on the number of collisions is reasonably zero[1]. Typically the scattering time is of the order $\sim 10^{-11}s$, which is smaller than $\tau_c = 10^{-7}s$, so it is possible to perform the time scales separation, so multiplying Eq. (2.1) by x and taking the average we get

$$\frac{1}{2}\frac{d^2}{dt^2}\langle x^2 \rangle - \langle v^2 \rangle = -\frac{1}{2\tau_c}\frac{d}{dt}\langle x^2 \rangle + \frac{1}{m}\langle x\xi \rangle$$

At this point Einstein introduced another fundamental assumption: the colloidal particles are in thermal equilibrium with the surrounding environment. This assumption enables us to identify the translational motion of the grain with a measure of its thermal energy via the relation $\langle v^2 \rangle = k_B T/m$, with k_B the Boltzmann constant and T the thermodynamic temperature. With the aim of the thermal equilibrium hypothesis we can solve Eq. (2.1) and the result is given by

$$\langle x^2(t) \rangle = \frac{2k_B T}{m}\tau_c^2 \left[\frac{t}{\tau_c} - (1 - \mathrm{e}^{-t/\tau_c})\right]$$

whose asymptotic behaviour ($t \gg \tau_c$) is

$$\langle x^2(t) \rangle = 2D_0 t \tag{2.2}$$

with D_0 the diffusion coefficient. If we recall that $\tau_c = m/6\pi\mu a$ we can express the diffusion coefficient as

$$D_0 = \frac{k_B T}{6\pi\mu a} = \frac{RT}{6N_A \pi\mu a} \tag{2.3}$$

with R the fundamental gas constant and N_A the Avogadro's number. Eq. (2.3) is the celebrated Einstein relation for the diffusion coefficient, it relates a macroscopic property like D_0, which is a measurable quantity, to a microscopic property like the Boltzmann constant k_B or Avogadro's number N_A, implying a strong indication of the discrete nature of the matter. The definitive proof of the atomic hypothesis was worked out by Jean Baptiste Perrin [Perrin, 1913], who measured the Avogadro's number N_A based on the Einstein theory of Brownian motion.

The relation $\langle x^2 \rangle \sim t$ implies that the variance of the process becomes infinite as $t \to \infty$. This means that the sample paths of Brownian particles are very variable on the molecular time scales. Thus, it is really difficult to perform a measure of the instantaneous velocity of a Brownian particle.

1 The condition $\langle x\xi \rangle = 0$ and the Eq. (2.1) , actually, were used by Langevin in his work on Brownian motion and not explicitly by Einstein. In particular the Langevin picture of Brownian motion led to the theory of stochastic calculus, subsequently improved by Wiener [Wiener, 1958], Itô [Itô and McKean, 1974] and Stratonovich [Gardiner, 2009] (see also Chap. 3).

Nowadays, with the advent of optical tweezers [Block, 1992], it is possible to measure such instantaneous velocity, thus testing the hypothesis of the time scales separation, however it is really astonishing that, only after more than one hundred years, such hypothesis is finally experimentally verified [Li et al., 2010; Huang et al., 2011; Franosch et al., 2011].

It is interesting to observe that Eq. (2.2) is identical to the Eq. (1.6). This result suggests that the macroscopic diffusion process described in the previous chapter can be described by the microscopic stochastic Langevin equation taken into account in this section (see Chap. 3 for a mathematical review on this point).

2.2 STATEMENT OF THE PROBLEM

Consider a two–dimensional channel with a non homogeneous boundary, as in Fig. 2.1. Suppose that the channel is filled, for example, by a water solution together with an ensemble of colloidal particles diffusing into the channel environment. If we assume that the interaction between the macroscopic sus-

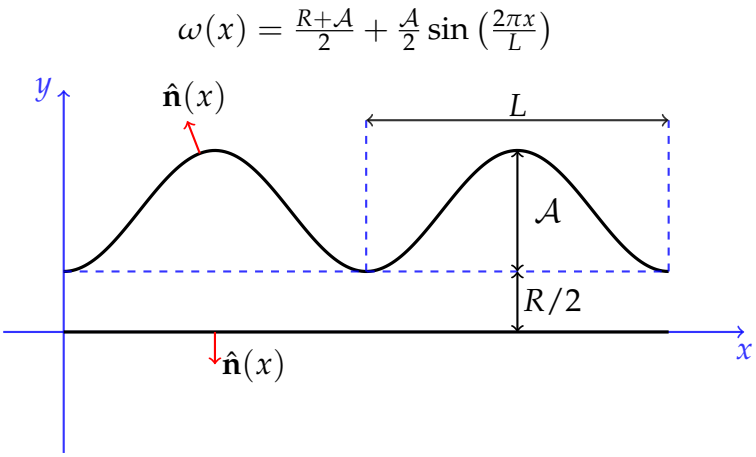

Figure 2.1: A simple periodic non homogeneous channel

pended particles is negligible as first approximation, then the time evolution of a colloidal particle of mass m can be explained with the single–particle Langevin equation

$$m\frac{d^2\mathbf{r}}{dt^2} = -\gamma\frac{d\mathbf{r}}{dt} - \boldsymbol{\nabla}V(\mathbf{r}) + \sqrt{2\gamma k_B T}\boldsymbol{\xi}_t \tag{2.4}$$

where $\mathbf{r} = r^{(x)}\hat{\mathbf{x}} + r^{(y)}\hat{\mathbf{y}} + r^{(z)}\hat{\mathbf{z}}$ is the position vector of the particle, $\gamma > 0$ the viscous friction coefficient, k_B the Boltzmann constant ($k_\mathrm{B} = 1{,}380\,6488\,(24) \times 10^{-23}\,\mathrm{J\,K^{-1}}$) and $V(\mathbf{r})$ a static conservative external potential [2]. The last term

2 The Eq. (2.4) is only a formal way to represent the brownian motion; indeed it can be shown (see Chap. 3 for a short review) that a stochastic quantity like $\mathbf{r}(t)$ is nowhere derivable in the usual sense [Chorin and Hald, 2009].

in Eq. (2.4) models the thermal fluctuations of the colloidal particles due to the coupling with the environment and it is chosen as a Gaussian white noise, that is

$$\langle \xi_t \rangle = 0, \quad \langle \xi_t^{(i)} \xi_{t'}^{(j)} \rangle = \delta_{ij}\delta(t-t'), \qquad i,j = x,y \tag{2.5}$$

When the viscous term is very large and therefore $|m\ddot{\mathbf{r}}| \ll |\gamma\dot{\mathbf{r}}|$, the resulting equation is called overdamped Langevin equation, namely the emerging dynamics is described by the stochastic model

$$\frac{d\mathbf{r}}{dt} = -\frac{\boldsymbol{\nabla} V(\mathbf{r})}{\gamma} + \sqrt{2D_0}\boldsymbol{\xi}_t \tag{2.6}$$

where we introduced the free diffusion coefficient $D_0 = k_B T/\gamma$ (see Sec. 2.1). Throughout the present work, we will consider always the overdamped situation described by Eq. (2.6).

Starting from the microscopic description modelled in Eq. (2.6) it is possible to derive the partial differential equation which rules the time and space evolution of the probability density $\mathscr{P}(\mathbf{r},t)$ to find a particle in a small volume element $d\mathbf{r}$ around $\mathbf{r}$ at time t [Risken, 1989; Chorin and Hald, 2009; Gardiner, 2009] (see also Chap. 3) . The equation for the probability density is called Fokker–Planck equation [Risken, 1989]:

$$\frac{\partial \mathscr{P}(\mathbf{r},t)}{\partial t} + \boldsymbol{\nabla}\cdot\mathbf{J}(\mathbf{r},t) = 0 \tag{2.7}$$

with $\mathbf{J}(\mathbf{r},t)$ the probability current given by

$$\mathbf{J}(\mathbf{r},t) = -\left[\frac{\boldsymbol{\nabla} V(\mathbf{r})}{\gamma} + D_0\boldsymbol{\nabla}\right]\mathscr{P}(\mathbf{r},t) \tag{2.8}$$

The problem of diffusion in a channel characterized by a non homogeneous cross–section in the overdamped regime is then fully classified by Eq. (2.7) and (2.8) together with the appropriate boundary conditions. In order to avoid a net flux out of the channel, that is, if we assume that there are not sources or sinks of matter into the channel, the boundary conditions read

$$\mathbf{J}(\mathbf{r},t)\cdot\hat{\mathbf{n}}(\mathbf{r}) = 0 \qquad \mathbf{r} \in \textit{ Channel wall} \tag{2.9}$$

with $\hat{\mathbf{n}}(\mathbf{r})$ the outgoing local versor from the channel walls (see Fig. 2.1). This condition is generally referred to as no–flux boundaries.

The normal versor reads

$$\hat{\mathbf{n}}(x) = \frac{1}{\sqrt{1+\left(\frac{d\omega}{dx}\right)^2}}\left(-\frac{d\omega}{dx}\hat{\mathbf{x}} + \hat{\mathbf{y}}\right) \tag{2.10}$$

where $\omega(x)$ is a smooth function which represents the boundary profile, see Fig. 2.1. If we take the external potential everywhere zero, $V(\mathbf{r}) = 0$, the

explicit analytical form of the problem which fully describes the overdamped motion is given by

$$\begin{cases} \partial_t \mathscr{P}(\mathbf{r},t) = D_0 \nabla^2 \mathscr{P}(\mathbf{r},t) \\ \left.\frac{\partial \mathscr{P}(\mathbf{r},t)}{\partial y}\right|_{y=\omega(x)} = \frac{d\omega}{dx} \left.\frac{\partial \mathscr{P}(\mathbf{r},t)}{\partial x}\right|_{y=\omega(x)} \\ \left.\frac{\partial \mathscr{P}(\mathbf{r},t)}{\partial y}\right|_{y=0} = 0 \end{cases} \tag{2.11}$$

Further generalizations to the three–dimensional case, as long as to a symmetric channel around the longitudinal axis, are straightforward, see for example Sec. 2.4 for a brief discussion on this point.

In the case of a periodic channel shape characterized by the spatial period L, it is useful to renormalize the physical position and time as [Burada et al., 2009]

$$\mathbf{r} \to \frac{\mathbf{r}}{L}, \quad t \to \frac{k_B T}{L^2 \gamma} t$$

in order to obtain the dimensionless Langevin equation

$$\frac{d\mathbf{r}}{dt} = -\boldsymbol{\nabla} \mathcal{V}(\mathbf{r}) + \sqrt{2}\boldsymbol{\xi}_t$$

where the dimensionless potential is defined as $\mathcal{V}(\mathbf{r}) = V(\mathbf{r})/k_B T$.

2.3 MAPPING THE PROBLEM ALONG THE LONGITUDINAL DIRECTION

The problem formulated in Eq. (2.11), in general, has no analytical solution. One of the possible approximation for the long time behaviour is to consider an effective equation which describes the motion along the longitudinal direction, so an effective one–dimensional problem. Such an approximation can be done by observing that along the longitudinal direction the quantity of interest is the marginal density $\mathscr{G}(x,t)$ which in two spatial dimensions reads

$$\mathscr{G}(x,t) = \int_0^{\omega(x)} dy \; \mathscr{P}(x,y,t) \tag{2.12}$$

To find an equation for the marginal density $\mathscr{G}(x,t)$ we work , just for simplicity, with dimensionless units, considering $\mathcal{V}(\mathbf{r}) = 0$ everywhere and following the one–dimensional reduction of the problem explained by Kalinay and Percus [2005a, 2006b].

Integrating $\mathscr{P}(\mathbf{r},t)$ on y from 0 to $\omega(x)$ we get

$$\int_0^{\omega(x)} dy \; \frac{\partial}{\partial t} \mathscr{P}(x,y,t) - \int_0^{\omega(x)} dy \; \frac{\partial^2}{\partial x^2} \mathscr{P}(x,y,t) - \int_0^{\omega(x)} dy \; \frac{\partial^2}{\partial y^2} \mathscr{P}(x,y,t) = 0$$

The first term yields simply $\partial_t \mathscr{G}(x,t)$, the third term is the integral of an exact differential, so we have

$$\int_0^{\omega(x)} dy\, \frac{\partial^2}{\partial y^2}\mathscr{P}(x,y,t) = \left.\frac{\partial \mathscr{P}(x,y,t)}{\partial y}\right|_{y=\omega(x)} - \left.\frac{\partial \mathscr{P}(x,y,t)}{\partial y}\right|_{y=0}$$

If we use the boundary conditions in Eq. (2.11) the third term becomes

$$\int_0^{\omega(x)} dy\, \frac{\partial^2}{\partial y^2}\mathscr{P}(x,y,t) = \frac{d\omega}{dx}\left.\frac{\partial \mathscr{P}(\mathbf{r},t)}{\partial x}\right|_{y=\omega(x)}$$

Finally the second term has to be calculated by remembering the differentiation rule about an integral whose extremes depend on the differentiation variable. In particular, let us consider the function $\mathscr{G}(x,t)$ defined in Eq. (2.12). If we take the derivative with respect to x and use the boundary conditions in (2.11), we find

$$\frac{\partial \mathscr{G}}{\partial x} = \int_0^{\omega} dy\, \frac{\partial \mathscr{P}}{\partial x} + \frac{d\omega}{dx}\mathscr{P}\Big|_{y=\omega(x)}$$

and so the second derivative takes the form

$$\frac{\partial^2 \mathscr{G}}{\partial x^2} = \int_0^{\omega} dy\, \frac{\partial^2 \mathscr{P}}{\partial x^2} + 2\,\frac{d\omega}{dx}\mathscr{P}\Big|_{y=\omega(x)} + \frac{d^2\omega}{dx^2}\mathscr{P}\Big|_{y=\omega(x)}$$

From the last relation we have

$$\int_0^{\omega} dy\, \frac{\partial^2 \mathscr{P}}{\partial x^2} = \frac{\partial^2 \mathscr{G}}{\partial x^2} - 2\,\frac{d\omega}{dx}\mathscr{P}\Big|_{y=\omega(x)} - \frac{d^2\omega}{dx^2}\mathscr{P}\Big|_{y=\omega(x)}$$

Putting all together the equation for the marginal density can be written as

$$\frac{\partial \mathscr{G}(x,t)}{\partial t} = \frac{\partial^2 \mathscr{G}(x,t)}{\partial x^2} - \frac{\partial}{\partial x}\left[\frac{d\omega(x)}{dx}\mathscr{P}(x,\omega(x),t)\right] \tag{2.13}$$

The one dimensional mapping on the longitudinal direction of the original two–dimensional Fokker–Planck equation is given by Eq. (2.13). In order to solve it, we have to take the appropriate boundary conditions at the channel ends, which we will take always at $x = \pm\infty$ [3]. However the boundary conditions are the last of our problems, indeed the mapped equation does not appear in a closed form and to find the marginal density we have to know the original probability density $\mathscr{P}$, at least the values that it takes on the channel walls.

The problem to find an expression for $\mathscr{P}(x,y,t)$ in terms of the marginal density $\mathscr{G}(x,t)$ was perturbatively solved by Kalinay and Percus [Kalinay and Percus, 2006a] (see also Sec. 2.8), however the solution is, in its general form,

3 This assumption embodies the notion of a finite channel which is much more greater than the longitudinal distance covered by the colloidal particles during the observation time.

too complicated for practical calculations, so other types of approximations and assumptions need to be taken in account; for example, the Fick–Jacobs [Jacobs, 1967] approximation and its generalizations [Burada et al., 2009, 2008] (see also Sec. 2.4, 2.6, 2.7 and 2.8) or the phenomenological approach due to Berezhkovskii et al. [2004]; Makhnovskii et al. [2006]; Berezhkovskii et al. [2006, 2009], called boundary homogenization (see also Sec. 2.10).

2.4 THE FICK–JACOB APPROXIMATION

The simplest approach to close the hierarchy in Eq. (2.13) comes by assuming a local structure of the full probability density in the form [Jacobs, 1967; Zwanzig, 1992]

$$\mathscr{P}(x,y,t) \approx \phi(y|x)\mathscr{G}(x,t)$$

with $\phi(y|x)$ the probability density to get a particle in a small volume element dy around y, given a local position x on the longitudinal axis. The last equation simply assumes that at every instant of time, on a fixed transversal section $\omega(x)$, the transversal and longitudinal motions are completely disentangled. In particular it is reasonable to assume that, after a finite relaxation time τ_y, the transversal motion becomes stationary and, on every transversal section of the channel, equilibrates to the uniform distribution $\phi(y|x) = 1/\omega(x)$, thus giving

$$\mathscr{P}(x,y,t) \approx \frac{\mathscr{G}(x,t)}{\omega(x)} \tag{2.14}$$

The assumption of local equilibrium along the transversal sections of the channel works well only if

$$\left|\frac{d\omega(x)}{dx}\right| \ll 1$$

as was firstly pointed out by R. Zwanzig [Zwanzig, 1992]. A way to understand this restriction is obtained by viewing at the normal versor $\hat{\mathbf{n}}(x)$ to the channel walls in Eq. (2.10). One can argue that, for the limiting case of a flat cylindrical channel, the second term on the right hand of Eq. (2.13) will be zero after the equilibration of the probability density along the transversal direction. Moreover in this case this equilibration does not depend on the particular position on the "x" axis, due to the fact that the simple cylindrical channel is homogeneous, that is the processes along the transversal and longitudinal directions are completely independent. On the other hand, when $\hat{\mathbf{n}}(x) = o(x)\hat{\mathbf{x}} + \hat{\mathbf{y}}$, that is, when the local versor normal to the channel is almost along the transversal direction, a condition verified only if $|d\omega(x)/dx| \ll 1$, it is reasonable to assume that the equilibration along the transversal direction will be still like the simple flat channel, justifying the assumption in Eq. (2.14).

The equilibration assumption along the transversal direction is also linked to the typical relaxation time τ_y, as showed by Burada et al. [2009, 2007, 2008].

Indeed the typical time scale τ_y of diffusion on the transversal direction over a distance Δ_y will be given by

$$\tau_y \approx \frac{\Delta_y^2}{2D_0}$$

and at the same manner along the longitudinal direction

$$\tau_x \approx \frac{\Delta_x^2}{2D_0}$$

The condition of local equilibrium along the transversal sections of the channel will result in the condition $\tau_y/\tau_x \ll 1$, that is

$$\frac{\Delta_y^2}{\Delta_x^2} \approx \left(\frac{d\omega}{dx}\right)^2 \ll 1$$

which clearly is the same result pointed out above, however this heuristic argument has the great value to elucidates in a really clear manner the relation between the validity of the assumption in Eq. (2.14) with the relaxation time along the transverse direction; moreover, can be immediately generalized to the case of a non vanishing external potential, leading to more stringent validity criteria for the FJ approximation [Burada et al., 2007], see also Sec. 2.9.

Assuming the local equilibrium condition, Eq. (2.13) becomes

$$\frac{\partial \mathcal{G}(x,t)}{\partial t} = \frac{\partial}{\partial x}\left\{\omega(x)\frac{\partial}{\partial x}\left[\frac{\mathcal{G}(x,t)}{\omega(x)}\right]\right\} \tag{2.15}$$

which is the so called Fick–Jacobs (FJ) equation.

It is interesting to observe that the FJ equation can be expressed in the equivalent form

$$\frac{\partial \mathcal{G}(x,t)}{\partial t} = -\frac{\partial}{\partial x}\left[\frac{d\mathcal{V}(x)}{dx}\mathcal{G}(x,t)\right] + \frac{\partial^2 \mathcal{G}(x,t)}{\partial x^2} \tag{2.16}$$

which has the same mathematical structure of Eq. (2.7) characterized by the "external" potential given by $\mathcal{V}(x) = -\ln\omega(x)$. This result is really interesting, indeed the particle motion is completely free, however the one dimensional reduction of the problem leads to a biased diffusion and the external field is pure entropic, namely it depends only by the geometry of the system. For this reason, frequently, transport in a non homogeneous channel is also called entropic particle transport [Reguera et al., 2006].

The generalization to a two–dimensional channel, symmetric respect to the longitudinal axis (i.e. the "x" axis in Fig. 2.1), can be made observing that in

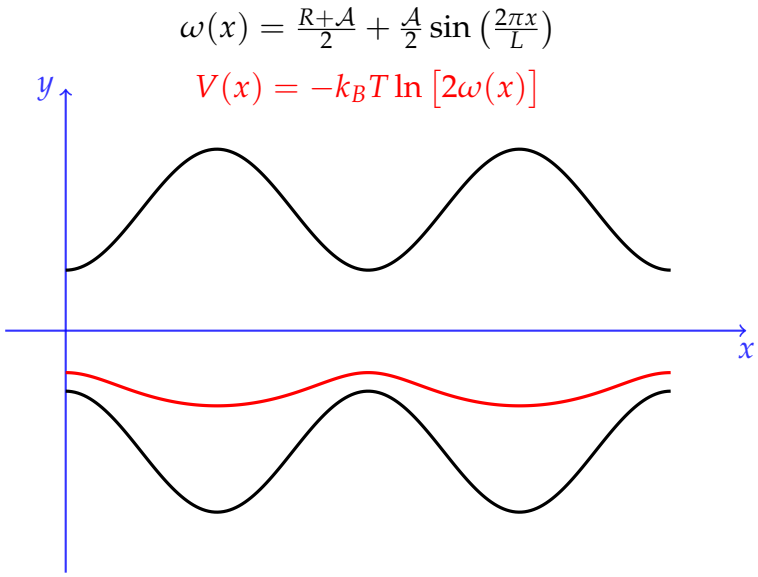

Figure 2.2: An example of entropic potential (red line), together the boundary profile (black line)

this case we have two boundaries, say $\pm\omega(x)$ $\left(\omega(x) > 0,\ \forall x \in \mathbb{R}\right)$ and so the problem in Eq. (2.11) must be replaced with the problem

$$\begin{cases} \partial_t \mathscr{P}(\mathbf{r},t) = D_0 \nabla^2 \mathscr{P}(\mathbf{r},t) \\ \left.\frac{\partial \mathscr{P}(\mathbf{r},t)}{\partial y}\right|_{y=+\omega(x)} = +\frac{d\omega}{dx}\left.\frac{\partial \mathscr{P}(\mathbf{r},t)}{\partial x}\right|_{y=+\omega(x)} \\ \left.\frac{\partial \mathscr{P}(\mathbf{r},t)}{\partial y}\right|_{y=-\omega(x)} = -\frac{d\omega}{dx}\left.\frac{\partial \mathscr{P}(\mathbf{r},t)}{\partial x}\right|_{y=-\omega(x)} \end{cases}$$

The relative marginal density now takes the form

$$\mathscr{G}(x,t) = \int_{-\omega(x)}^{+\omega(x)} dy\ \mathscr{P}(x,y,t)$$

and the resulting 1D model will be the same as in Eq. (2.15), where now the transversal section $\omega(x)$ is replaced by the function $\sigma(x) = 2\omega(x)$ for the two–dimensional case, being $\pm\omega(x)$ respectively the upper and lower boundary of the symmetric channel [4].

The three–dimensional case can be treated at the same manner; the final result, for a symmetric channel respect to the longitudinal direction, is another time in the form of Eq. (2.15), where now $\omega(x)$ must be replaced with the transversal section of the 3D channel, i.e. $\sigma(x) = \pi\omega^2(x)$. From now on we will always treat the case of a 2D channel.

4 Actually, in order to get this result, it must be assumed that, given the symmetry of the channel with respect the longitudinal axis, then $\mathscr{P}(x,\omega(x),t) = \mathscr{P}(x,-\omega(x),t)$. This assumption is reasonable as long as there are no external field acting along the transversal direction, whereas the assumption remains correct if the external field has its only component along the longitudinal direction.

2.5 A MULTISCALE ANALYSIS OF THE FJ DIFFUSION EQUATION

The FJ equation is the first approximation to the problem of entropic particles transport within periodic channels. Before to proceed with other types of improved approximations we present here a multiscale analysis of Eq. (2.16).

Consider the general case of a periodic entropic potential $\mathcal{V}(x) = \mathcal{V}(x+1)$, being 1 the period in dimensionless units. Our intuitive idea is related to the fact that the periodic potential like that depicted in Fig. 2.2 acts as a confining one, trapping the motion of the particles for a certain time, before the transport continues to go on along the longitudinal direction. Following this idea, we can suppose that there is a fast motion on the length scale x and a slow motion on the length scale $Z = \epsilon x$, with $\epsilon > 1$. In addition, we introduce two time scales, the first one is $\tau = \epsilon t$, intuitively associated with the emergence of a longitudinal drift with a constant velocity, the second one is $\Sigma = \epsilon^2 t$, associated to a diffusive motion on the length scale Z; the idea is that on the scale Z, Eq. (2.16) can be recast by an effective diffusion equation of the form

$$\frac{\partial \psi(Z,\Sigma)}{\partial \Sigma} = D_{\text{eff}} \frac{\partial^2 \psi(Z,\Sigma)}{\partial Z^2}$$

with D_{eff} an effective diffusion coefficient expected to be lower than 1, which is the value of the free diffusion coefficient D_0 within the dimensionless units used in the present section. We solve the problem in a single period, assuming periodic boundary conditions; the periodic boundary conditions embody the notion that solving the problem in a given period must be the same as solving the problem in another period; in addition we ignore boundary effects, that is, we assume $-\infty < x < +\infty$.

The multiscale analysis proposed in this section is a standard technique in solving partial differential equation, see for example [Johnson, 2005]. Here we apply this technique to derive D_{eff}, focusing on the reasoning which reinforces the notion of two types of motion mixed in the same system. The marginal density $\mathcal{G}(x,t)$ can be seen as a function $\mathcal{G}(x,Z,t,\tau,\Sigma)$ that we can put in the form

$$\mathcal{G}(x,Z,t,\tau,\Sigma) = \sum_{n=0}^{\infty} \epsilon^n \mathcal{G}^{(n)}(x,Z,t,\tau,\Sigma) \tag{2.17}$$

Moreover the differentiation rules have to be changed as

$$\begin{aligned} \frac{\partial}{\partial t} &\to \frac{\partial}{\partial t} + \epsilon \frac{\partial}{\partial \tau} + \epsilon^2 \frac{\partial}{\partial \Sigma} \\ \frac{\partial}{\partial x} &\to \frac{\partial}{\partial x} + \epsilon \frac{\partial}{\partial Z} \end{aligned}$$

Substituting Eq. (2.17) in Eq. (2.16) and equating all the terms of the same order in ϵ we obtain the follow hierarchy

$$\begin{aligned}\frac{\partial \mathscr{G}^{(n)}}{\partial t} + \frac{\partial \mathscr{G}^{(n-1)}}{\partial \tau} + \frac{\partial \mathscr{G}^{(n-2)}}{\partial \Sigma} &= \frac{\partial}{\partial x}\left[\frac{d\mathcal{V}}{dx}\mathscr{G}^{(n)}\right] \\ &+ \frac{\partial}{\partial Z}\left[\frac{d\mathcal{V}}{dx}\mathscr{G}^{(n-1)} + 2\mathscr{G}^{(n-1)}\right] \\ &+ \left[\frac{\partial^2 \mathscr{G}^{(n)}}{\partial x^2} + \frac{\partial^2 \mathscr{G}^{(n-2)}}{\partial Z^2}\right]\end{aligned} \tag{2.18}$$

where we defined $\mathscr{G}^{(n)} = 0$ for $n < 0$. To the order zero we get the equation

$$\frac{\partial \mathscr{G}^{(0)}}{\partial t} = \frac{\partial}{\partial x}\left[\frac{d\mathcal{V}}{dx}\mathscr{G}^{(0)}\right] + \frac{\partial^2 \mathscr{G}^{(0)}}{\partial x^2} \tag{2.19}$$

which contains only the function $\mathscr{G}^{(0)}$, this means that the hierarchy in Eq. (2.18) is closed and, in principle, it is possible to solve the multiscale problem to every order in ϵ

ORDER ϵ^0

To the order zero in ϵ we have to solve the equation Eq. (2.19). In particular due to the fact that we are looking for a solution on large length and time scales, we can focus only on the stationary solution, that is on the equation

$$\frac{\partial}{\partial x}\left[\frac{d\mathcal{V}}{dx}\mathscr{G}^{(0)} + \frac{\partial \mathscr{G}^{(0)}}{\partial x}\right] = 0$$

which gives immediately

$$\frac{d\mathcal{V}}{dx}\mathscr{G}^{(0)} + \frac{\partial \mathscr{G}^{(0)}}{\partial x} = -J \tag{2.20}$$

with J a constant. Now, let us define the function

$$P(x) = \frac{\mathrm{e}^{-\mathcal{V}(x)}}{\int_0^1 dz\, \mathrm{e}^{-\mathcal{V}(z)}}$$

which is the normalized solution obtained by solving the homogeneous equation (i.e., $J = 0$); moreover, observe that Eq. (2.20) can be written in terms of $P(x)$ as

$$-J = -\frac{1}{P}\frac{\partial P}{\partial x}\mathscr{G}^{(0)} + \frac{\partial \mathscr{G}^{(0)}}{\partial x}$$

Dividing both sides of the last equation by P (which we assume always different from zero) we get

$$-\frac{J}{P(x)} = \frac{\partial}{\partial x}\left(\frac{\mathscr{G}}{P}\right)$$

that is, integrating from $x = 0$ to $x = 1$, namely, integrating on a period in dimensionless units, we find

$$-J \int_0^1 \frac{dx}{P(x)} = \left. \frac{\mathscr{G}^{(0)}}{P} \right|_0^1$$

By using the periodic boundary conditions imposed to the problem, we find the solubility condition $J = 0$. This condition implies that $\mathscr{G}^{(0)}$ will be proportional to $P(x)$, where the proportionality constant will be a function independent from the fast variables x and t, thus

$$\mathscr{G}^{(0)} = P(x)\psi(Z, \tau, \Sigma)$$

The function $\psi(Z, \tau, \Sigma)$ can be determined by looking at higher orders in the perturbation series.

ORDER ϵ^1

To the order one, the equation for $\mathscr{G}^{(1)}$ is given by

$$\frac{\partial \mathscr{G}^{(1)}}{\partial t} + \frac{\partial \mathscr{G}^{(0)}}{\partial \tau} = \frac{\partial}{\partial x}\left[\frac{d\mathcal{V}}{dx}\mathscr{G}^{(1)}\right] + \frac{\partial^2 \mathscr{G}^{(1)}}{\partial x^2} + \frac{d\mathcal{V}}{dx}\frac{\partial \mathscr{G}^{(0)}}{\partial Z} + 2\frac{\partial^2 \mathscr{G}^{(0)}}{\partial x \partial Z}$$

As usual, we neglect the derivative with respect to the fast variable t, so integrating both sides of the equation on a period and using the periodic boundary conditions we find

$$\frac{\partial \psi}{\partial \tau} = v_{\text{eff}} \frac{\partial \psi}{\partial Z}$$

which corresponds to a simple transport equation on the length scale Z and time scale τ, with an effective drift velocity given by

$$v_{\text{eff}} = \frac{\int_0^1 dx \, \frac{d\mathcal{V}}{dx} \mathrm{e}^{-\mathcal{V}(x)}}{\int_0^1 dz \, \mathrm{e}^{-\mathcal{V}(z)}} \propto \left. \mathrm{e}^{-\mathcal{V}(x)} \right|_0^1 = 0$$

being $\mathcal{V}(x) = V(x + 1)$; for example we have $\partial\psi/\partial\tau = 0$, from which follows that $\psi = \psi(Z, \Sigma)$ is only a function of the slow variables. Finding an effective equation for this function is the goal of the perturbation analysis to the second order.

Now we can solve the equation for $\mathscr{G}^{(1)}$, obviously the derivative with respect to τ is not present, thanks to the above reasoning, while the derivative with respect to the fast variable t, will be neglected due to the fact that we are searching for a solution on the time scale $\Sigma \gg t$; we have

$$-\frac{\partial}{\partial x}\left[\frac{d\mathcal{V}}{dx}\mathscr{G}^{(1)}\right] - \frac{\partial^2 \mathscr{G}^{(1)}}{\partial x^2} = \left[\frac{d\mathcal{V}}{dx}P(x) + 2\frac{\partial P(x)}{\partial x}\right]\frac{\partial \psi}{\partial Z} \tag{2.21}$$

The last equation can be solved, for example, by taking a solution in the form

$$\mathscr{G}^{(1)} = \Omega(x)\frac{\partial\psi(Z,\Sigma)}{\partial Z}$$

Substituting in Eq. (2.21) and remembering the result obtained to the order zero, i.e.

$$\frac{d\mathcal{V}}{dx}P + \frac{\partial P}{\partial x} = -J = 0$$

we get

$$\frac{\partial}{\partial x}\left[\frac{d\mathcal{V}}{dx}\Omega(x,t) + \frac{\partial\Omega(x,t)}{\partial x} + P\right] = 0$$

which identifies another time a constant, say $\tilde{J}$, given by the expression between the square brackets in the last equation. Remembering that

$$\frac{d\mathcal{V}}{dx} = -\frac{1}{P(x)}\frac{\partial P}{\partial x}$$

we can also write $\tilde{J}$ as

$$-\frac{1}{P(x)}\frac{\partial P}{\partial x}\Omega(x,t) + \frac{\partial\Omega(x,t)}{\partial x} + P = \tilde{J}$$

from which, dividing both sides by $P(x)$ follows

$$\frac{\partial}{\partial x}\left(\frac{\Omega}{P}\right) = \frac{\tilde{J}}{P} - 1 \tag{2.22}$$

By taking another time the integral of the last equation on a period and applying the periodic boundary conditions it is simple to show that

$$\tilde{J} = \frac{1}{\int_0^1 dx\ \frac{1}{P(x)}} \tag{2.23}$$

At this point the first order solution in ϵ follows immediately from Eq. (2.22), indeed by direct integration we find the (stationary) solution

$$\Omega(x) = P(x)\left\{\frac{\int_0^x d\tilde{x}\ \frac{1}{P(\tilde{x})}}{\int_0^1 dz\ \frac{1}{P(z)}} - x + \frac{\Omega(0)}{P(0)}\right\}$$

thus giving

$$\mathscr{G}^{(1)}(x,Z,\Sigma) = \Omega(x)\frac{\partial\psi(Z,\Sigma)}{\partial Z}$$

ORDER ϵ^2

Finally we see the equation to the order ϵ^2, it is given by

$$\frac{\partial \mathscr{G}^{(2)}}{\partial t} + \frac{\partial \mathscr{G}^{(0)}}{\partial \Sigma} = \frac{\partial}{\partial x}\left[\frac{d\mathcal{V}}{dx}\mathscr{G}^{(2)} + 2\frac{\partial \mathscr{G}^{(1)}}{\partial Z}\right] + \frac{\partial}{\partial x}\left[\frac{d\mathcal{V}}{dx}\mathscr{G}^{(1)}\right]\frac{\partial^2 \mathscr{G}^{(2)}}{\partial x^2} + \frac{\partial^2 \mathscr{G}^{(0)}}{\partial Z^2}$$

As usual, we neglect the fast variable t and integrate both sides on x from 0 to 1, thus using the periodic boundary conditions we find finally the equation for the slow variables Z, Σ

$$\frac{\partial \psi}{\partial \Sigma} = \left[1 + \int_0^1 dx\ \Omega(x)\frac{d\mathcal{V}}{dx}\right]\frac{\partial^2 \psi}{\partial Z^2}$$

Remembering the equation for $\tilde{J}$ explained to the first order in ϵ, say

$$\Omega(x)\frac{d\mathcal{V}}{dx} = \frac{1}{\int_0^1 dx\ \frac{1}{P(x)}} - \frac{\partial \Omega}{\partial x} - P$$

and using the usual periodic boundary conditions, we get the final effective equation for the slow variables

$$\frac{\partial \psi(Z,\Sigma)}{\partial \Sigma} = D_{\text{eff}}\frac{\partial^2 \psi(Z,\Sigma)}{\partial Z^2} \tag{2.24}$$

$$D_{\text{eff}} = \frac{1}{\int_0^1 dx\ \mathrm{e}^{\mathcal{V}(x)}\int_0^1 dz\ \mathrm{e}^{-\mathcal{V}(z)}} \tag{2.25}$$

The above reasoning shows that under the validity of the FJ approximation we expect asymptotically in time and on large scales, an effective motion which along the longitudinal direction appears as a standard diffusive one, with an effective diffusion coefficient given by Eq. (2.25), see Chap. 5 for numerical verifications of this result compared to our results.

Restoring all the physical units, the above analysis shows that if we take $V(x) = -k_B T \ln \sigma(x)$ and we introduce the notation

$$\langle f(x)\rangle = \frac{1}{L}\int_0^L dx\ f(x)$$

with $f(x) = f(x+L)$, then the effective diffusion coefficient can be put in the usual form explained through the Lifson–Jackson formula [Lifson and Jackson, 1962], that is

$$D_{\text{eff}} = \frac{D_0}{\langle \sigma(x)\rangle \left\langle \frac{1}{\sigma(x)}\right\rangle} \tag{2.26}$$

2.6 THE ZWANZIG TREATMENT OF THE FJ EQUATION

Zwanzig [Zwanzig, 1992] was the first who proposed an improvement of the FJ equation. In particular by leaving the local equilibrium assumption, Zwanzig showed that FJ equation has to be modified with the equation

$$\frac{\partial \mathscr{G}(x,t)}{\partial t} = \frac{\partial}{\partial x}\left\{ D(x)\sigma(x)\frac{\partial}{\partial x}\left[\frac{\mathscr{G}(x,t)}{\sigma(x)}\right]\right\} \tag{2.27}$$

with $D(x)$ a microscopic position–dependent diffusion coefficient. We refer to the literature [Zwanzig, 1992] for an exhaustive treatment of the Zwanzig reasoning, which is a perturbative expansion performed assuming "small" perturbations from the local equilibrium condition. Here we want just to show how Eq. (2.27), characterized by a generalized microscopic diffusion coefficient, can be used to go beyond the local equilibrium condition, strictly related with the FJ equation.

The starting point is to write the full probability density as

$$\mathscr{P}(x,y,t) = \frac{\mathscr{G}(x,t)}{\sigma(x)} + \delta\mathscr{P}(x,y,t) \tag{2.28}$$

with $\delta\mathscr{P}(x,y,t)$ a perturbation such that the condition ("small" perturbations)

$$\frac{\sigma(x)\delta\mathscr{P}(x,y,t)}{\mathscr{G}(x,t)} \ll 1 \tag{2.29}$$

holds for every space point (x,y) and for every instant of time t. Using Eq. (2.13) with $\mathscr{P}(x,y,t)$ given by (2.28), we obtain Eq. (2.27) with $D(x)$ given by

$$D(x) = 1 + \frac{\partial\delta\mathscr{P}}{\partial(\mathscr{G}/\sigma)}$$

with $\partial\delta\mathscr{P}/\partial(\mathscr{G}/\sigma) \ll 1$, due to the condition above.

The above reasoning explains well how, by leaving the local equilibrium assumption, a position–dependent microscopic diffusion coefficient naturally comes into play, thus generalizing the FJ approach [Jacobs, 1967]. However the calculation of $D(x)$ is all another history and, up to now, it does not exist a general accepted analytical expression for $D(x)$, also if a series of proposals was done by various authors [Zwanzig, 1992; Reguera and Rubí, 2001; Kalinay and Percus, 2006a], as we will explain better in the next sections.

The Zwanzig's [Zwanzig, 1992] calculation about the microscopic diffusion coefficient $D(x)$ is based on the analysis of the evolution equation for the fluctuation $\delta\mathscr{P}(x,y,t)$, in particular he showed that when the condition (2.29) is fulfilled, then we can write $D(x)$ as

$$D_{Zw}(x) = \frac{D_0}{1+\theta\left(\frac{d\omega}{dx}\right)^2} \tag{2.30}$$

with $\theta = 1/3, 1/2$, respectively in two and three spatial dimensions. Observe that we used the subscript "Zw" in order to distinguish the Zwanzig result from others calculation and proposals for the microscopic diffusion coefficient.

The Eq. (2.26) for the effective diffusion coefficient can be generalized to those cases characterized by a non local microscopic diffusion coefficient $D(x)$. The result is given by the modified LJ formula [Lifson and Jackson, 1962]

$$D_{\text{eff}} = \frac{1}{\langle \sigma(x) \rangle \left\langle \frac{1}{D(x)\sigma(x)} \right\rangle}$$

The same result was also derived by Martens et al. [2011] using perturbabive techniques and by Reimann et al. [2001] analyzing the *nth* moment of the first passage time from a point a to $b > a$ for a stochastic trajectory obeying the overdamped Langevin equation with an external periodic potential.

To conclude this section, we observe that small fluctuations of the probability density "around" the local equilibrium condition, are not enough to justify the Zwanzig treatment. Indeed in order to have a nearly one–dimensional motion, the linear size of a single cell must be greater than the linear dimension of the transversal pores, that is $L \gg R/2$, see Fig. 2.1.

2.7 THE HEURISTIC ARGUMENT OF REGUERA AND RUBÍ

The Zwanzig's perturbative reasoning on the generalization of the FJ equation, reinforces the idea that Eq. (2.27) is essentially the correct one to describe the longitudinal diffusive motion within non homogeneous channel, once more deeper approximations for $D(x)$ to higher orders in the fluctuations from local equilibrium assumption can be worked out. By giving an heuristic argument Reguera and Rubí firstly suggested a possible generalization of Zwanzig's result [Reguera and Rubí, 2001].

Practically it is well known that the microscopic diffusion coefficient D_0 for the free case determines the particle displacement $(\Delta \mathbf{r})^2 = \Delta x^2 + \Delta y^2$ in the plane, that is

$$D_0 \approx \frac{(\Delta \mathbf{r})^2}{t} = \frac{\Delta x^2 \left[1 + \left(\frac{\Delta y}{\Delta x}\right)^2\right]}{t}$$

This relation implies that if we map the two–dimensional motion along the longitudinal direction, the effects of the entropic potential have to be taken in account as a consequence of the re–scaling of the microscopic diffusion coefficient from D_0 to $D \approx D_0/[1 + (\Delta x/\Delta y)^2]$ so, in particular, the microscopic

diffusion coefficient $D(z)/D_0$ should be a function $h(z)$ of the z variable only, defined by the relation

$$\frac{D}{D_0} = h(z), \qquad z = \frac{1}{1+\left(\frac{d\omega}{dx}\right)^2}$$

Reguera and Rubí proposed for the function $h(z)$ the power law relation [Reguera and Rubí, 2001] $h(z) = z^\alpha$ By expanding the suggested result in terms of $(d\omega/dx)^2$ and comparing it with the Zwanzig's result follows that a reasonable choice for the exponent α is given by $\alpha = 1/3$ for the 2D case[5]. The final expression of the Reguera and Rubí (RR) local diffusion coefficient is then given by

$$D_{RR}(x) = \frac{D_0}{\left[1+\left(\frac{d\omega}{dx}\right)^2\right]^{1/3}} \tag{2.31}$$

2.8 THE PERTURBATIVE APPROACH OF KALINAY AND PERCUS

In the previous sections we showed that the concept of entropic potential naturally comes into play when we consider a diffusion problem within non homogeneous periodic channels. We also analyzed the FJ equation perturbatively, using a multiscale analysis and showing how this analysis highlights the fact that FJ equation can be seen asymptotically as a simple effective diffusion equation with an appropriate diffusion coefficient D_{eff}. The problem is how we can go beyond the FJ approximation, considering also those channel shapes such that $|d\omega(x)/dx| > 1$, that is, by leaving the local equilibrium condition hypothesis.

The perturbative way to find the solution is due to Kalinay and Percus [Kalinay and Percus, 2005a,b, 2006a,b, 2008]. In particular they split the diffusion coefficient D_0 in two pieces, a transversal one $D_y = D_0/\varepsilon$ ($\varepsilon \ll 1$) and a longitudinal one $D_x = D_0$. This "trick" is equivalent to the scaling of y and $\omega(x)$ by $\sqrt{\varepsilon}$ and leads to the diffusion equation in the form

$$\frac{\partial \mathscr{P}(x,y,t)}{\partial t} = \left(\frac{\partial^2}{\partial x^2} + \frac{1}{\varepsilon}\frac{\partial^2}{\partial y^2}\right)\mathscr{P}(x,y,t) \tag{2.32}$$

where the time is also rescaled according to the relation $D_0 t \to t$.

We refer for simplicity to Fig. 2.1 in order to simplify the boundary conditions (BCs); indeed, in this case, the transversal section $\sigma(x)$ is equivalent to $\omega(x)$ and the BCs read:

$$\begin{cases} \partial_y \mathscr{P}(x,y,t)\Big|_{y=\omega(x)} & = \varepsilon\omega'(x)\partial_x \mathscr{P}(x,y,t)\Big|_{y=\omega(x)} \\ \partial_y \mathscr{P}(x,y,t)\Big|_{y=0} & = 0 \end{cases}$$

5 For the 3D case the result is $\alpha = 1/2$

The mapped equation along the longitudinal direction takes the same form as in Eq. (2.13), that is

$$\frac{\partial \mathscr{G}(x,t)}{\partial t} = \frac{\partial^2 \mathscr{G}(x,t)}{\partial x^2} - \frac{\partial}{\partial x}\left[\omega'(x)\mathscr{P}(x,\omega(x),t)\right] \tag{2.33}$$

If $\varepsilon \to 0$ the transverse relaxation is so fast that $\mathscr{P}(x,y,t)$ is flat in the transverse direction, namely $\mathscr{P}(x,\omega(x),t) \approx \mathscr{G}(x,t)/\omega(x)$ and the Eq. (2.33) leads to the FJ equation (see Sec. 2.3 and Sec. 2.4).

When $\varepsilon > 0$ the transverse relaxation is slower and $\mathscr{P}(x,y,t)$ becomes curved in the transverse direction and the local equilibrium assumption has to be replaced with the more general hypothesis

$$\mathscr{P}(x,y,t) = \hat{Q}(x,y,\partial_x)\frac{\mathscr{G}(x,t)}{\omega(x)}$$

where $\hat{Q}(x,y,\partial_x)$ is the so called operator of backward mapping. Due to the fact that we are looking for a model in the stationary regime along the transverse direction, Kalinay and Percus assume

- $\hat{Q}(x,y,\partial_x)$ does not depend on time, hence

$$\frac{\partial \hat{Q}(x,y,\partial_x)}{\partial t} = \hat{Q}(x,y,\partial_x)\frac{\partial}{\partial t}$$

- $\hat{Q}(x,y,\partial_x)$ satisfies the unitary relation

$$\frac{1}{\omega(x)}\int_0^{\omega(x)} dy\ \hat{Q}(x,y,\partial_x)\frac{\mathscr{G}(x,t)}{\omega(x)} = \frac{\mathscr{G}(x,t)}{\omega(x)}$$

- $\hat{Q}(x,y,\partial_x)$ can be expanded in ε as

$$\hat{Q}(x,y,\partial_x) = 1 + \sum_{k=1}^{\infty} \varepsilon^k \hat{Q}_k(x,y,\partial_x) \tag{2.34}$$

Substituting Eq. (2.34) into Eq. (2.32) we get

$$\sum_{k=0}^{\infty} \varepsilon^{k+1}\left(\frac{\partial}{\partial t} - \frac{\partial^2}{\partial x^2} - \frac{1}{\varepsilon}\frac{\partial^2}{\partial y^2}\right)\hat{Q}_k(x,y,\partial_x)\frac{\mathscr{G}(x,t)}{\omega(x)} = 0$$

with Neumann BCs at $y = 0$ and $y = \omega(x)$, namely

$$\frac{\partial \mathscr{G}(x,t)}{\partial t} = \frac{\partial}{\partial x}\left[\frac{\partial \omega(x)}{\partial x} - \omega'(x)\sum_{k=0}^{\infty}\varepsilon^k \hat{Q}_k(x,y,\partial_x)\right]\frac{\mathscr{G}(x,t)}{\omega(x)} =$$
$$= \frac{\partial \omega(x)}{\partial x}\left(1 - \sum_{k=1}^{\infty}\varepsilon^k \hat{Z}_k(x,\partial_x)\right)\frac{\partial}{\partial x}\frac{\mathscr{G}(x,t)}{\omega(x)}$$

In the last equation it was defined another differential operator $\hat{Z}(x,\partial_x)$, related to the operator $\hat{Q}$ by the recurrence relations

i)

$$\frac{\partial^2 \hat{Q}_{k+1}}{\partial y^2} = -\frac{\partial^2}{\partial x^2}\hat{Q}_k - \sum_{s=0}^{k} \hat{Q}_{k-s}\frac{1}{\omega(x)}\frac{\partial}{\partial x}\omega(x)\hat{Z}_k\frac{\partial}{\partial x}$$

ii)

$$\hat{Z}_k\frac{\partial}{\partial x} = \frac{\omega'(x)}{\omega(x)}\hat{Q}_k, \qquad k > 0$$

The recurrence relations can be used to find $\hat{Q}_k$. The starting point is the case with $k = 0$ which gives $\hat{Q}_0 = 1$ and $\hat{Z}_0 = -1$; observe that in this case we recover the simple FJ description. To perform higher order corrections we have to use the recurrence relations, using the BCs and the unitary assumption on $\hat{Q}$ to fix the integration constants at the double integration of $\partial_y^2\hat{Q}_{k+1}$. The final result of this calculation gives

$$\frac{\partial \mathcal{G}(x,t)}{\partial t} = \frac{\partial}{\partial x}\left\{\omega(x)\hat{D}(x)\frac{\partial}{\partial x}\frac{\mathcal{G}(x,t)}{\omega(x)}\right\} \tag{2.35}$$

The microscopic diffusion coefficient $\hat{D}(x)$ appearing in Eq. (2.35) can be now expressed as [Kalinay and Percus, 2006a]

$$\begin{aligned}\hat{D}(x) = 1 &- \frac{\varepsilon}{3}\omega'^2 \\ &+ \frac{\varepsilon^2}{45}\left[9\omega'^4 + \omega\omega'^2\omega'' - \omega^2\omega'\omega^{(3)}\right] \\ &- \frac{\varepsilon^3}{945}\left[135\omega'^6 + 45\omega\omega'^4\omega'' + \cdots\right] + \cdots\end{aligned} \tag{2.36}$$

As a first approximation it is possible to consider only the "linear" terms in Eq. (2.36) (highlighted in green), that is all those terms expressed as a linear function of the profile or its first derivative. In particular we have

$$\hat{D}(x) \approx D_{KP}(x) = \sum_{k=0}^{\infty}\frac{(-\varepsilon)^k}{2k+1}\omega'^{2k} \tag{2.37}$$

Remembering that the expansion was executed by scaling the transversal direction with the factor $\sqrt{\varepsilon}$ and coming back to the original units we get the final result

$$D_{KP}(x) = D_0\frac{\arctan\left[\omega'(x)\right]}{\omega'(x)} \tag{2.38}$$

obtained by summing up the the series in Eq. (2.37)

Repeating the reasoning for a 3D channel which is symmetric about its longitudinal axis leads to the microscopic diffusion coefficient given by the formula

$$D_{KP}^{(3D)}(x) = D_0\frac{1}{\sqrt{1+[\sigma'(x)]^2}}$$

where $\sigma(x)$, as usual, is the local transversal section. It is interesting to observe that the last expression is exactly the same expression obtained heuristically by Reguera and Rubí [Reguera and Rubí, 2001] for the three–dimensional case. However when we consider a two dimensional channel, the Eq. (2.38) is different from the Eq. (2.31).

Further observations about the Kalinay and Percus (KP) perturbative treatment need to be carried out at this point:

- the series expansion of $D(x)$ contains a lot of terms emerging as linear and non linear combinations of the boundary derivatives and despite the fact that the "linear" approximation used to calculate $D_{KP}(x)$ converges, it is not obvious that the entire series presents the same convergence property.
- The procedure is based on the assumption that $\omega(x)$ is a smooth function, infinitely differentiable, thus implying that for a sharp channel, like, for example, those treated in Chap. 5, the singularities in the boundary profile invalidate the KP approach.
- Some periodic channels, also if they are not differentiable, can be however expanded in Fourier series, which is differentiable term by term and in this limit it is possible to think that the Kalinay and Percus approach can be recovered, however if $\omega(x)$ is a multivalued function of the space point (see for example Chap. 5) the Kalinay and Percus treatment fails.

2.9 ASYMPTOTIC NON LINEAR MOBILITY

In this section, we consider the overdamped stochastic Lagevin dynamics within a periodic channel in the case of a non vanishing external field given by $V(\mathbf{r}) = -\mathbf{F}\cdot\mathbf{r}$ with $\mathbf{F} = f\hat{\mathbf{x}}$ The stochastic equation describing such dynamics is given by (See Sec. 2.2).

$$\frac{d\mathbf{r}}{dt} = \frac{f}{\gamma}\hat{\mathbf{x}} + \sqrt{2D_0}\xi_t \tag{2.39}$$

with $D_0 = k_B T/\gamma$ the free diffusion coefficient and considering no–flux boundaries.

The one–dimensional reduction of the Fokker–Planck equation related to the Eq. (2.39) can be immediately worked out, extending the previous reasoning on the unbiased case to the biased dynamics considered in this section [Burada et al., 2009]. The resulting equation is given by

$$\frac{\mathcal{G}(x,t)}{\partial t} = \frac{\partial}{\partial x}\left\{D(x)\left[\frac{\partial \mathcal{G}(x,t)}{\partial x} + \frac{U'(x)}{k_B T}\mathcal{G}(x,t)\right]\right\} \tag{2.40}$$

The free energy $U(x) = E(x) - TS(x)$ is made up of a contribution due to the external applied field, $E(x) = -fx$, and an entropic term $S(x) = k_B \ln\sigma(x)$,

with $\sigma(x)$ the transversal section of the channel. The local diffusion coefficient $D(x)$ can be considered as $D_{Zw}(x)$ (Eq. (2.30)), $D_{RR}(x)$ (Eq. (2.31)) and $D_{KP}(x)$ (Eq. (2.38)) and in principle there is not a way to know what is the best choice which ensures a good matching with the simulated data.

One of the key quantities to describe the behaviour of a diffusive process within a quasi one–dimensional structure is the average particle current $\langle \dot{x} \rangle$ [Marchesoni, 2010], useful to define the mobility as the ratio between the averaged current and the applied external field f, namely

$$\mu = \frac{\langle \dot{x} \rangle}{f} \tag{2.41}$$

To find an asymptotic analytical expression for the mobility in terms of the external geometrical parameters, applied field and temperature, we follow Burada et al. [2007]. The Eq. (2.40) results from the continuity equation

$$\frac{\partial \mathscr{G}(x,t)}{\partial t} = -\frac{\partial J(x,t)}{\partial x}$$

where the probability current can be expressed in the form

$$J(x,t) = -D(x)\, \mathrm{e}^{-\beta U(x)} \frac{\partial}{\partial x}\, \mathrm{e}^{\beta U(x)} \mathscr{G}(x,t), \qquad \beta = \frac{1}{k_{\mathrm{B}} T}$$

All the proposed microscopic diffusion coefficients are periodic smooth functions. Indeed they can be expressed in terms of $\sigma(x)$ and/or its first derivatives; in particular $\sigma(x)$ is a function of the periodic boundary profile $\omega(x) = \omega(x + L)$. Another immediate property is related to the free energy $U(x)$; more specifically we have $U(x + L) = U(x) - \beta f L$, that is, $U(x)$ is a tilted periodic potential [Constantini and Marchesoni, 1999; Hänggi and Marchesoni, 2009; Hänggi et al., 2005], so it is convenient to introduce the (reduced) quantities ($k \in \mathbb{Z}$)

$$\mathcal{G}(x,t) = \sum_k \mathscr{G}(kL + x, t)$$
$$\mathcal{J}(x,t) = \sum_k J(kL + x, t)$$

The above quantities are periodic by definition. Moreover, provided that $\mathscr{G}(x,t)$ is normalized to the unity on $\mathbb{R}$, then $\mathcal{G}(x,t)$ is normalized on $[0, L]$ (and more generally on $[x_0, x_0 + L]$). Asymptotically in time, the current is expected to reaches a steady state value, so $\mathcal{J}(x,t) = \mathcal{J}_{st}$, with $\mathcal{J}_{st}$ a constant. Similarly $\mathcal{G}(x,t)$ approaches a steady state density $\mathcal{G}_{st}(x)$ and we have

$$\mathcal{J}_{st} = -D(x)\, \mathrm{e}^{-\beta U(x)} \frac{\partial}{\partial x}\, \mathrm{e}^{\beta U(x)} \mathcal{G}_{st}(x)$$

Multiplying both sides of the last equation by $\mathrm{e}^{\beta U(x)}/D(x)$ and integrating over a channel period we get

$$\mathcal{J}_{st} \int_{x_0}^{x_0+L} dx'\, \frac{\mathrm{e}^{\beta U(x')}}{D(x')} = \int_{x_0}^{x_0+L} dx'\, \frac{\partial}{\partial x'}\, \mathrm{e}^{\beta U(x')} \mathcal{G}_{st}(x')$$

Using the conditions $\mathcal{G}_{st}(x) = \mathcal{G}_{st}(x+L)$ and $U(x+L) = U(x) - \beta f L$ the last equation can be written as

$$\mathcal{J}_{st} \int_{x_0}^{x_0+L} dx' \; \frac{\mathrm{e}^{\beta U(x')}}{D(x')} = \mathcal{G}_{st}(x)(1 - \mathrm{e}^{-\beta f L}) \, \mathrm{e}^{\beta U(x)}$$

which, after rearranging the terms and integrating from 0 to L gives

$$\mathcal{J}_{st} = \frac{(1 - \mathrm{e}^{-\beta f L})}{\int_0^L dx \; \mathrm{e}^{-\beta U(x)} \int_{x_0}^{x_0+L} dx' \; \frac{\mathrm{e}^{\beta U(x')}}{D(x')}} \tag{2.42}$$

Now, recall that the general relation between the asymptotic averaged velocity $\langle \dot{x} \rangle$ and the steady current is given by

$$\langle \dot{x} \rangle = \int_0^L dx \; \mathcal{J}_{st} = \mathcal{J}_{st} L$$

thus from Eq. (2.42) we get the final result

$$\mu(f, L, \beta) = \frac{L(1 - \mathrm{e}^{-\beta f L})}{f \int_0^L dx \; \mathrm{e}^{-\beta U(x)} \int_{x_0}^{x_0+L} dx' \; \frac{\mathrm{e}^{\beta U(x')}}{D(x')}} \tag{2.43}$$

which is also the same result derived by [Reguera et al., 2006] using the mean first–passage time approach.

The picture 2.3 shows the comparison between the analytical expression in Eq. (2.43) and the simulation results, as performed by Burada et al. [2009], taking as $D(x)$ the microscopic diffusion coefficient (in two space dimension) proposed by Reguera and Rubí, $D_{RR}(x)$ (Eq. (2.31)) and considering $2\pi\omega(x) = \mathcal{A}[\sin(2\pi x/L) + R]$ with $L = 1$, $R = 1.02$ and $\mathcal{A} = 1$. The authors highlight how the mobility derived by the application of the generalized FJ approach considering the effect of a constant external field acting on the system, is in agreement with the simulated data up to a critical field f_c, so establishing a generalized validity criteria for the application of the generalized FJ equation. In order to estimate f_c it is possible to use a phenomenological criterion based on the comparison of the characteristic time scales of the problem [Burada et al., 2007]. In particular we can compare the typical length scale related to the transversal motion,

$$\tau_y = \frac{2}{D_0} \frac{\mathcal{A}^2}{(1+R)^2}$$

with the typical length scale related to the longitudinal motion

$$\tau_x = \frac{2}{D_0 L^2}$$

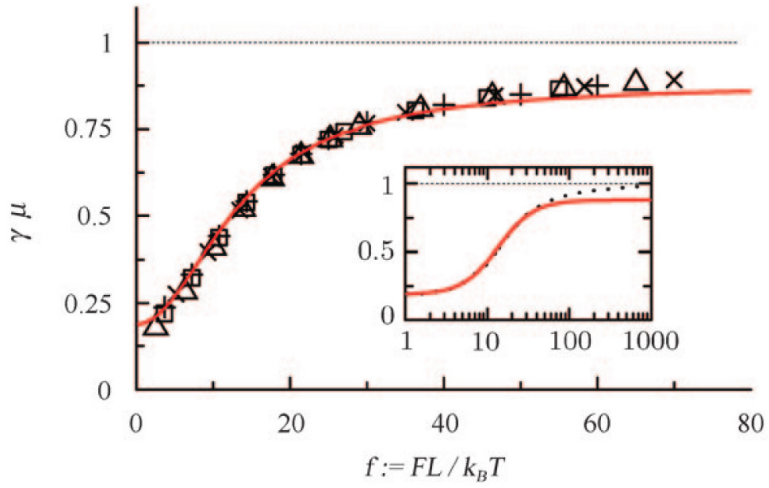

Figure 2.3: *Plot of the non linear mobility $\gamma\mu$ (with γ the friction coefficient) as a function of the rescaled field $f \to fL/k_BT$ for a 2D channel at different temperatures: $k_BT = 0.01(\times), 0.1(+), 0.2(\square), 0.4(\triangle)$. After rescaling all the data collapse onto one curve which is in a wonderful agreement at low field with the analytical solution in Eq. (2.43) (red continuum line). The inset shows the same plot in log–linear scale in order to highlight how the approximation does not work after a critical field f_c. Adapted from Burada et al. [2009]*

and the length scale τ_f useful to the external field f in order to move a particle across one period of the channel, namely

$$\tau_f = \frac{\gamma L}{f}$$

The FJ approximation is accurate when the transversal motion equilibrates faster than the longitudinal one, a condition which can be satisfied only if $\tau_y \ll \min\{\tau_x, \tau_f\}$. In particular, for large drives it suffices to require $\tau_x \ll \tau_f$, which leads to the following expression for the critical field f_c [Burada et al., 2007],

$$f_c = \frac{1}{2(1+R)^2}\left(\frac{L}{a}\right)^2$$

where the value of f_c is given in dimensionless form, that is using the substitution $f_c \to f_c L/k_BT$, see Sec. 2.2.

2.10 THE BOUNDARY HOMOGENIZATION APPROACH

The boundary homogenization approach belongs to a class of methods called effective–medium theories [Zwanzig, 1990; Choy, 1999; Torquato, 2002]. It is based on the replacement of the real medium by a fictitious uniform medium with prescribed effective parameters.

The idea of the boundary homogenization was historically introduced in a biological context by Berg and Purcell [1977] (see also [Berg, 1983]), in order to study the problem of diffusing particles trapped by patchy surfaces, such as the ligand binding to cell surface receptors. Such a problem can be generally formulated as follow [Zwanzig, 1990; Zwanzig and Szabo, 1991]. Consider a sphere of radius R randomly covered with N non overlapping disks of radius $a \ll R$. Let be $\mathscr{C}(\mathbf{r}, t)$ the ligands concentration at spatial position $\mathbf{r}$ and time t; it satisfies the diffusion equation

$$\frac{\partial \mathscr{C}(\mathbf{r}, t)}{\partial t} = D_0 \boldsymbol{\nabla}^2 \mathscr{C}(\mathbf{r}, t)$$

where D_0 is the diffusion coefficient.

Initially the ligand concentration is uniform outside the sphere,

$$\mathscr{C}(\mathbf{r}, t) = \mathscr{C}_0, \qquad |\mathbf{r}| > R$$

The BCs are taken such that off the disks the sphere is perfectly reflecting, while the disks, namely the receptors placed on it are partially absorbing, thus giving

$$\begin{aligned} D_0 \hat{\mathbf{n}}(\mathbf{r}) \cdot \boldsymbol{\nabla} \mathscr{C}(\mathbf{r}, t) &= \kappa \mathscr{C}(\mathbf{r}, t) \ , \qquad \text{on the receptors} \\ D_0 \hat{\mathbf{n}}(\mathbf{r}) \cdot \boldsymbol{\nabla} \mathscr{C}(\mathbf{r}, t) &= 0 \ , \qquad \text{off the receptors} \end{aligned}$$

being $\hat{\mathbf{n}}(\mathbf{r})$ the local versor outgoing from the sphere surface and κ the trapping rate of a given receptor. The main problem is to find the total steady–state flux into the receptors, which is given by the surface integral

$$\lim_{t \to \infty} \oint_{\text{Sphere}} dS \ D_0 \hat{\mathbf{n}}(\mathbf{r}) \cdot \boldsymbol{\nabla} \mathscr{C}(\mathbf{r}, t)$$

The effective medium approximation comes into play observing that, rather than searching for the total flux, a possible approximate solution can be found by considering the whole surface of the sphere as a partial absorbing surface, characterized by an effective trapping rate.

The first approximation for κ was found by Berg and Purcell [1977]. They found for the stationary case the expression

$$\kappa_{\text{BP}} = \frac{N \kappa_{\text{disk}}}{4\pi R^2} = \frac{4 D_0}{\pi a} \nu, \qquad \nu = \frac{N a^2}{\pi R^2}$$

with $\kappa_{\text{disk}} = 4 D_0 a$ the stationary rate for a perfectly absorbing disk of radius a located on the otherwise reflecting sphere of radius $R \gg a$[6]. The parameter ν can be interpreted as the trap–covered fraction of the spherical surface and

6 Actually the expression $\kappa_{\text{disk}} = 4 D_0 a$ is the stationary rate for a perfectly absorbing disk placed on a perfectly reflecting plane, however in the limit $a \ll R$, the same result can be used also in the case of a spherical surface, being the sphere locally flat on the length scale a.

$4D_0/\pi a$ is the ratio of κ_{disk} to the disc area. The *BP* result shows a good agreement with the simulated data [Berezhkovskii et al., 2004] only in the limiting case $\nu \ll 1$. Zwanzig [Zwanzig, 1990; Zwanzig and Szabo, 1991] extended the *BP* result to arbitrary surface coverages:

$$\kappa_{\text{Zw}} = \frac{4D_0}{\pi a}\frac{\nu}{1-\nu} = \frac{\kappa_{\text{BP}}}{1-\nu}$$

Generally speaking, from dimensional arguments, it follows that the trapping rate entering the homogenized boundary condition can be written as

$$\kappa = \frac{4D_0}{\pi a}F(\nu) \tag{2.44}$$

where $F(\nu)$ is a dimensionless function.

The function $F(\nu)$ tends to zero as $\nu \to 0$ and to infinity as $\nu \to 1$, since the surface becomes perfectly reflecting and absorbing in these limiting cases. In particular the Berg–Purcell and Zwanzig expressions for κ lead to $F(\nu)$ of the form $F_{\text{BP}}(\nu) = \nu$ and $F_{\text{Zw}}(\nu) = \nu/(1-\nu)$ respectively. While $F_{\text{BP}}(\nu)$ describes only the limiting case $\nu \ll 1$, $F_{\text{Zw}}(\nu)$ captures both of the asymptotes: it reduces to $F_{\text{BP}}(\nu)$ when $\nu \to 0$ and diverges when $\nu \to 1$. However the range of applicability of $F_{\text{Zw}}(\nu)$ is unknown. Berezhkovskii and coworkers showed numerically that $F(\nu)$ grows much faster than it is predicted by $F_{\text{Zw}}(\nu)$[Berezhkovskii et al., 2004] and, in particular, they found that over a wide range of ν, $F(\nu)$ is well approximated by the formula

$$F(\nu) = F_{\text{Zw}}(\nu)(1 + 3.8\nu^{1.25}) \tag{2.45}$$

To find the result in Eq. (2.45) Berezhkovskii et al. [2004] performed Brownian dynamics in planar and spherical geometries, taking $a \ll R$ (which is the condition for the validity of the boundary homogenization). The function $F(\nu)$ is related to the average lifetime $\langle t \rangle$ thanks to the formula

$$\langle t \rangle = \frac{\pi a R}{12 D_0 F(\nu)}$$

This relation was used to determine $F(\nu)$ from $\langle t \rangle$ found in simulations, fitting the simulation results with the formula $F(\nu) = F_{\text{Zw}}(\nu)(1 + A\nu^B)$ with A and B two fit parameters.

The same homogenization procedure was applied by Berezhkovskii et al. [2006] to the case of a reflecting surface covered by disks with $a \ll R$, arranged on a regular lattice. In particular they considered triangular, square and hexagonal lattices of perfectly absorbing disks showing that in this case

$$F(\nu) = \frac{\nu(1 + A\sqrt{\nu} - B\nu^2)}{(1-\nu)^2}$$

with A and B depending on the type of the considered microstructural lattice[Berezhkovskii et al., 2006]. In particular they found that the values for κ for all the trap arrangements are quite close to each other (the difference is within 20%), indicating that the homogenized boundary condition is not too sensitive to the microstructure of the surface. In particular they showed that a reasonable choice for the fit parameters is given by considering $A = 1.37$ and $B = 0.37$.

In the next section we review a possible application of the boundary homogenization procedure to the problem of diffusion within non homogeneous channels.

2.10.1 *Diffusion in a tube of alternating diameter*

In this section we propose an application of the boundary homogenization to the problem of diffusion within a non homogeneous two–dimensional channel, see Fig. 2.4, following the work of Makhnovskiia et al. [2010].

On large time and length scales, the transversal motion saturates, while when $\langle \Delta x_t^2 \rangle \gg L^2$, the longitudinal diffusion process is expected to be standard with

$$\langle \Delta x_t^2 \rangle \approx 2D_{\text{eff}} t, \qquad t \gg D_{\text{eff}}/L^2$$

One of the most interesting problem regarding the diffusion in a periodic channel is related to the effective diffusion coefficient, D_{eff} which is expected to be lower than the microscopic diffusion coefficient D_0, i.e. the diffusion coefficient arising when there are not geometrical constraints acting on the particles motion. The approach of Makhnovskiia et al. [2010] is based on the

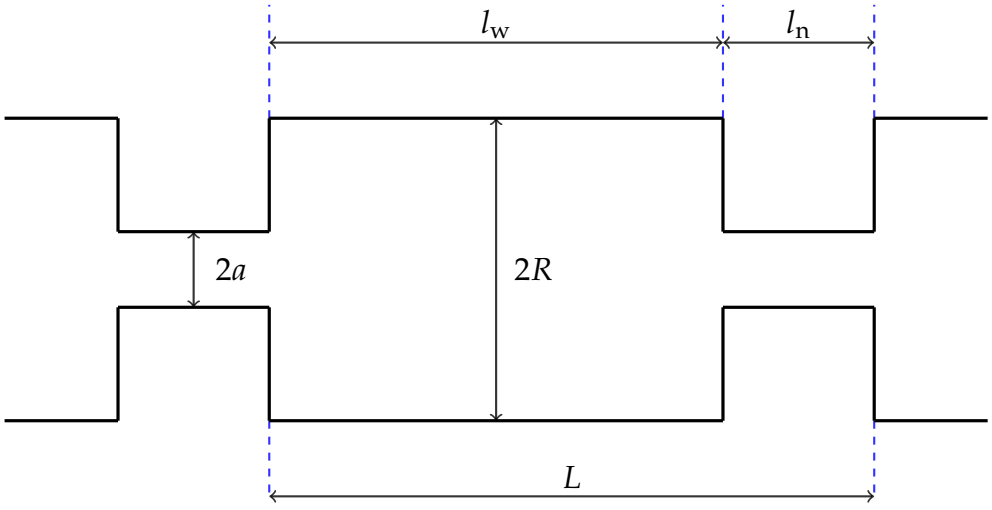

Figure 2.4: A simple periodic non homogeneous channel.

estimation of D_{eff} by means of the formula [Weiss, 1994]

$$D_{\text{eff}} = \frac{L^2}{2\langle t \rangle} \tag{2.46}$$

being $\langle t \rangle$ the mean first–passage time of the particle from an initial cross–section to one of the two neighbouring cross–section separated from the initial on by distance L, with L the spatial period of the structure. The idea is based on the replacement of the original two–dimensional problem with non uniform boundary condition, with a simpler one–dimensional problem with uniform radiation–type boundary condition with a properly chosen trapping rate. In particular Makhnovskiia and coworkers introduce the follow problem, defined in one period of the channel, for the one–dimensional propagator $\mathscr{G}(x,t)$ (see Fig. 2.4):

$$\mathscr{G}(x,t) = \begin{cases} \mathscr{G}_1(x,t), & 0 < x < l_{\text{w}}/2 \\ \mathscr{G}_2(x,t), & l_{\text{w}}/2 < x < l_{\text{n}} + l_{\text{w}}/2 \\ \mathscr{G}_3(x,t), & l_{\text{n}} + l_{\text{w}}/2 < x < L \end{cases}$$

In each of the three intervals, the component of the propagators satisfy

$$\frac{\partial \mathscr{G}_i(x,t)}{\partial t} = D_0 \frac{\partial^2 \mathscr{G}_i(x,t)}{\partial x^2}$$

Moreover they have chosen the initial particle density as

$$\mathscr{G}_1(x,0) = 0, \quad \mathscr{G}_2(x,0) = 0, \quad \mathscr{G}_3(x,0) = \delta(x-L)$$

as well as the absorbing and reflecting boundary conditions at $x = 0$ and $x = L$:

$$\mathscr{G}_1(0,t) = \left.\frac{\partial \mathscr{G}_3(x,t)}{\partial x}\right|_{x=L} = 0$$

The solution at $x = l_{\text{w}}/2$ and $x = l_{\text{n}} + l_{\text{w}}/2$ must be opportunely matched. To this end it is possible to introduce two trapping rates, κ_{w} and κ_n. The former, κ_{w}, describes transitions of the particle from wide sections to the narrow one of the channel, whereas, κ_{n} describes the particles transition in the opposite direction. The matching conditions have the form [Makhnovskiia et al., 2010]

$$\begin{aligned} D_0 \left.\frac{\partial \mathscr{G}_1}{\partial x}\right|_{x=l_{\text{w}}/2} &= D_0 \left.\frac{\partial \mathscr{G}_2}{\partial x}\right|_{x=l_{\text{w}}/2} \\ &= \left.\left(\kappa_{\text{n}} \mathscr{G}_2 - \kappa_{\text{w}} \mathscr{G}_1\right)\right|_{x=l_{\text{w}}/2} \\ D_0 \left.\frac{\partial \mathscr{G}_2}{\partial x}\right|_{x=l_{\text{n}}+l_{\text{w}}/2} &= D_0 \left.\frac{\partial \mathscr{G}_3}{\partial x}\right|_{x=l_{\text{n}}+l_{\text{w}}/2} = \\ &= \left.\left(\kappa_3 \mathscr{G}_3 - \kappa_{\text{n}} \mathscr{G}_2\right)\right|_{x=l_{\text{n}}+l_{\text{w}}/2} \end{aligned}$$

The two trapping rates κ_w and κ_n are not independent. They are related by the relationship

$$\kappa_w R^2 = \kappa_n a^2 \tag{2.47}$$

which follows from the requirement of no net fluxes at equilibrium (i.e. by requiring detailed balance).

One of the usual technique to find the mean first–passage time $\langle t \rangle$ is related to the survival probability, defined by

$$S(t) = \int_0^L dx\, \mathscr{G}(x,t)$$

from which follows the particle lifetime probability density

$$\phi(t) = -\frac{dS(t)}{dt}$$

and finally the mean lifetime of the particle [Weiss, 1994; Gardiner, 2009]

$$\langle t \rangle = \int_0^\infty d\tau\, \tau\phi(\tau)$$

The result of this technical calculation is given by

$$\begin{aligned} 2D_0\langle t \rangle = l_n^2 + l_w^2 + 2D_0\left(\frac{l_n}{\kappa_n} + \frac{l_w}{\kappa_w}\right) \\ + l_n l_w\left(\frac{\kappa_w}{\kappa_n} + \frac{\kappa_n}{\kappa_w}\right) \end{aligned} \tag{2.48}$$

To express the last formula in terms of the geometrical parameters of the channel, in agreement with the boundary homogenization discussed in the previous section, Makhnovskiia et al. [2010] assume that the trapping rates can be expressed as functions of the ratio $\nu = a/R$. In particular the "narrow" transition rate, κ_n, can be taken as in Eq. (2.44):

$$\kappa_n = \frac{4D_0}{\pi a} f(\nu)$$

and, thanks to the detailed balance condition expressed in Eq. (2.47)

$$\kappa_w = \frac{4D_0 a}{\pi R^2} f(\nu)$$

Introducing the last expression of the rates κ_n and κ_w in the equation Eq. (2.46) and using the result in Eq. (2.48) it is possible to find the general formula of the tortuosity, i.e. the ratio between D_0 and D_{eff}:

$$\frac{D_0}{D_{\text{eff}}} = 1 + \frac{l_n l_w}{(l_n + l_w)^2}\left(\frac{R}{a} - \frac{a}{R}\right)^2 + \frac{\pi(a^2 l_n + R^2 l_w)}{2f(\nu)a(l_n + l_w)^2}$$

thus measuring the effective diffusion coefficient it is possible to model $f(\nu)$ exactly as in the previous section and so to infer the effective diffusion coefficient in all the similar cases.

3

THE REALM OF RANDOM WALK AND DIFFUSION

"The diffusion or spontaneous intermixture of two gases in contact, is effected by an interchange in position of indefinitely minute volumes of the gases, which volumes are not necessarily of equal magnitude, being, in the case of each gas, inversely proportional to the square root of the density of that gas"

Graham [1833]

In this chapter we present a review of the main concepts related to the random walk theory and the connections between random walk and diffusion.

The crucial role of the Central Limit Theorem [Feller, 1968; Fisher, 2010] is pointed out, emphasizing the motivations which explain why the Gaussian probability density must be considered as the standard one which describes a diffusive process. However, despite the reasonability of the hypothesis of the CLT (Central Limit Theorem), it is possible to observe and describe anomalous diffusive processes [Metzler and Klafter, 2000; Klages et al., 2008], that is, processes characterized by $\langle x^2 \rangle \sim t^{2\nu}$ ($2\nu \neq 1$), related obviously to the violations of the CLT assumptions.

3.1 THE RANDOM WALK MODEL FOR DIFFUSION

A simple microscopic model which describes the diffusion process can be obtained by assuming that the colloidal particles undergo random displacements as a result of the scattering with the microscopic particles composing the underlying fluctuating environment. More specifically, to every finite time step δt is associated a random displacement $\Delta\mathbf{s}$, sampled from a given probability density $\mathscr{P}(\Delta\mathbf{s})$ [1]. Under these assumptions, a particle which starts from

1 There are not physical reasons to take a constant jump frequency. A more realistic model can be constructed by considering δt as a random variable, drawn from a given probability density. We briefly discuss this point in Sec. 3.6.1

$\mathbf{r}(t_0) \equiv \mathbf{r}_0$ at some reference instant of observation t_0, after N steps, that is at time $t = N\delta t$, will be at the space point $\mathbf{r}(t)$ given by

$$\mathbf{r}(t) - \mathbf{r}(t_0) = \sum_{i=1}^{N} \Delta \mathbf{s}_i \tag{3.1}$$

Given Eq. (3.1), the general problem is to find the probability density $\mathscr{P}(\mathbf{r}, t \mid \mathbf{r}_0, t_0) \equiv \mathscr{P}(\mathbf{r}, t)$, namely the probability to find a particle in a volume element $d\mathbf{r}$ around $\mathbf{r}$ at time t, starting from $\mathbf{r}_0$ at time t_0; clearly if the random displacements are discrete random variables, then we have to talk about probability distribution rather than probability density, however here we do not stress this type of distinction, we assume that it will be clear by the context.

The Eq. (3.1) introduces a microscopic point of view on the Brownian motion; the final position of a particle is obtained by summing up a series of independent and identically distributed random variables, for this reason the particle motion is called random walk [Smoluchowski, 1906; Chandrasekhar, 1943; Weiss, 1994].

3.2 THE ROLE OF THE CENTRAL LIMIT THEOREM

The random walk model introduced in the last section provides a microscopic point of view on diffusion. Generally speaking, the problem is reduced to find the probability density of a sum of random variables. More specifically, consider the case of independent and identically distributed random variables $X_1, X_2, \cdots, X_N$, each one sampled from a probability density $\mathscr{P}(X)$. In addition, we assume that the ensemble average $\mu = \langle X \rangle$ and the standard deviation $\sigma = \sqrt{\langle X^2 \rangle - \langle X \rangle^2}$ are both finite; under these hypothesis the CLT asserts that the random variable

$$Z_N = \frac{1}{\sigma\sqrt{N}} \sum_{s=1}^{N} \Big(X_s - \mu \Big),$$

in the limit $N \to \infty$, will be distributed as [Bouchaud and Georges, 1990; Prokhorov and Statulevičius, 1991; Adams, 2009; Fisher, 2010; Boffetta and Vulpiani, 2012]

$$\mathscr{P}(Z_N) = \frac{1}{\sqrt{2\pi}} \exp\left(-\frac{Z_N^2}{2} \right) \tag{3.2}$$

An exhaustively treatment of the CLT is far from the scope of this work; here we present just a simple derivation of the above result, considering independent and identically distributed random variables. The CLT however can be generalized to case of "weakly" dependent random variables [Bouchaud and Georges, 1990; Boffetta and Vulpiani, 2012] and/or to those

variables which are not identically distributed, i.e. $X_i \sim \mathscr{P}(X_i)$ with, as before $|\mu_i|, \sigma_i < +\infty$ [Prokhorov and Statulevičius, 1991; Fisher, 2010; Boffetta and Vulpiani, 2012];

To prove Eq. (3.2) we consider without loss of generality that $\mu = 0$, that is, instead of $X_1, \cdots, X_N$ we take simply $\tilde{X}_1, \cdots, \tilde{X}_N$ with $\tilde{X} = X - \mu$; for the case of discrete random variables, just to fix the ideas, suppose $\tilde{X}_k = k/m$ with $k = -m, \cdots, m$ $(m \in \mathbb{Z})$, each one with probability p_k; thus the sum $\tilde{Z} = \sum_l^N \tilde{X}_l$ can take values j/m $(-Nm \leq j \leq Nm)$, each one with probability $\mathcal{P}_j$.

We introduce the characteristic functions

$$\begin{aligned} \phi_{\tilde{X}}(\tilde{x}) &= \sum_{k=-m}^{m} p_k \, \mathrm{e}^{ik\tilde{x}} \\ \phi_{\tilde{Z}}(\tilde{z}) &= \sum_{s=-Nm}^{Nm} \mathcal{P}_s \, \mathrm{e}^{is\tilde{z}} \end{aligned} \tag{3.3}$$

moreover observe that, due to the independence of the variables $\tilde{X}$ we have $\phi_{\tilde{Z}}(\tilde{z}) = \left[\phi_{\tilde{X}}(\tilde{x})\right]^N$; in particular, using the identity

$$\frac{1}{2\pi} \int_{-\pi}^{\pi} d\tilde{x} \, \mathrm{e}^{-ik\tilde{x}} \, \mathrm{e}^{ik'\tilde{x}} = \delta_{kk'}, \quad (k, k' \in \mathbb{Z})$$

we can write $\mathcal{P}_j$ as

$$\begin{aligned} \mathcal{P}_j &= \frac{1}{2\pi} \int_{-\pi}^{\pi} d\tilde{x} \, \mathrm{e}^{-ij\tilde{x}} \phi_{\tilde{Z}}(\tilde{z}) = \frac{1}{2\pi} \int_{-\pi}^{\pi} d\tilde{x} \, \mathrm{e}^{-ij\tilde{x}} \left[\sum_{k=-m}^{m} p_k \, \mathrm{e}^{ik\tilde{x}} \right]^N \\ &= \frac{1}{2\pi} \int_{-\pi}^{\pi} d\tilde{x} \, \mathrm{e}^{-ij\tilde{x}} \left[\sum_{k=-m}^{m} p_k \left(1 + ik\tilde{x} - \frac{k^2 x^2}{2} - \frac{ik^3 \tilde{x}^3}{6} + \cdots \right) \right]^N \end{aligned}$$

Using the fact that $\mu = \sum_k p_k m^{-1} k = 0$ and $m^2\sigma^2 = \sum_k p_k k^2$ we obtain

$$\mathcal{P}_j = \frac{1}{2\pi} \int_{-\pi}^{\pi} d\tilde{x} \, \mathrm{e}^{-ij\tilde{x}} \left[1 - \frac{m^2\sigma^2\tilde{x}^2}{2} - iB\tilde{x}^3 + \cdots \right]^N$$

with B a constant depending on the the sum $\sum_k p_k k^3$. Observe that in the last expression we used the hypothesis on the first two moments. We will see immediately that the higher order moments (i.e. all the details of the distribution $\mathscr{P}(\tilde{X})$) do not affect the final result. To this end we introduce the quantity

$$\ln \left\{ \left[1 - \frac{m^2\sigma^2\tilde{x}^2}{2} - iB\tilde{x}^3 + \cdots \right]^N \right\} \approx -\frac{m^2 N\sigma^2\tilde{x}^2}{2} - iBN\tilde{x}^3 + \cdots$$

thus

$$\left[1-\frac{m^2\sigma^2\tilde{x}^2}{2}-iB\tilde{x}^3+\cdots\right]^N \approx \mathrm{e}^{-\frac{Nm^2\sigma^2\tilde{x}^2}{2}}\left(1-iB\tilde{x}^3+\cdots\right)$$

Taking the transformation $\tilde{x}=y/\sqrt{N}$ we get the final result

$$\mathcal{P}_j=\frac{1}{2\pi\sqrt{N}}\int_{-\pi\sqrt{N}}^{\pi\sqrt{N}}dy\,\mathrm{e}^{-i\frac{j}{\sqrt{N}}y}\,\mathrm{e}^{-\frac{m^2\sigma^2y^2}{2}}\left(1-\frac{iBy^3}{\sqrt{N}}+\cdots\right)$$

For an approximation with a "very large" N we ignore all the series terms with a power of N in the denominator, and at the same time, set the limits of integration equal to $\pm\infty$. In this way we obtain the asymptotic formula

$$\mathcal{P}_j\approx\frac{1}{m\sigma\sqrt{2\pi N}}\exp\left(-\frac{j^2}{2m^2\sigma^2N}\right) \tag{3.4}$$

which is nothing that Eq. (3.2) for the variable $\tilde{Z}=\sum_l\tilde{X}_l$.

The continuum case can be heuristically obtained by summing up Eq. (3.4) on $j\in[mx_1\sqrt{N},mx_2\sqrt{N}]$ with x_1 and x_2 two real numbers and taking $dx\approx 1/\sqrt{N}$:

$$\begin{aligned}\mathscr{P}(x_1\sqrt{N}\le\tilde{Z}\le x_2\sqrt{N})\approx&\sum_j\frac{1}{m\sigma\sqrt{2\pi N}}\exp\left(-\frac{j^2}{2m^2\sigma^2N}\right)\\ \approx&\int_{mx_1}^{mx_2}dx\frac{1}{m\sigma\sqrt{2\pi}}\exp\left(-\frac{x^2}{2m^2\sigma^2}\right)\\ =&\frac{1}{\sigma\sqrt{2\pi}}\int_{x_1}^{x_2}dx\,\mathrm{e}^{-x^2/2\sigma^2}\end{aligned}$$

The importance of the CLT requires further observations:

- the standard Gaussian behaviour for the renormalized random variable Z_N is an asymptotic formula; it is valid only in the limit $N\to\infty$. Practically N is a fixed "great" number, however CLT does not say anything about how much must be large N in order to consider the system in the asymptotic regime. This means that before the cross–over between the asymptotic regime and the pre–asymptotic one, there are no reasons to expect a standard Gaussian behaviour;

- CLT does not specify what is the shape of the tails of the probability density. Indeed it was derived by assuming only that $|\mu|,\sigma<+\infty$, however this assumption neglects the higher order moments, which give contribution to the tails of the probability density. For this reason the Gaussian behaviour is expected only within the scale region, associated to the typical values of Z_N.

- Outside the scale region, CLT does not grant anything and the standard scenario can fail.

- A formal way to characterize the "attraction basin" of the Gaussian probability density as a result of the sum of a large number of independent random variables is given by the Khintchine, Feller, Lévy theorem which we state here without proof [Feller, 1945; Bouchaud and Georges, 1990].

  Consider N independent and identically distributed random variables $X_1, \cdots, X_N$, each one sampled from a probability density $\mathscr{P}(X)$. If the random variable

  $$S_N = \sum_{s=1}^{N} X_s,$$

  opportunely renormalized, is distributed according to a standard Gaussian distribution, we will say that $\mathscr{P}(X)$ belongs to the attraction basin of the normal law.

  The Khintchine, Feller, Lévy theorem states that $\mathscr{P}(X)$ belongs to the attraction basin of the normal law if and only if

  $$\lim_{X\to\infty} X^2 \frac{\int_{|x|>X} dx\ \mathscr{P}(x)}{\int_{|x|>X} dx\ x^2 \mathscr{P}(x)} = 0$$

  The above theorem is more powerful than the CLT. For example on large scale ($X \to \infty$) the density $\mathscr{P}(X) \sim X^{-3}$ belongs to the attraction basin of the normal law also if the variance is infinite.

- It is interesting to observe that the modern technologies enable scientists to perform experiments also at mesoscale ($\sim 10^{-6}$ m), characterized by a small number of particles (also 10 molecules per micrometer), depending on the details of the systems considered. Such "middle way" has attracted in the last years an increasing interest by the scientific community. Various experiments can be performed, ranging from the emergent organized behaviour (crystallinity, ferromagnetism, superconductivity, etc.) [Laughlin et al., 2000], diffusion–driven island growth on nano–structures [Sachs et al., 2001], up to the measurement of the instantaneous velocity of Brownian particles [Li et al., 2010; Huang et al., 2011; Franosch et al., 2011]. From a theoretical point of view, such problems constitute the test–bed for modeling and computational approaches where the thermodynamic limit or the CLT, in principle, cannot be invoked as applicable. However it is really astonishing the fact that also at mesoscale, effective "macroscopic" theories can be used, once the constrained geometry of the environment is taken into account. When the number of particles becomes really small (1 molecules per micrometer), quantum effects, like the size quantization [Inn, 2004], can emerge, however we will not discuss here similar situations.

3.3 CONNECTION WITH THE LANGEVIN EQUATION

The random walk model embodies the notion of stochastic evolution. Indeed the time evolution of a single particle trajectory can be thought as a recurrence scheme of the form [Gardiner, 1985; Hald, 1987; Kloeden and Platen, 1995]

$$x_{t+\delta t} = x_t + \Delta W_t$$

$\Delta W_t \equiv W_{t+\delta t} - W_t$ being an opportune stochastic process [Chorin and Hald, 2009; Gardiner, 2009] which plays the role of the random displacement. Now if we think to a random walker as a colloidal particle within a fluctuating environment, during the time step δt, the walker experiences a great number of collisions with the surrounding environment because the time scales separation between the colloidal particle motion and the heavy particles composing the thermal bath, as we pointed out in Sec. 2.1; thus, the stochastic noise ΔW_t can be considered as the sum of a large number of random variables during the time interval δt. Assuming that the CLT hypothesis hold true, the process W_t can be reasonably characterized by the following proprieties [Chorin and Hald, 2009]:

- $W_0 = 0$, which means that we know exactly the initial condition;
- W_t is a continuous function of the time t, i.e. the displacement links two space points in a continuous way;
- for each $s < t$, $W_t - W_s$ is a Gaussian variable with zero mean and variance $t - s$; this property follows from the CLT thesis;
- W_t has independent increments, namely if $t_1 < t_2 < \cdots < t_n$, then

  $$W_{t_2} - W_{t_1}, \quad W_{t_3} - W_{t_2}, \quad \cdots, \quad W_{t_n} - W_{t_{n-1}}$$

  are independent random variables; this property follows from the CLT hypothesis.

The process W_t is called Wiener process [Wiener, 1958]; from its definition follows immediately that

i) $\langle W_t W_{t'} \rangle = \min\{t, t'\}$;

ii) the random variable ξ_t defined by

$$\xi_t = \frac{W_{t+\delta t} - W_t}{\delta t}$$

is distributed according to a Gaussian with zero mean and standard deviation δt^{-1}, which tends to infinity as δt goes to zero. So we can guess that W_t is nowhere differentiable in the usual sense with probability one.

iii) the derivative ξ_t of the Wiener process is called white noise and it is defined in the distributional sense by the relation

$$\int_{t_1}^{t_2} ds\ \xi_s = W_{t_2} - W_{t_1} \quad \langle \xi_t \xi_{t'} \rangle = \delta(t - t')$$

Keeping in mind the remarks about the derivative of the Wiener process, the random walk process in the limit $\delta t \to 0$ can be represented by the formal equation

$$\frac{dx}{dt} = \xi_t$$

which is the overdamped Langevin equation in the case of a vanishing external field.

To conclude the review on the realm of random walk and diffusion we discuss in the next section how it is possible to find the Fokker–Planck equation related to a stochastic dynamics described by a Langevin–like evolution equation, finally we will pass to describe the anomalous transport.

3.4 FROM THE LANGEVIN EQUATION TO THE FOKKER–PLANCK EQUATION

Consider the overdamped Langevin equation in the form

$$\frac{du}{dt} = -\gamma u + \frac{dW}{dt} \tag{3.5}$$

where $W(t)$ is the Wiener process introduced in the last section and γ is a fixed constant.

The correct way to understand the Langevin equation is by looking at the finite increments of the Eq. (3.5); for example integrating from $n\delta t$ to $(n+1)\delta t$, where δt is the time step and $n \in \mathbb{N}$, we find[2]

$$u_{n+1} - u_n = -\gamma \delta t u_n + W_{n+1} - W_n \tag{3.6}$$

Starting from the Langevin equation, which describes the time evolution of a single trajectory, it makes sense to define the follow problem. Consider the Wiener process W_t and define the function $\mathscr{K}(x,t)$ as the probability density that at a fixed time t, W_t is within a small element dx around x, namely

$$\mathscr{K}(x,t)dx = P(x \leq W_t \leq x + dx)$$

2 There are two common choice in approximating stochastic integrals [Chorin and Hald, 2009]. In particular in this work we refer always to the Itô prescription [Itô and McKean, 1974] , for more details we refer the reader to the literature [Gardiner, 1985, 2009; Chorin and Hald, 2009].

Our main interest is to find the evolution equation for the probability density $\mathscr{K}(x,t)$, which we assume continuous and once differentiable; such an evolution equation is called Fokker–Planck [Risken, 1989] equation associated to the Eq. (3.6). Generally speaking, to any given stochastic differential equation, is associated a Fokker–Planck equation which can be find, in principle, using the following technique[3].

Using the fact that the Wiener process is characterized by independent increments, we can write the equation (Chapman–Kolmogorov equation, see [Chorin and Hald, 2009])

$$\mathscr{K}(x,t+\delta t) = \int_{-\infty}^{+\infty} dy\ \mathscr{K}(x+y,t)\psi(x,t+\delta t \mid x+y,t) \tag{3.7}$$

The last equation states that the probability to reach the point x at time $t+\delta t$ is the sum of the probabilities to be at the point $x+y$ at time t multiplied by the probabilities to effectuate a transition from $x+y$ at time t to x, during the time interval δt.

From the Eq. (3.6) we know that, if W_t is the Wiener process, then the variable $u_{n+1} - u_n + \gamma u_n \delta t$ will be characterized by a Gaussian probability density; indeed by definition $W_{n+1} - W_n$ is sampled from a Gaussian density. Moreover $W_{n+1} - W_n$ is related exactly to the transitional kernel, namely to the probability density to find u_{n+1} in a small volume element dx around x at time $(n+1)\delta t$, given that at time $n\delta t$ the particle was in a small volume element around $x+y$, thus the transitional kernel for the present case is given by

$$\begin{aligned}\psi(x,t+\delta t \mid x+y,t) = & \\ & \frac{1}{\sqrt{2\pi\delta t}} \exp\left\{-\frac{\left[x-(x+y)+\gamma(x+y)\delta t\right]^2}{2\delta t}\right\} \\ =& \frac{1}{\sqrt{2\pi\delta t}} \exp\left\{-\frac{\left[(1-\gamma y\delta t)-\gamma x\delta t\right]^2}{2\delta t}\right\}\end{aligned} \tag{3.8}$$

Inserting Eq. (3.8) in the Chapman–Kolmogorov equation (3.7) we get

$$\mathscr{K}(x,t+\delta t) = \int_{-\infty}^{+\infty} dy\ \mathscr{K}(x+y,t) \frac{\exp\left\{-\frac{\left[(1-\gamma y\delta t)-\gamma x\delta t\right]^2}{2\delta t}\right\}}{\sqrt{2\pi\delta t}} \tag{3.9}$$

At this point we expand $\mathscr{K}(x+y,t)$ in y; up to the fourth order we have

$$\begin{aligned}\mathscr{K}(x+y,t) =& \mathscr{K}(x,t) + y\mathscr{K}_x(x,t) + \frac{y^2}{2}\mathscr{K}_{xx}(x,t) \\ &+ \frac{y^3}{6}\mathscr{K}_{xxx}(x,t) + \mathrm{O}(y^4)\end{aligned} \tag{3.10}$$

3 A more general technique is the so called Kramers–Moyal expansion, for a discussion see for example Risken [1989]

The next step is to substitute Eq. (3.10) into Eq. (3.9) and evaluate the integral on the right hand side. The technical details of the calculation can be found in Chorin and Hald [2009]. Here we give the final result

$$\frac{\mathscr{K}(x,t+\delta t)-\mathscr{K}(x,t)}{\delta t}=\mathscr{K}(x,t)\gamma+\mathscr{K}_x(x,t)\gamma x+\frac{1}{2}\mathscr{K}_{xx}(x,t)+\mathrm{O}(\delta t)$$

which, after letting $\delta t \to 0$, becomes

$$\frac{\partial \mathscr{K}(x,t)}{\partial t}=\frac{\partial}{\partial x}\Big[\gamma x\mathscr{K}(x,t)\Big]+\frac{1}{2}\frac{\partial^2\mathscr{K}(x,t)}{\partial x^2} \tag{3.11}$$

The Eq. (3.11) is the Fokker–Planck equation associated to the stochastic dynamics described by the Eq. (3.5).

In the same way it is possible to show that the Fokker–Planck equation associated to the most general Langevin equation

$$\frac{dx}{dt}=a(x)+\sqrt{2D(x)}\frac{dW_t}{dt}$$

with $a(x)$ and $D(x)$ differentiable functions of their argument, is given by

$$\frac{\partial \mathscr{K}(x,t)}{\partial t}=-\frac{\partial}{\partial x}\Big[a(x)\mathscr{K}(x,t)\Big]+\frac{1}{2}\frac{\partial^2}{\partial x^2}\Big[D(x)\mathscr{K}(x,t)\Big]$$

which is the diffusion equation discussed in the previous chapters characterized by a (local) diffusion coefficient $D(x)$ and an external force field given by $a(x)$.

The result derived in this section i s strictly based on a regularization procedure, called the Itô regularization. Such assumption has a microscopic interpretation, that is, the transition probability of a given particle is evaluated exclusively on the space point where is the particle before its transition. Obviously, other types of regularization procedure are allowed. Choosing between these different procedures depends on the details of the microscopic dynamics of the system under consideration, especially those properties related to the time correlations at short times.

One of the most common choice, different from the Itô prescription described in this section, is the so called Stratonovich regularization, that is, the stochastic integrals are evaluated at the middle point between the time step $n\delta t$ and $(n+1)\delta t$. The Stratonovich regularization leads to the "Langevin" equation [Gardiner, 2009]

$$\frac{dx}{dt}=a(x)+\sqrt{D(x)}\frac{\partial\sqrt{D(x)}}{\partial x}+\sqrt{2D(x)}\frac{dW_t}{dt}$$

which is different from the standard Langevin equation discussed up to now. More specifically, the second term in the last equation is the so called *drift induced by the noise*.

3.5 FIRST PASSAGE PROBLEMS

The First Passage Time Density (FPTD) $f(t)$ is the probability that a particle has first reached a point x_c at time t. The usual way to obtain the FPTD is based on the survival probability, defined by

$$S(t) = \int_0^{x_c} dx \; \mathscr{P}(x, t \mid x_0, 0)$$

which is the probability that a particle is still at a position $x < x_c$ at time t, related to $f(t)$ by the relation

$$f(t) = -\frac{\partial S(t)}{\partial t}$$

Using, for example, the method of images borrowed from Electrodynamics [Jackson, 1971], the explicit FPTD for a one–dimensional diffusion process takes the form

$$f(t) = \frac{|x_c - x_0|}{\sqrt{4\pi D_0 t^3}} \exp\left(-\frac{(x_c - x_0)^2}{4D_0 t}\right) \xrightarrow[t\to+\infty]{} \sim t^{-3/2}$$

This equation states that the probability for a Brownian particle achieving a first passage at some long time becomes increasingly small, but always finite. The FPTD belongs to the class of the so called heavy–tailed distribution, in particular it is characterized by a diverging first moment, implying that it is not possible to calculate the average FPT. However it is possible to calculate the typical time t^*, which follows from the condition $\partial f(t)/\partial t = 0$:

$$t^* \sim (x_c - x_0)^2$$

The simple treatment given above can be generalized to higher space dimensions. Let be $\Omega \subseteq \mathbb{R}^d$ the available state space of a d–dimensional unbiased diffusive process described by the model

$$\frac{\partial}{\partial t}\mathscr{P}(\mathbf{x}, t) + \sum_{i=1}^{d} \frac{\partial J_i(\mathbf{x}, t)}{\partial x_i} = 0$$

$$\mathbf{J}(\mathbf{x}, t) + D_0 \sum_{i=1}^{d} \frac{\partial \mathscr{P}(\mathbf{x}, t)}{\partial x_i}\hat{\mathbf{x}}_i = 0$$

If we assume the independence of the motion along the different coordinates, the joint probability density $\mathscr{P}(\mathbf{x}, t)$ will be given by,

$$\mathscr{P}(\mathbf{x}, t) = \prod_{k=1}^{d} \mathscr{P}_{\chi_k}(x_k, t)$$

and consequently the fundamental solution of a d–dimensional diffusion process can be written as

$$\mathscr{P}(\mathbf{x}, t|\mathbf{x}_0, 0) = \frac{1}{(4\pi D_0 t)^{d/2}} \exp\left[-\frac{(\mathbf{x}-\mathbf{x}_0)^2}{2D_0 t}\right]$$

being $\mathbf{x}_0 \in \mathcal{V}_d$, with $\mathcal{V}_d \subseteq \Omega$.

The mean FPT $\langle T \rangle$ within the region $\mathcal{V}_d$ can be evaluated as [Gardiner, 2009]

$$\langle T \rangle = \int_0^{+\infty} dt \int_{\mathcal{V}_d} d^d x \mathscr{P}(\mathbf{x}, t|\mathbf{x}_0, 0) = \int_0^{+\infty} dt\ S(t)$$

We assume, for simplicity, that $\mathcal{V}_d$ is a spherical region with radius ε and $\mathscr{P}(\mathbf{x}, 0) = \delta(\mathbf{x}-\mathbf{x}_0)$. When $t \ll \varepsilon^2/2D_0$, the above integration over the volume $\mathcal{V}_d$ is well approximated by 1, indeed in this case almost all the particles started in $\mathbf{x}_0$ are still in the region $\mathcal{V}_d$ and so the time integration gives a contribution of the order $t_\varepsilon = \varepsilon^2/2D_0$. On the other hand, when $t \gg t_\varepsilon$, the contribution to the mean FPT will be given by those walkers that, after an excursion out of the sphere $\mathcal{V}_d$, come back near the starting point $\mathbf{x}_0$. In this case the exponential in the probability density $\mathscr{P}(\mathbf{x}, t \mid \mathbf{x}_0, 0)$ is approximately 1, thus

$$\mathscr{P}(\mathbf{x}, t|\mathbf{x}_0, 0) \approx \frac{1}{(4\pi D_0 t)^{d/2}}$$

and the integral over the space region $\mathcal{V}_d$ gives $\varepsilon^d \Gamma_d$, with Γ_d the volume of the d–dimensional hyper–sphere of radius 1. Thus we have

$$\langle T \rangle \approx t_\varepsilon + \frac{\Gamma_d \varepsilon^d}{(4\pi D_0)^{d/2}} \int_{t_\varepsilon}^{+\infty} dt\ t^{-d/2}$$

The latter integral diverges for $d \leq 2$ (as we just saw above for the case $d = 1$), that is, the mean time spent by a particle near its starting point is infinitely high: in one and two dimension the Brownian motion is recurrent. When $d > 2$ the integral converges and the mean time spent by a walker around $\mathbf{x}_0$ goes to zero when $\varepsilon \to 0$, implying that in dimension higher than 2, Brownian motion is not recurrent [Redner, 2001] (see also Chap. 4 for a deeper discussion and examples on this point). The dimension $d = 2$ presents a logarithmic divergence and separates recurrent walks by not recurrent ones.

A classical and interesting result is related to the FPT probability to the origin for a one–dimensional random walk on a line of length $L \gg 0$, considering as initial condition all the particles starting from the origin. If we consider the case of unitary length and time steps, the first return probability decays as $t^{-3/2}$ for $t \ll L^2$ and as e^{-t/L^2} thereafter [Redner, 2001], thus giving

$$\langle T \rangle \sim \int_0^{\infty} dt\ t \times t^{-3/2}\, \mathrm{e}^{-t/L^2} \sim \int_0^{L^2} dt\ \times t^{-1/2} \sim L$$

Another relevant example, useful to treat the case of the intracellular transport, concerns the mean FPT related to the escape problem of a free diffusing molecule from a two or three dimensional bounded domain trough small absorbing windows on the otherwise reflecting boundary, see for example Holcman and Schuss [2004]; Shuss et al. [2007]; Holcman and Schuss [2011]; Bressloff and Newby [2013].

3.6 BEYOND CLT: ANOMALOUS TRANSPORT

We already saw that the remarkable property of a diffusion process is given by the linear growth with the time of the second order moment, that is

$$\langle x^2 \rangle \sim t$$

It is natural to wonder if there can be physical situations where the CLT hypothesis do not hold true, thus implying an anomalous transport, i.e. a transport mechanism which is different by the expected one, with

$$\langle x^2 \rangle \sim t^{2\nu}$$

Anomalous transport is a well established phenomenon, both from theoretical [Gefen et al., 1983; Bouchaud and Georges, 1990; Shlesinger et al., 1993; Klafter et al., 1996; Metzler and Klafter, 2000; ben Avraham and Havlin, 2000; Havlin and ben Avraham, 2002] and experimental [Solomon et al., 1993; Schütz et al., 1997; Wong et al., 2004; Barthelemy et al., 2008; Santamaria et al., 2006] point of view, the exponent ν is called anomalous exponent; in particular when $\nu < 1/2$ we speak of subdiffusion, whereas the case with $\nu > 1/2$ is referred to as superdiffusion. Actually, nowadays "*The evidence for natural phenomena exhibiting anomalous diffusion with* $2\nu \neq 1$ *has grown so compelling as to prompt punchlines such as "anomalous is normal" "* [Marchesoni and Taloni, 2006]

In order to get an anomalous behaviour, the CLT assumptions (see Se. 3.2) must be violated. The implications of such violations are discussed in the next sections.

3.6.1 *The continuous time random walk model*

The continuous time random walk model (CTRW) is a natural extension of the simple random walk introduced in the last sections [Montroll and Weiss, 1965; Kenkre et al., 1973; Klafter and Silbey, 1980; Barkai et al., 2000]. In particular it is based on the idea that the length of a given jump as well as the elapsed time between two successive jumps are both random variables, sampled from a probability density $\phi(\delta x, \delta t)$.

As a simple example, consider a one–dimensional discrete states random walk. Moreover, suppose that δt is a random variable sampled from a certain

distribution $\psi(\delta t)$; at the same way δx is drawn independently from a distribution $\lambda(\delta x)$, whose first two moments are both finite. In addition, suppose that, up to the time t, a walker has performed N steps.

In the long time limit ($N \to \infty$), applying CLT, we have that the sum of N independent displacements behaves as

$$\langle X^2 \rangle \approx N \langle \delta x^2 \rangle$$

with

$$\langle \delta x^2 \rangle = \int d\xi \xi^2 \lambda(\xi)$$

Now the elapsed time is itself given by a sum of independent random variables

$$t = \sum_{i=0}^{N} \delta t_i$$

and we must distinguish two different cases:

- $\langle \delta t \rangle = +\infty$, for example $\psi(\delta t) \sim \delta t^{1+\mu}$. In this case CLT does not apply to the time–like random variable. To estimate the elapsed time t, we ask for the largest term $t_m(N)$ in the above sum. It will be occurred at least once up to time t, namely

  $$\int_{t_m(N)}^{\infty} d\tau \psi(\tau) \approx \frac{1}{N}$$

  from which we get

  $$t \approx t_m \sim N^{1/\mu}$$

  that is

  $$\langle X^2 \rangle \approx N \langle \delta x^2 \rangle \sim \begin{cases} t^{\mu} & 0 < \mu < 1 \\ t / \ln t & \mu = 1 \end{cases}$$

- $\langle \delta t \rangle < +\infty$. In this case CLT applies and we have $t = \sum_s \delta t_s \approx N \nu_t$ and so the mean square displacement behaves as

  $$\langle X^2 \rangle \approx N \langle \delta_x^2 \rangle = 2 D_{\text{eff}} t$$

  with

  $$D_{\text{eff}} = \frac{\langle \delta x^2 \rangle}{2 \langle \delta t \rangle}$$

  Comparing the last equation with the case of free diffusion in one spatial dimension follows that the asymptotic diffusion is still standard, however with a renormalized diffusion coefficient D_{eff}. Indeed for the free diffusion case we have

  $$D_{\text{eff}} = \frac{\langle \delta x^2 \rangle}{2 \delta t}$$

  Practically taking $\langle \delta t \rangle$ finite, one has only to recast the CTRW with a simple random walk whose jump frequency is given by $\langle \delta t \rangle$.

Another situation can arise when $\langle \delta x \rangle = +\infty$, see for example Klages et al. [2008] for more detailed calculations.

An application of the CTRW described above is provided by the random walk on the comb structure (see Chap. 4). More specifically, the comb lattice (see Fig. 3.1) is composed by a main transport direction, the backbone, on which is arranged an infinite one–dimensional chain and, to every site of this chain, is attached a transversal tooth of length L.

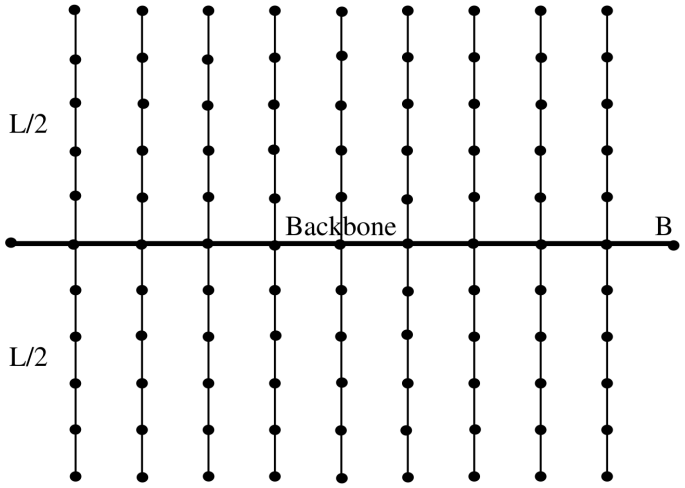

Figure 3.1: *Simple comb–lattice.*

This model was proposed by Goldhirsch and Gefen [1986] as an elementary structure able to describe some properties of transport in disordered networks and can be well adapted to all physical cases where particles diffuse freely along a main direction but can be temporarily trapped by lateral dead–ends.

Despite the simple structure of the comb–lattice, its main features can be applied in nature; an example is provided by the case of diffusion on biological and synthetic polyelectrolytes [Papagiannopoulos et al., 2006; Waigh and Papagiannopoulos, 2010], see Fig. 3.2.

On a comb lattice the longitudinal diffusion is a process determined by the return statistics of the walkers to the backbone. Practically we are observing a CTRW where waiting times δt are the return times to the backbone sites [Weiss and Havlin, 1986; Bouchaud and Georges, 1990; Weiss, 1994; Redner, 2001], see also Sec. 3.5. Thus, on the comb–lattice, the waiting–time distribution $\psi(\delta t)$ coincides with the distribution of first–return time to the backbone sites, which for infinite sidebranches is long tailed and asymptotically decays as $\psi(\delta t) \sim \delta t^{-3/2}$ [Redner, 2001]. We can thus identify the longitudinal motion along the comb–lattice as a CTRW, whose time increments are drawn from a probability density $\psi(\delta t) \sim \delta t^{-(1+\mu)}$ with $\mu = 1/2$. In this

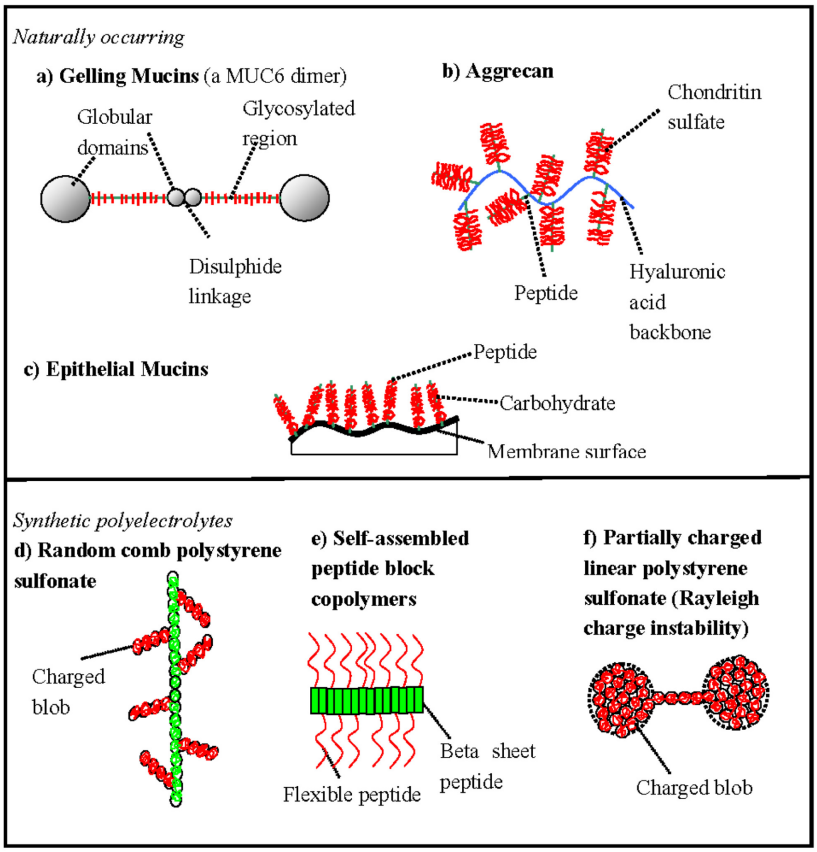

Figure 3.2: *Morphology of some polymers along with their relates polyelectrolyte structure;* ***a)*** *Gelling mucins;****b)*** *proteoglycans, e.g., bovine aggrecan,* ***c)*** *epithelial mucins,* ***d)*** *synthetic flexible comb polyelectrolytes, e.g., polystyrene sulfonate,* ***e)*** *synthetic self–assembled peptide block copolymers;* ***f)*** *synthetic hydrophobic linear polyelectrolytes, e.g., partially charged linear polystyrene sulfonate. Adapted from Waigh and Papagiannopoulos [2010]*

case, as explained above, we expect a mean square displacement of the form $\langle x^2 \rangle \sim t^{-1/2}$[4].

Another example of subdiffusion is strictly related to the effects due to the non vanishing particle size. For example, diffusion of particles in a narrow channel where mutual passage is forbidden, and thus the sequence of particles remains the same over time, is known as single–file diffusion (SFD) [Hahn et al., 1996; Hahn and Kärger, 1996; Mon and Percus, 2003]. As shown by Marchesoni and Taloni [2006], the case of a file of N indistinguishable Brownian particles of unitary mass, moving on a circle of length L in the thermodynamic limit (i.e. $N, L \to \infty$ with N/L a constant), despite the finiteness of the time and space increments, is characterized a subdiffusive behaviour, as a consequence of a persistent anticorrelation of the jump sequences.

4 When $L < +\infty$ this result is valid only for $t \sim L^2$ [Forte et al., 2013a], due to the fact that $\psi(t)$ decays as $t^{-3/2}$ for $t \ll L^2$ and as e^{-t/L^2} thereafter, as we quoted in Sec. 3.5

3.6.2 *Fractional Diffusion*

In this section we briefly review the continuum limit of a CTRW process. We just derived the Fokker–Planck equation related to the simple random walk and to the Langevin equation. It is natural to wonder how we can describe the time and space evolution of the probability density $\mathscr{P}(x,t)$ in the case of a CTRW.

To this end, let us consider the CTRW model whose space and time increments distribution is given by

$$\phi(\delta x, \delta t) = \psi(\delta t)\lambda(\delta x)$$

where the stochastic independence of the increments is a reasonable physical assumption.

The probability $\mathscr{P}(x,t)$ to reach a small volume element dx around x at time t can be written as the contribution of two terms [Metzler and Klafter, 2000]; more specifically, let us introduce the probability

$$\mathcal{P}(\delta t \geq t) = 1 - \int_0^t d\tau\ \psi(\tau) \equiv \Psi(t)$$

which is the probability for a walker to remain somewhere up to the time t. Now we have:

$$\mathscr{P}(x,t) = \int_0^t d\tau\ Q(x,\tau)\Psi(t-\tau) \tag{3.12}$$

The distribution $Q(x,t)$ is called turning points distribution [Zumofen and Klafter, 1993]. Practically it represents the probability distribution associated to those points just reached by a walker, which subsequently starts to move elsewhere from those points. In particular we can expand $Q(x,t)$ essentially by requiring "mass" conservation [Metzler and Klafter, 2000; Klages et al., 2008], that is

$$Q(x,t) = \int_{-\infty}^{+\infty} dz\ \lambda(z) \int_0^t d\tau\ Q(x-z, t-\tau)\psi(\tau) + \delta(x)\delta(t) \tag{3.13}$$

where the second term in the sum represents the initial condition.

Taking the Laplace transform with respect to the time and the Fourier transform with respect to the position of the Eq. (3.13) and Eq. (3.12) we get

$$\begin{aligned} \hat{\tilde{Q}}(k,s) &= \hat{\tilde{Q}}(k,s)\tilde{\psi}(s)\hat{\lambda}(k) + 1 \\ \hat{\tilde{\mathscr{P}}}(k,s) &= \frac{1-\tilde{\psi}(s)}{s}\hat{\tilde{Q}}(k,s) \end{aligned} \tag{3.14}$$

The last equations can be solved explicitly with respect to the probability density $\hat{\tilde{\mathscr{P}}}(k,s)$, whose representation in the Fourier–Laplace space is given

by the so called Weiss–Montroll equation [Montroll and Weiss, 1965; Zumofen and Klafter, 1993; Klafter et al., 1987]

$$\hat{\tilde{\mathscr{P}}}(k,s) = \frac{1-\tilde{\psi}(s)}{s\left[1-\tilde{\psi}(s)\hat{\lambda}(k)\right]} \tag{3.15}$$

The Eq. (3.15) represents the full solution of the CTRW problem under the hypothesis that the space and time increments are stochastically independent and the related model is also known as the waiting model.

Another popular model is the velocity model. Here the space and time increments are not independent, so, generally speaking we have $\phi(\delta x, \delta t) = p(\delta t|\delta x)\lambda(\delta x)$; the velocity model is defined by taking

$$p(\delta t|\delta x) = \delta\left(\delta t - \frac{|\delta x|}{v}\right)$$

with v a fixed constant whose physical dimension is the same as a velocity. We refer the reader to the literature for more detailed calculation on the velocity model [Klages et al., 2008]

In order to specify the random walk problem completely, we need to specify the probability densities $\tilde{\psi}(s)$ and $\hat{\lambda}(k)$. Consider the case characterized by [Metzler and Klafter, 2000]

$$\begin{aligned} \hat{\lambda}(k) &\sim \mathrm{e}^{-a|k|^{\alpha}} \\ \tilde{\psi}(s) &\sim \mathrm{e}^{-bs^{\beta}} \end{aligned} \tag{3.16}$$

On large scales ($k \to 0$) and asymptotically in time ($s \to 0$), we can expand the space and time increments distributions as

$$\hat{\lambda}(k) \approx 1 - a|k|^{\alpha}$$

$$\tilde{\psi}(s) \approx 1 - bs^{\beta}$$

Substituting the last expansions in the Eq. (3.15) we find the asymptotic analytical expression for the probability density in the Fourier–Laplace space, namely

$$\hat{\tilde{\mathscr{P}}}(k,s) = \frac{bs^{\beta-1}}{bs^{\beta} + a|k|^{\alpha}} \tag{3.17}$$

which can we written as

$$s^{\beta}\hat{\tilde{\mathscr{P}}}(k,s) - s^{\beta-1} = -\frac{a}{b}|k|^{\alpha}\hat{\tilde{\mathscr{P}}}(k,s) \tag{3.18}$$

For example, let us take $\beta = 1$ and $\alpha = 2$, moreover recall that one of the Laplace transform properties is given by

$$\frac{d\psi(t)}{dt} \to s\tilde{\psi} - \psi(0)$$

At the same way, when the Fourier transform is applied, we have

$$\frac{d^2\lambda(x)}{dx^2} \to -k^2\hat{\lambda}(k)$$

Thus Eq. (3.18) becomes

$$\frac{\partial \mathscr{P}(x,t)}{\partial t} = \frac{a}{b}\frac{\partial^2 \mathscr{P}(x,t)}{\partial x^2}$$

It is possible to express the ratio a/b in terms of the first moment of the time increments probability density and the second moment of the space increments probability density; indeed, generally speaking, we can write the Taylor expansion

$$\hat{\lambda}(k) \approx 1 - \langle \delta x^2 \rangle k^2 + \cdots$$

$$\tilde{\psi}(s) \approx 1 - \langle \delta t \rangle s + \cdots$$

from which we have $a/b \equiv D_0 = \langle \delta x^2 \rangle / 2\langle \delta t \rangle$ and so

$$\frac{\partial \mathscr{P}(x,t)}{\partial t} = D_0\frac{\partial^2 \mathscr{P}(x,t)}{\partial x^2}$$

and we have obtained another time the standard Fokker–Planck equation which describes diffusive processes on the macroscopic scale.

For general values of the exponents α and β, the associate macroscopic equation is called fractional Fokker–Planck equation [Klages et al., 2008].

A very quick digression on fractional derivatives at this point can be useful in order to better clarify the fractional Fokker–Planck equation

Fractional derivatives

Given any smooth function $f(x)$ and $\alpha \in \mathbb{N}$, it is well defined the n-th order derivative of $f(x)$. Leibnitz, during its studies on differential calculus, just expressed his curiosity about a possible extension of the standard derivative to the case of non integer α.

An exhaustive mathematical treatment of fractional derivative could require an entire book (maybe a collection, see for example Podlubny [1999]; Pramukkul et al. [2013], Chap. one of Klages et al. [2008] or the extended appendix of Baluscu [2006]); moreover several definitions of fractional derivative exist, thus here we just give the definition and some properties of the fractional derivatives we need.

We just discussed the case of standard diffusion when $\alpha = 2$ and $\beta = 1$ of the Eq. (3.18). For other values of α and β the question is to find a definition of "derivative" whose Laplace transform is equivalent to the left hand side of Eq. (3.18).

To this end we introduce the so called Caputo fractional derivative defined by

$$\mathscr{D}_x^\beta f(x) = \frac{1}{\Gamma(n-\beta)} \int_0^x d\bar{x}\, \frac{1}{(x-\bar{x})^{\beta+1-n}} \frac{d^n}{d\bar{x}^n} f(\bar{x}) \tag{3.19}$$

with n an integer such that $n-1 \leq \beta < n$ and $\Gamma(x)$ is the Euler gamma function.

Taking $0 \leq \beta < 1$ and Laplace transforming Eq. (3.19) we find the expression

$$\mathscr{D}_x^\beta f(x) \to s^\beta \tilde{f}(s) - s^{\beta-1} f(0) \tag{3.20}$$

which "sounds good" as a generalization of the the standard rule

$$\frac{df(x)}{dx} \to s\tilde{f}(s) - f(0)$$

It is possible to consider also situation for which $\beta > 1$ however Eq. (3.20) doesn't take a so simple form.

Looking at the right side of the Eq. (3.18), at the same way we done for the left side, we have to introduce some type of operation whose Fourier transform produces $-a/b|k|^\alpha$. For this purpose we introduce the Riemann–Liouville left–fractional derivative

$${}_a\mathcal{D}_x^\alpha f(x) = \frac{1}{\Gamma(n-\alpha)} \frac{d^n}{dx^n} \int_a^x d\bar{x}\, \frac{f(\bar{x})}{(x-\bar{x})^{\alpha+1-n}} \tag{3.21}$$

as well as the Riemann-Liouville right–fractional derivative

$${}_x\mathcal{D}_b^\alpha f(x) = \frac{1}{\Gamma(n-\alpha)} \frac{d^n}{dx^n} \int_x^b d\bar{x}\, \frac{f(\bar{x})}{(\bar{x}-x)^{\alpha+1-n}} \tag{3.22}$$

with a and b two fixed constant and $n-1 \leq \alpha < n$. The fractional derivatives in Eq. (3.21) and (3.22) can be combined to give the so called Riesz fractional derivative:

$$\mathcal{D}_{|x|}^\alpha f(x) = -\frac{1}{2\cos(\pi\alpha/2)} \left({}_{-\infty}\mathcal{D}_x^\alpha + {}_x\mathcal{D}_{+\infty}^\alpha \right) f(x) \tag{3.23}$$

The Riesz fractional derivative has the interesting property that its representation in Fourier space is

$$\mathcal{D}_{|x|}^\alpha f(x) \to -|k|^\alpha \hat{f}(k) \tag{3.24}$$

which is a natural generalization of the simple rule

$$\frac{d^n f(x)}{dx^n} \to (-ik)^n \hat{f}(k)$$

The Fractional Fokker–Planck equation

Using the results in the previous section we can immediately write the macroscopic "diffusion" equation related to the Eq. (3.18); such an equation is known as the fractional Fokker–Planck equation and takes the form

$$\mathscr{D}_t^{\beta}\mathscr{P}(x,t) = \frac{a}{b}\mathcal{D}_{|x|}^{\alpha}\mathscr{P}(x,t) \tag{3.25}$$

with $0 \leq \beta \leq 1$ and $0 \leq \alpha \leq 2$.

As we explained in the last sections the case $\beta = 1$ and $\alpha = 2$ corresponds to the standard diffusion scenario. In particular when $\beta = 2$ only we get

$$\frac{\partial\mathscr{P}(x,t)}{\partial t} = \frac{a}{b}\mathcal{D}_{|x|}^{\alpha}\mathscr{P}(x,t)$$

namely a fractional diffusion only in the spatial dimension. On the other hand, when $\alpha = 2$ we get a fractional diffusion only with respect to the time; for example, taking $\beta = 1/2$ the time fractional diffusion equation becomes

$$\mathscr{D}_t^{1/2}\mathscr{P}(x,t) = D_0\frac{\partial^2\mathscr{P}(x,t)}{\partial x^2}$$

To calculate the mean square displacement recall that

$$\langle x^2(s)\rangle = -\left.\frac{\partial^2\hat{\tilde{\mathscr{P}}}(k,s)}{\partial k^2}\right|_{k=0}$$

thus using Eq. (3.17) we find

$$\langle x^2(s)\rangle = \frac{\langle\delta x^2\rangle}{bs^{3/2}}$$

with $a = \langle\delta x^2\rangle/2$ for the case of $\alpha = 2$. This expression is valid for small s, and with the help of the Tauberian theorems, which relate the power–law scaling of a Laplace transform at small s to the scaling in original space for large t [Feller, 1971; Hughes, 1995; Yakimiv, 2005] it follows that

$$\langle x^2(t)\rangle \sim t^{1/2}$$

recovering the result just established for the comb–case.

3.7 SUMMARY

In this chapter we discussed briefly the general features related with the standard and anomalous transport.

The anomalous case was discussed by taking as an example the CTRW performed by a walker diffusing on the backbone of a comb lattice and showing

how the anomalous behaviour experienced by such a system can be derived both from the fractional Fokker–Planck equation and from simple scaling arguments. In the next Chapter we will show our approach to the problem of diffusion on comb lattice and more generalized branched structures, discussing also the fluctuation–dissipation relations in the anomalous transport regime .

An interesting analysis of the diffusion process on the comb–lattice in the continuum space and time limit is reported in [Arkhincheev, 2002, 2010] starting from an usual (i.e. not fractional) Fokker–Planck equation. The feature of the diffusion in the considered model is that the displacement in the x–direction is possible only at $y = 0$. This means that the longitudinal diffusion coefficient D_x differs from zero only at $y = 0$:

$$D_x = D_1 \delta(y)$$

with $\delta(y)$ the Dirac delta function [Dirac, 1958]. On the other hand the diffusion along the teeth is characterized by a transversal diffusion coefficient $D_y = D_2$. Thus, the random walk on the comb structure is described by the diffusion tensor:

$$\begin{bmatrix} D_1\delta(y) & 0 \\ 0 & D_2 \end{bmatrix}$$

Accordingly, we have the following diffusion equation:

$$\left[\frac{\partial}{\partial t} - D_1\delta(y)\frac{\partial^2}{\partial x^2} - D_2\frac{\partial^2}{\partial y^2}\right] \mathscr{P}(x, y, t) = 0$$

The longitudinal MSD for this model grows as $t^{1/2}$, which is the expected anomalous behaviour explained for the comb lattice in this chapter, showing once again how geometrical limitations (here expressed by the Dirac delta function) are able to strongly influence the dynamical properties of a diffusive process.

4

ANALYTICAL AND NUMERICAL RESULTS ON BRANCHED STRUCTURES

"Never–ending wonders pop out from simple rules, if these are repeated ad infinitum."

Mandelbrot [2010]

INTRODUCTION

In this chapter we focus on the random walk performed on a certain class of ramified structures. We will take as examples (see Sec. 4.1 and Sec. 4.1.2) the comb–lattice [Goldhirsch and Gefen, 1986] and some generalizations of it [Forte et al., 2013a]. In particular, using simple scaling arguments, we will show how it is possible to predict the correct anomalous behaviour of the Mean Square Displacement (MSD) during the pre–asymptotic regime and how such regime is related with the geometrical parameters of the surrounding environment.

As usual in all the non equilibrium transport problems, a special attention will be devoted to the Fluctuation–Dissipation Relations (FDRs) [Kubo et al., 1991; Marconi et al., 2008]. The first example of a FDR was pointed out by A. Einstein; in his seminal paper on Brownian motion, Einstein [1905] showed that the average position of a random walker under the action of an external field $\mathbf{F} = f\hat{\mathbf{x}}$ must satisfy at long time the relation

$$\frac{\langle \delta x_t \rangle_f}{\langle (x_t - x_0)^2 \rangle_0} = \frac{f}{2k_B T} \tag{4.1}$$

where $\langle \delta x_t \rangle_f = \langle (x_t - x_0) \rangle_f - \langle (x_t - x_0) \rangle_0$, being $\langle \cdots \rangle_\phi$ the average over the particle ensemble calculated with ($\phi = f$) or without ($\phi = 0$) considering the influence of the external field; k_B is the Boltzmann constant and T the absolute temperature.

It is natural to wonder if Eq. (4.1) still holds true in the case of anomalous transport, thus generalizing the Einstein result. One of the main contribution of our work is thus related to the FDR. Indeed, using our approach, we are able to discuss the "fate" of the FDR, at least within the linear response approximation. In particular we found that, despite an anomalous transport regime, which can be controlled up to become the predominant one, there

are situations such that the FDR still holds true, suggesting that FDR does not depend on the details of the dynamics. On the other hand it is possible to construct particular comb–like structures (see Sec. 4.5) whose peculiar geometry along the transversal direction acts as a sort of an external drift, thus breaking the FDR at short times.

Another important part of our work is devoted to the study of those "apparently" standard diffusive processes. More specifically, we show how the standard scaling $\langle |x^q| \rangle \sim t^{q/2}$ is not always associated to a Gaussian probability density. To highlight such behaviour we will take into account a simple model of Continuous Time Random Walk (CTRW, see Sec. 4.3) and some examples of walks performed on a certain class of fractal trees (see Sec. 4.4.1 and Sec. 4.4.2), called Nice Trees of dimension k (NT_k) [Burioni and Cassi, 1994, 1995; Forte et al., 2013b] and a possible generalization of such trees [Forte et al., 2013b].

4.1 THE COMB MODEL

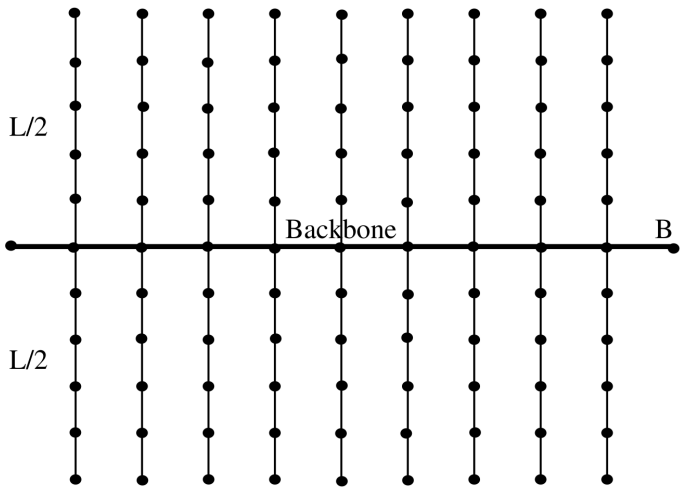

Figure 4.1: *Simple comb–lattice.*

The comb–lattice was introduced in Sec. 3.6.1, in order to provide an example of the CTRW process.

A walker occupying a site of the lattice can jump to one of the nearest neighbor sites according to the transition rules

$$\mathscr{W}(x \to x') = \left(\frac{1}{4} \pm \Delta p\right) \delta_{y,0}\delta_{x,x'\pm 1} \tag{4.2}$$

$$\mathscr{W}(y \to y') = \delta_{y,y'\pm 1}\left[\frac{\delta_{y,0}}{4} + \frac{1}{2}(1-\delta_{y,0})\right] \tag{4.3}$$

where $\Delta p \in [0, 1/4)$ represents an unbalance in the jump probabilities along the longitudinal direction introduced in order to take into account the possible effect of an external field, applied along the longitudinal direction. Observe that the external drift is never applied along the transversal direction, whose jump probabilities will be always $1/4$ if we move from $y = 0$ to $y' = \pm 1$ and $1/2$ otherwise.

We review firstly the simple case with $\Delta p = 0$, taking an unitary displacement between two consecutive teeth; denoting by $\mathbf{r}_t = (x_t, y_t)$ the position vector of a given particle, the total displacement up to time t along the backbone will be given by

$$x_t - x_0 = \sum_{j=1}^{t} \xi_j \delta_{y_j,0}$$

where the random variable ξ_j takes values in $\{1, 0, -1\}$, respectively with probability $\{1/4, 1/2, 1/4\}$, in agreement with the above transition rules defined in Eq. (4.2) and (4.3) specialized for the case $\Delta p = 0$.

The mean square displacement can be computed as

$$\langle (x_t - x_0)^2 \rangle = \sum_{j=1}^{t} \langle (\xi_j \delta_{y_j,0})^2 \rangle + 2 \sum_{j=1}^{t} \sum_{i>j}^{t} \langle \xi_j \xi_i \delta_{y_j,0} \delta_{y_i,0} \rangle$$

In the last equation all the terms given by $\langle (\xi_j \delta_{y_j,0})^2 \rangle$ are zero if $y_j \neq 0$ (i.e., if a walker is out of the backbone), otherwise $\langle (\xi_j \delta_{y_j,0})^2 \rangle = \langle \xi_j^2 \rangle = 1/2$; on the other hand $\langle \xi_j \xi_i \delta_{y_j,0} \delta_{y_i,0} \rangle = 0$ if $j \neq i$ and so we can write

$$\langle (x_t - x_0)^2 \rangle = \frac{1}{2} t \mu_t \tag{4.4}$$

with μ_t the mean percentage of time which a given walker spends in the backbone B during the time interval $[0, t]$. To evaluate μ_t we begin from the case $t > t_*(L)$, $t_*(L)$ being the homogenization time, meant as the time taken by a walker to span a whole tooth, visiting at least once all the sites [Weiss, 1994; Bouchaud and Georges, 1990; Redner, 2001]. Since along the y–direction the one–dimensional random walk is fast enough to explore exhaustively the size L $\left(\langle y_t^2 \rangle \approx 2 D_0 t\right)$ and, more important, it is recurrent, $t_*(L)$ can be taken as the time such that $\langle y_t^2 \rangle \sim L^2$, thus $t_*(L) \sim L^2$. After $t_*(L) \sim L^2$, the probability for a walker to be on the tooth can be considered almost uniform, namely

$$\mu_t = \frac{1}{1 + L} \approx L^{-1}$$

implying that for $t \gtrsim L^2$ the mean square displacement behaves as

$$\langle (x_t - x_0)^2 \rangle \approx \frac{1}{2(1 + L)} t \tag{4.5}$$

and after a time of the order of L^2 the diffusion along the transport direction will be normal, with an effective diffusion coefficient given by $D_{\text{eff}}(L) = 1/[4(1+L)]$.

To find the time behaviour of the MSD for $t \lesssim t_*(L)$ we observe that the diffusion on the comb lattice with infinite teeth length is known to be anomalous [Weiss and Havlin, 1986; Bouchaud and Georges, 1990; Weiss, 1994; Redner, 2001], a result which can be understood by viewing the longitudinal motion along the backbone of the comb lattice as a Continuous Time Random Walk, as we explained in Chap. 3. In particular the time behaviour of the mean square displacement is given by

$$\langle (x_t - x_0)^2 \rangle \sim t^{1/2}$$

which can be derived, under certain geometrical conditions, also for the case of diffusion in non homogeneous channels, using an effective one–dimensional Fokker–Planck equation [Dagdug et al., 2007] (see also Chap. 5).

For finite L, the diffusion will remain anomalous, as long as the RW does not feel the finite size of the sidebranches. Therefore for times $t \lesssim t_*(L)$, we expect an anomalous behaviour of the type

$$\langle (x_t - x_0)^2 \rangle \sim t^{2\nu}$$

The exponent ν can be computed by matching the last equation with the behaviour in Eq. (4.5) at the cross–over time $t \sim t_*(L)$, that is $t_*^{2\nu}(L) \approx t_*(L) L^{-1}$ yielding

$$\nu = \frac{1}{4}$$

It is interesting to note that, as the homogenization time $t_*(L)$ diverges with the size L, upon choosing the appropriate L, the anomalous regime can be made arbitrarily long till it becomes the dominant feature of the process.

The generalization to the case of a non vanishing external field f applied along the longitudinal direction can be made by introducing an unbalance $\Delta p \neq 0$ in the jump probabilities along the backbone. In this case, the displacement takes the form

$$x_t - x_0 = \sum_{j=1}^{t} \xi_j^{(f)} \delta_{y_j,0}$$

where $\xi^{(f)} \in \{-1, 0, 1\}$ with probabilities $\{1/4 - \Delta p, 0, 1/4 + \Delta p\}$; f is linked to Δp through the relation $\langle \xi_j^{(f)} \delta_{y_j,0} \rangle = f \delta_{y_j,0}$; indeed we have $\langle \xi_j^{(f)} \delta_{y_j,0} \rangle = 2\Delta p \delta_{y_j,0}$ and so $f = 2\Delta p$. By the same argument used for the case $f = 0$, we obtain

$$\langle \delta x \rangle_f \equiv \langle (x_t - x_0) \rangle_f - \langle (x_t - x_0) \rangle_0 = f t \mu_t \tag{4.6}$$

The notation $\langle \cdots \rangle_f$ is introduced to emphasize the fact that the average is taken over the perturbed ensemble of the diffusing particles, whereas $\langle \cdots \rangle_0$

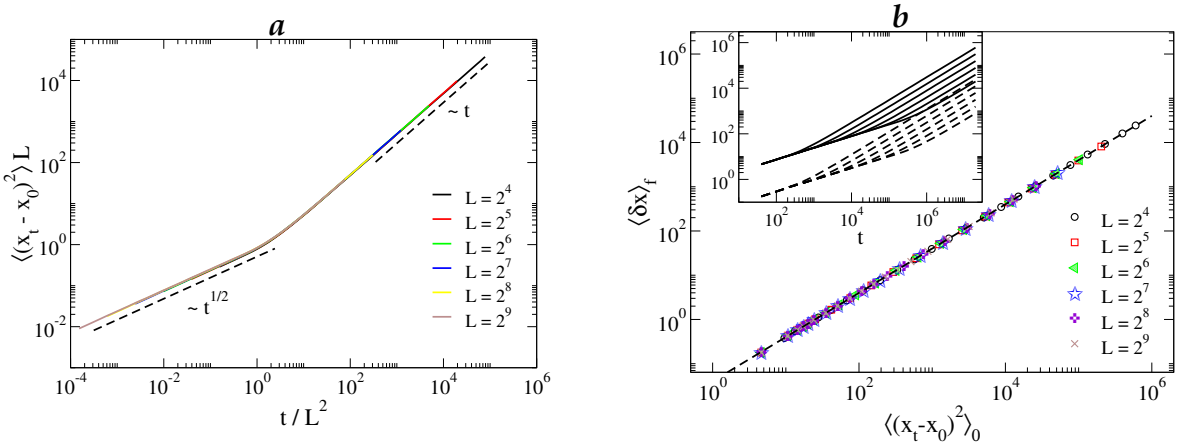

Figure 4.2: ***(a)*** *Log–log plot of $\langle x^2 \rangle L$ as a function of the rescaled time t/L^2. Observe the cross–over time from the subdiffusive regime to the standard one near $t/L^2 \approx 1$, supporting the assumptions at the heart of the matching argument explained in the text;* ***(b)*** *log–log parametric plot of $\langle \delta x_t \rangle_f$ versus $\langle (x_t - x_0)^2 \rangle$ (coloured symbols). The dashed line represents the theoretical prediction in Eq. (4.7); the inset shows the time behaviour of $\langle (x_t - x_0)^2 \rangle$ (black continuum lines) together with the time behaviour of $\langle \delta x_t \rangle_f$ (black dashed lines) for different values of the teeth size.*

simply gives the average with respect to the simple case with $f = 0$. Comparing the last equation with Eq. (4.4) we find that

$$\frac{\langle (x_t - x_0)^2 \rangle}{\langle \delta x_t \rangle_f} = \frac{1}{2f} \tag{4.7}$$

Despite the fact that Eq. (4.7) is formally identical to the Eq. (4.1) found by Einstein, it works both in the anomalous regime ($t \lesssim t_*(L)$) and in the standard diffusive one ($t \gtrsim t_*(L)$), so emphasizing its generality also in the case of anomalous transport, as was also previously found by [Barkai and Fleurov, 1998; Villamaina et al., 2008; Chechkin and Klages, 2009; Villamaina et al., 2011; Chechkin et al., 2012a,b; Gradenigo et al., 2012].

To verify the above results we performed numerical simulations taking $N_p = 7 \times 10^4$ walkers for $t = 2 \times 10^7$ unitary time steps. In particular we considered different values of L to probe the homogenization effects characterized by the cross–over time $t_*(L) \sim L^2$ between the two diffusive regimes, see Fig. 4.2

4.1.1 *The role of the fractal and spectral dimension*

In the following sections, we will frequently use the concept of spectral and fractal dimension. In particular, diffusion in fractal–like environment is strongly influenced by these two quantities. Thus we recall here what is the

meaning of the fractal and spectral dimension, in order to clarify the role of the space dimension on a diffusive process.

The intuitive idea of (topological) dimension is related to the number d of independent directions accessible to a point sampling a given object. This integer number, however, might be insufficient to fully quantify the dimensionality of a generic set of points, characterized by a "bizarre" arrangement of segmentation, voids or discontinuities. An example of such peculiar arrangement is provided by the typical trajectory of a two–dimensional Brownian motion, see Fig. 4.3. It is then useful to introduce an alternative definition of

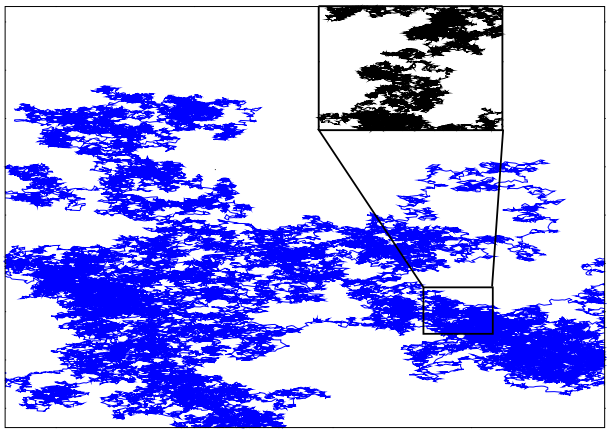

Figure 4.3: *Typical path (topological dimension $d = 1$) of a Brownian particle in a two dimensional space. The inset shows a zoom of the small box in the main figure, emphasizing the self–similarity of the process.*

dimension based on the "measure" of the considered object. Such measure is called the fractal dimension d_f and it is defined by the relation[Mandelbrot, 1983; Cencini et al., 2010]

$$d_f = -\lim_{\ell \to 0} \frac{\ln N(\ell)}{\ln \ell}$$

with $N(\ell)$ the number of points within a sphere of radius ℓ. As an example, consider a diffusion process for which we have, as we discussed in the previous sections,

$$\langle x^2(t) \rangle \sim t^{2/d_w}$$

being d_w the so called walk dimension[1]. Thus, within a sphere of radius ℓ, we have, at time t

$$\ell^{d_w} \sim N(\ell)$$

and the so called walk dimension d_w, for a standard diffusive process, can be interpreted as the fractal dimension of the typical set of points visited by the walk. In particular it takes the value $d_w = 2$ and this value is independent

1 Obviously for a standard diffusive process we have $d_w = 2$

by the topological dimension of the environment within which the process is going on.

An interesting question concerns the walk dimension d_w when we consider a random walk performed on a fractal network characterized by the fractal dimension d_f. In general a fractal network can be viewed as a graph. An undirected graph is a collection of vertices pairwise connected, or not, by links. To each graph of $\mathcal{N}$ vertices, we can associate an $\mathcal{N} \times \mathcal{N}$ matrix $\mathbf{A}$ (adjacency matrix), such that , $A_{ij} = 1$ if there is a link between vertices i and j, otherwise $A_{ij} = 0$ [Thulasiraman and Swamy, 1992; Caldarelli and Vespignani, 2007].

An unbiased random walk on a graph can be defined in a natural way [Woess, 2000; Burioni and Cassi, 2005; Philippe and Volchenkov, 2011]: a walker at time t on a site i can jump at time $t+1$ on the node j only if $A_{ij} = 1$, with a transition probability $\mathscr{W}_{i\to j} = 1/s_i$. Here $s_i = \sum_j A_{ij}$ is called the coordination number of the node i and represents the number of links which leave i. The assumption on the transition rates embodies the notion that there are not in a given graph privileged links, that is, the probability to jump on a site located on a given branch depends only by the coordination number, however not by the branch itself. Obviously such hypothesis can be relaxed, but we will not consider here such cases.

The probability $\mathcal{P}_t(m)$ to be on a given site m at time t satisfies the equation

$$\begin{aligned}\frac{d\mathcal{P}_t(m)}{dt} &= \sum_n \mathscr{W}_{n\to m} P_t(n) - \sum_n \mathscr{W}_{m\to n} P_t(m) \\ &= \sum_n \mathscr{W}_{nm} \Big[\mathcal{P}_t(n) - \mathcal{P}_t(m)\Big]\end{aligned}$$

where, in the last equation, we assumed for simplicity that the transition matrix is symmetric (which is always true in the unbiased case). The last equation resembles the equation for the vibrational modes ("*fractons*") of an elastic fractal network consisting of particles connected by harmonic springs and can be solved in analogy with the "vibrational problem" [Alexander and Orbach, 1982; Nakayama et al., 1994; ben Avraham and Havlin, 2000].

Here we use a simple scaling approach [ben Avraham and Havlin, 2000] in order to calculate the approximate time behaviour of the probability density in the long time limit, in particular we will focus on the return probability to the origin $\mathcal{P}_t(0)$. By definition of fractal dimension , the number of points of the fractal network, contained in a sphere of radius ℓ, is given by ℓ^{d_f}. In particular, in the long time limit, we can assume that the probability to be on one of these points is approximately uniform, thus $\mathcal{P}_t(0) \sim \ell^{-d_f}$. Moreover, using the relation $\langle x^2 \rangle \sim t^{2/d_w}$, we have $\ell \sim t^{1/d_w}$ and so, asymptotically in time, $\mathcal{P}_t(0) \sim t^{-d_f/d_w}$. This means that the return probability decreases in time as

$$\mathcal{P}_t(0) \sim t^{-\frac{d_s}{2}} \tag{4.8}$$

where we introduced a new type of (generally fractional) dimension: the so called spectral dimension d_s, given by

$$d_s = 2\frac{d_f}{d_w}$$

Using the last relation, the time behaviour of the MSD, $\langle x^2 \rangle \sim t^{2/d_w}$, related to a diffusive process defined on a fractal network with fractal dimension d_f and spectral dimension d_s, can be finally written as

$$\langle x^2 \rangle \sim t^{d_s/d_f} \tag{4.9}$$

The relation $d_w = d_s/2d_f$ implies that diffusive processes on a fractal structure are anomalous whenever $d_f \neq d_s$. However, consider now the general average $\langle |x|^q \rangle$ ($q \in \mathbb{N}$). If the walk dimension is a function of q, that is $d_w = d_w(q)$, depending on q, we could observe a standard diffusive behaviour ($\langle x^2 \rangle \sim t$) also for those processes which are not characterized by a Gaussian probability density, a situation which we could call standard, but not normal (i.e. not Gaussian) diffusion. We will focus on such pathological systems in Sec. 4.3 and Sec. 4.4.2, discussing our personal results on the "hidden" anomalies underlying the apparently standard case $\langle x^2 \rangle \sim t$.

4.1.2 *Generalized Comb structures*

The goal of this section is to present a derivation based on a simple physical reasoning, i.e. without sophisticated mathematical formalism, of both the anomalous exponent ν and the Einstein FDR for RWs on a class of comb– like structures [Forte et al., 2013a], consisting of a main backbone, decorated by an array of sidebranches, as in Fig. 4.4, thus generalizing the simple comb introduced in the last section. Comb–like structures are frequently observed in condensed matter and biological frameworks: they describe the topology of polymers [Casassa and Berry, 1966; Douglas et al., 1990], in particular of amphiphilic molecules, and can be also engineered at the nano- and microscale. Moreover, they are studied as simple models for channels in porous media and a general account of these systems can be found in [ben Avraham and Havlin, 2000]. The diffusion along the backbone, longitudinal diffusion, can be strongly influenced by the shape and the size of such branches and anomalous regimes arise by simply tuning their geometrical importance over the backbone. In other words, the dangling lateral structures, dead-ends, introduce a delay mechanism in the hopping to the neighboring backbone sites that easily leads to non–Gaussian behaviour, as has been observed for instance in flows across porous media [Tarafdar et al., 2001].

The analysis for the simple comb considered in Sec. 4.1, can be easily extended to the cases where each tooth is replaced by a more complicated structure, for example a two dimensional plaquette, a cube or a graph with fractal

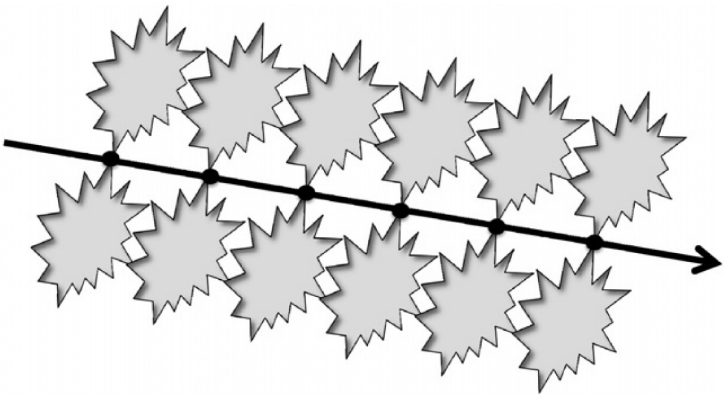

Figure 4.4: *Cartoon of a one–dimensional lattice (backbone) decorated by identical arbitrary–shaped sidebranches or dead–ends, depicted as lateral irregular objects. Such sidebranches act as temporary traps for the random walk along the backbone.*

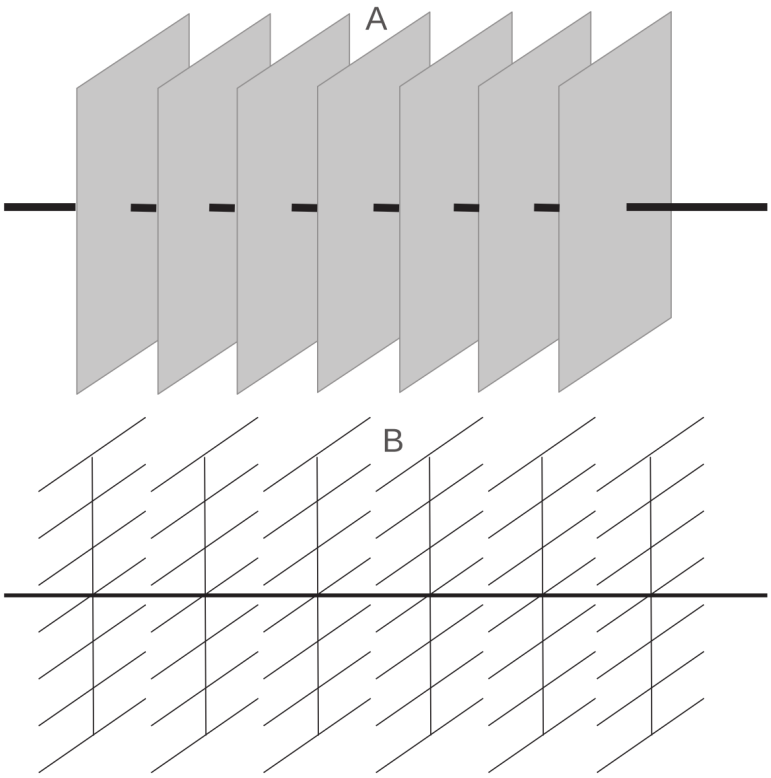

Figure 4.5: *Sketch of the Comb structures used in the text and obtained as an infinite periodical arrangement of the same geometrical element:* ***(a)*** *comb of plaquettes (dubbed "kebab") and* ***(b)*** *two–nested comb lattices ("antenna")*

dimension d_f and spectral dimension d_s (see Sec. 4.1.1), as reported in Fig. 4.5. According to the Eq. (4.9), One has, for the lateral diffusion

$$\langle y^2(t) \rangle \sim t^{d_s/d_f}$$

and then, the homogenization time can be estimated as $t_*(L) \sim L^{2d_f/d_s}$ if $d_s < 2$. Here, and in the following, y_t indicates the transversal process with respect to the backbone ($d_s = d_f = 2, 3$ if the lateral structure is a plaquette or a cube, respectively). The previous argument used in Sec. 4.1 for the homogenization time stems straightforwardly noting that a walker on an infinite graph, in an interval t, visits a number of different sites [Weiss and Havlin, 1986; Alexander and Orbach, 1982]

$$N(t) \sim \begin{cases} t^{d_s/2}, & \text{if } d_s \leq 2 \\ t, & \text{if } d_s > 2 \end{cases} \tag{4.10}$$

and accordingly, in a finite lattice of linear size L, for $t \approx t_*$, we have $N(t_*) \sim L^{d_f}$, implying that $t_*(L) \sim L^{2d_f/d_s}$ when the spectral dimension $d_s \leq 2$. If the lattice has $d_s > 2$, the random walk is shown to be not recurrent [Itzykson and Drouffe, 1989; Bouchaud and Georges, 1990; Redner, 2001]; its exploration of the sidebranches over a diffusive time scale $t_*(L) \sim L^2$ is not exhaustive, a full exploration takes a much longer time which can be obtained by the condition $N(t_*(L)) = L^{d_f}$ leading to $t_*(L) \sim L^{d_f}$, directly from the second of Eqs. (4.10). By matching the behaviour at the cross–over time $t_*(L)$, we obtain in the case $d_s < 2$

$$\langle (x_t - x_0)^2 \rangle \sim t^{2\nu}, \quad 2\nu = 1 - \frac{d_s}{2} \tag{4.11}$$

These results coincide with the exact relations obtained by a direct calculation of the spectral dimension on branched structures, based on the asymptotic behaviour of the return probability on the graph, or on renormalization techniques [Cassi and Regina, 1995; Burioni and Cassi, 2005; Haynes and Roberts, 2009].

The case $d_s = 2$ deserves a specific treatment. Indeed $d_s = 2$ is the critical dimension separating recurrent ($d_s < 2$) and not recurrent ($d_s > 2$) random walks (see Sec. 3.5). Thus $d_s = 2$ is the marginal dimension which reflects into the logarithmic scaling of the lateral mean square displacement $\langle y_t^2 \rangle \sim t/\ln t$ [Itzykson and Drouffe, 1989; Bouchaud and Georges, 1990; Metzler and Klafter, 2000] (see also Chap. 3), therefore the homogenization time is now $t_*(L) \sim L^2 \ln L$. To illustrate this point we consider the case of the "kebab–lattice" (Fig.4.5 **(a)**) where each plaquette is a regular two dimensional square lattice, for which $d_s = d_f = 2$.

Applying once again the matching argument we have

$$\langle (x_t - x_0)^2 \rangle \sim \ln t \tag{4.12}$$

indicating a logarithmic pre–asymptotic diffusion along the backbone, see Fig. 4.6 **(a)**.

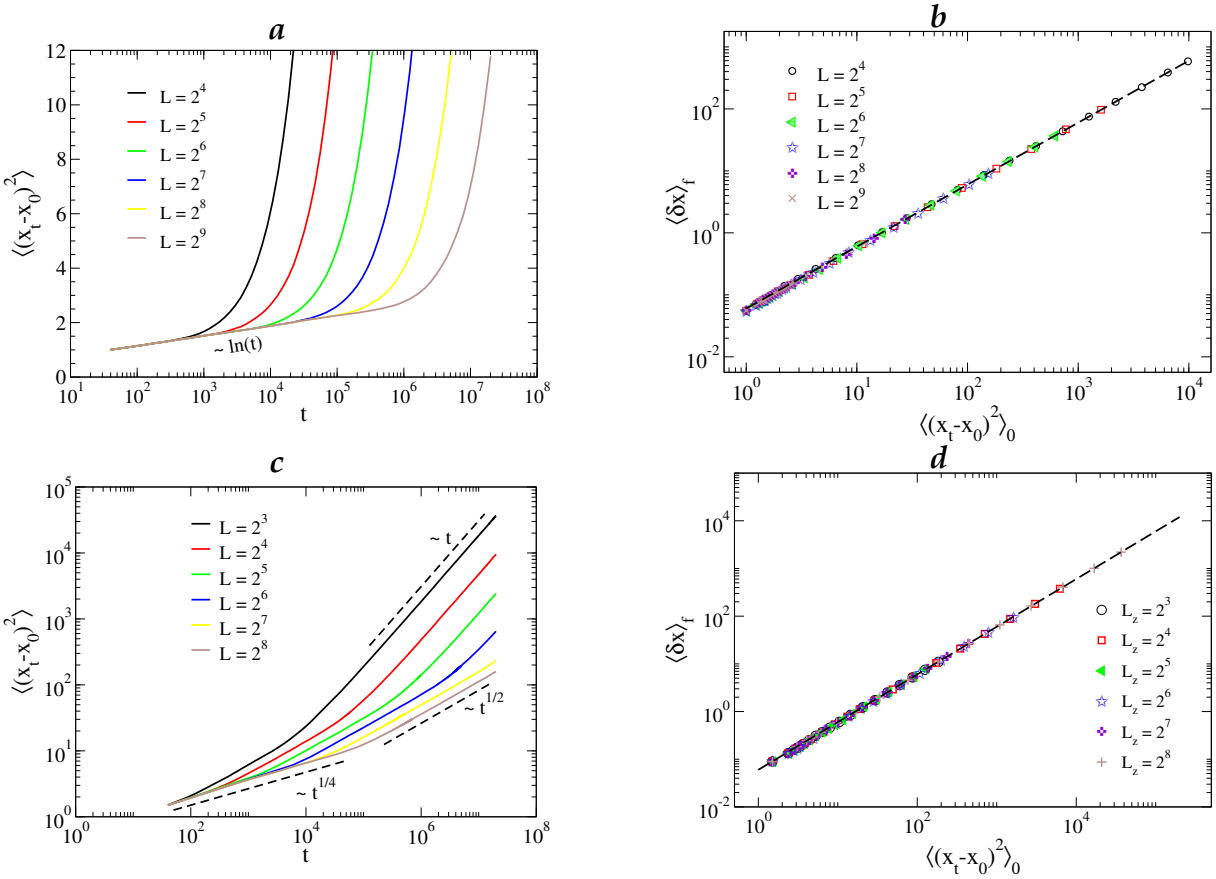

Figure 4.6: ***(a)*** *Log–linear plot of the mean square displacement for the case of the kebab–lattice (see Fig. 4.5* ***(A)****), as a function of the time, together with* ***(b)*** *the parametric log–log plot of* $\langle \delta x_t \rangle_f$ *vs* $\langle (x_t - x_0)^2 \rangle_0$ *(coloured symbols) and the theoretical prediction in Eq. (4.13) (dashed line);* ***(c)*** *mean square displacement (log–log scale) and* ***(d)*** *fluctuation–dissipation relation for the case of the antenna–lattice (see Fig. 4.5* ***(B)****)*

Following the same steps as those described for the comb lattice, the generalized fluctuation–dissipation relation also holds for all the branched structures described in this section[2]. In particular we have:

$$\frac{\langle (x_t - x_0)^2 \rangle}{\langle \delta x_t \rangle_f} = \frac{1}{3f} \tag{4.13}$$

Numerical simulations show that the time behaviour of the MSD (Fig. 4.6 **(a)**) on the kebab–lattice exhibits the initial $\ln t$ behaviour, at different sizes L, in agreement with Eq.(4.12). Panel **(b)** of Fig. 4.6 reports the verification of the fluctuation–dissipation relation, independently of the lattice size, with the prefactor $1/3$, as the probability to jump back and forth along the backbone is $1/6$.

To show the effect of d_s of the homogenization time on the diffusion process, we consider a structure composed by two–nested comb lattices that we dub "antenna", sketched in Fig. 4.5 **(b)**, i.e. a comb lattice where the teeth are comb lattices themselves on the y, z plane. This structure is then characterized by two length–scales, the vertical, L_y , and transversal, L_z , teeth length; only for sake of simplicity we assume all these scales of the same order of magnitude, namely $L_y \sim L_z \sim L$. Also in this case, a cross–over time, (related to the length of the teeth along z, L) $t_*(L) \sim L^2$ exists such that for $t \gtrsim t_*(L)$, the diffusion is standard, whereas for $t \lesssim t_*(L)$, an anomalous diffusive regime takes place. Since $d_s = 3/2$ for a simple comb lattice [Weiss and Havlin, 1986], from Eq. (4.11) we obtain

$$\langle (x_t - x_0)^2 \rangle \sim t^{1/4} \tag{4.14}$$

For finite L, the mean square displacement in Fig. 4.6, **(c)** exhibits an initial regime $t^{1/4}$ followed by a $t^{1/2}$ behaviour with a final cross–over to the standard one. Such a particular scaling is due to the "double structure" of the sidebranches

The case of $d_s > 2$ must be carefully considered. For simplicity we present here our analysis for the particular condition $d_s = d_f = 3$, so we consider a comb–like structure where the lateral teeth are compenetrating but non–communicating cubes. For computational simplicity the cubes are arranged with centers at a unitary distance from one another along the backbone. Actually, the minimal distance among the centers of non–compenetrating cubes with edge L, is $L/2 + L/2 = L$ which is of course larger than 1 as soon as $L > 1$, but in our model the cubes, despite their large overlap, are still considered as distinct sidebranches connected only through the backbone. The homogenization time will be $t_*(L) \sim L^d$ and $D(L) \sim L^{-d}$. Therefore, for

2 It is possible to construct structures whose peculiar geometry acts as a sort of an external field along the transversal direction, thus implying that the generalized FDR does not hold, such an example will be discussed in Sec. 4.5

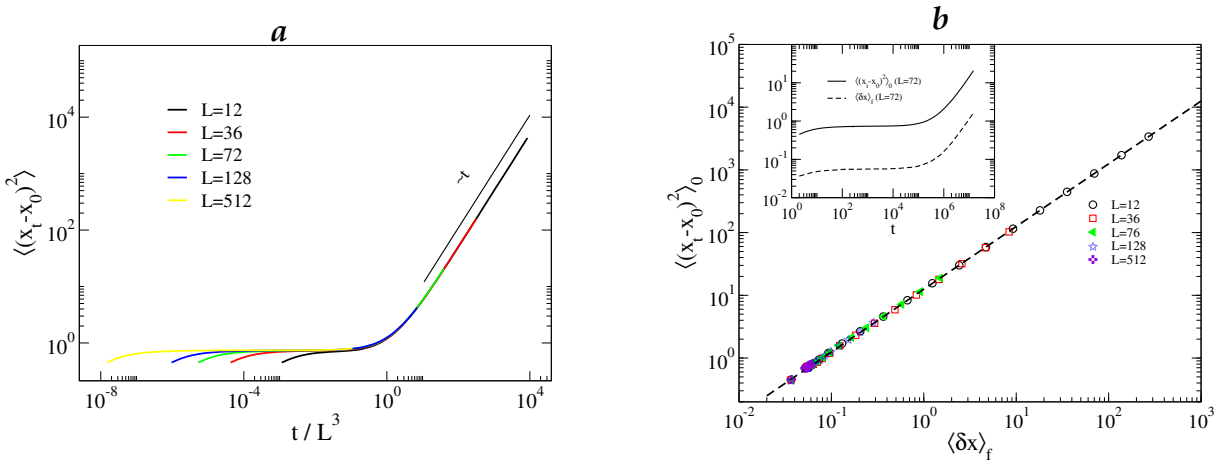

Figure 4.7: ***(a)*** *Mean square displacement and* ***(b)*** *fluctuation–dissipation relation for the case of a comb–lattice composed by non compenetrating cubes; dashed line represents the relation in Eq.* (4.13)

$t \gg t_*(L)$, we expect the standard diffusive growth $\langle (x_t - x_0)^2 \rangle_0 \sim t/L^d$, while below $t_*(L)$, $\langle (x_t - x_0)^2 \rangle_0 \sim t^{2\nu}$ and the matching condition at $t_*(L)$ predicts the existence of a plateau $\langle (x_t - x_0)^2 \rangle_0 \sim const$, as derived by exact relations based on return probabilities [Goldhirsch and Gefen, 1986]. The simulation data are in agreement with the above results, see Fig. 4.7, and also the proportionality between fluctuation and response is again perfectly verified.

4.2 STRONG ANOMALOUS DIFFUSION

In the last sections we introduced a simple analysis of comb–like based structures , using essentially the physical concept of matching two different behaviors and requiring continuity at the cross–over between the two regimes. We derived a series of anomalous behaviour of the MSD with the elapsed time; in general we can write $\langle x^2 \rangle \sim t^{\nu_1} \ln^{\nu_2} t$ [Bouchaud and Georges, 1990] with ν_1 and ν_2 anomalous exponents tuned by choosing in an appropriate way the geometrical morphology of the diffusive environment.

Generally speaking, deviations from standard diffusive behaviour are well known and frequently observed in experiments, computer simulations, natural and economic phenomena [Klafter et al., 1996; Solomon et al., 1993; Shlesinger et al., 1993; Santamaria et al., 2006; Klages et al., 2008] and typically are classified according to the anomalous scaling

$$\langle x^2(t) \rangle \sim t^{2\nu} \tag{4.15}$$

If a process, for example in one spatial dimension, is characterized by anomalous diffusion, the simplest occurring scenario is that for large enough t its probability density satisfies the ordinary scaling

$$\mathscr{P}(x,t) = t^{-\nu/2} f\left(\frac{x}{t^{\nu/2}}\right) \tag{4.16}$$

with $f(x/t^{\nu/2})$ an homogeneous function of $x/t^{\nu/2}$ only. The scaling law (4.16) implies a precise properties of the moments

$$\langle |x(t)|^q \rangle \sim t^{q\nu/2}, \quad q \in \mathbb{N}$$

The general assumption on the scaling property of the probability density in Eq. (4.16) is numerically verified for a large class of models, as for example the comb lattice (see Sec. 4.1); however it is not verified for all the models exhibiting anomalous diffusion, as for example the case of those models which show strong anomalous diffusion [Andersen et al., 2000; Castiglione et al., 1999; Gradenigo et al., 2012], see also Sec. 4.3; such systems are characterized by the scaling law

$$\langle |x(t)|^q \rangle \sim t^{q\nu(q)}, \quad q \in \mathbb{N} \tag{4.17}$$

where $q\nu(q)$ is a function of q which can be both linear or non–linear. Clearly the spectrum of exponents $\nu(q)$ in Eq. (4.17) implies that the scaling law in Eq. (4.16) fails, so there is no possibility to have a unique collapse of the probability density at different times onto a single curve. The above observations reinforce the idea that the anomalous character of a diffusive process is not only related to the exponent ν in Eq. (4.15).

The following sections are dedicated to the analysis of some examples showing strong anomalous diffusion; in addition we will also take into account systems characterized by the standard scaling $q\nu(q) = q/2$, however with a non Gaussian probability density, showing how the standard scaling of the moments is not always connected with a normal (i.e. Gaussian) diffusion. In particular we start from the analysis of a CTRW model in one spatial dimension and we will proceed by taking into account the random walk performed on a class of fractal trees.

4.3 CTRW AND STRONG ANOMALOUS DIFFUSION

Consider the following model of CTRW: a particle (for simplicity in one spatial dimension) can undergoes a series of collisions at random times $t_1, t_2, \cdots, t_n, \cdots$ and between two successive collisions the velocity v_n remains constant. The particle position $x(t)$ at time t between t_n and t_{n+1} will be given by

$$x(t) = x(t_n) + v_n(t - t_n) \tag{4.18}$$

being $v_n = \pm 1$ with equal probability and the time intervals $\tau_n = t_{n+1} - t_n$ independent random variables distributed according to the power law

$$\mathscr{P}(\tau) \sim \begin{cases} \tau^{-g} & , \quad 1 \leq \tau \leq T \\ 0 & , \quad \text{otherwise} \end{cases} \tag{4.19}$$

In Eq. (4.19) $g > 1$, the lower cutoff $t_c = 1$ is a regularization to avoid the singularity from infinitesimally short steps. Moreover, as in real physical systems step size are always bounded, we also introduced an upper cutoff T. The presence of the cutoff T implies that the hypothesis of the CLT for the process in (4.18) are fulfilled, thus as $t \gtrsim T$, it converges to a Gaussian process. However if T is chosen sufficiently large, this convergence is slow enough that a long and robust pre–asymptotic regime of strong anomalous diffusion can be observed as explained by the following reasoning.

Consider n_t as the stochastic process counting the number of collisions that a particle underwent within the time t such that

$$x(t) = \sum_{i=1}^{n_t} v_i \tau_i$$

When the time is so large that enough collisions occurred ($n_t \gg 1$) we have in a good approximation $t \approx \sum_{i=1}^{n_t} \tau_i$ giving $t \approx N\langle\tau\rangle$, N being the mean number of time steps necessary to reach the time t, say $N = \langle n_t \rangle$. In this limiting regime we can express moments of order q as

$$\langle x^q(t) \rangle = \left\langle \left(\sum_{i=1}^{N} v_i \tau_i \right)^q \right\rangle = \sum_{\{\mathbf{k}\}} \frac{q!}{k_1! k_2! \cdots k_N!} \prod_{j=1}^{N} \langle (v_j \tau_j)^{k_j} \rangle$$

with $\{\mathbf{k}\}$ indicating the set of non negative integers such that $k_1 + k_2 + \cdots + k_N = q$. The odd–order moments $\langle x^q(t) \rangle$ vanishes for the symmetry $v \to -v$ of the velocity distribution. Even order moments are non zero and can be evaluated exploiting the following properties: $\langle v_i \tau_j \rangle = 0$, $\langle v_i v_j \rangle = \delta_{ij}$, $\langle \tau_i \tau_j \rangle = \langle \tau^2 \rangle \delta_{ij}$, moreover it is useful to observe also that the q–order moments of the waiting time τ for large T can be obtained from Eq. (4.19) as

$$\langle \tau^q \rangle \sim \begin{cases} T^{1-g+q} & , \text{ if } q > g-1 \\ a(q,g) & , \text{ if } q < g-1 \end{cases} \tag{4.20}$$

with $a(q,g)$ a constant independent from T. Substituting N with $t/\langle\tau\rangle$ in the (4.20) we obtain

$$\begin{aligned}
\langle x^2(t)\rangle &= t\frac{\langle\tau^2\rangle}{\langle\tau\rangle} \sim t \\
\langle x^4(t)\rangle &= t\frac{\langle\tau^4\rangle}{\langle\tau\rangle} + 3\left(t\frac{\langle\tau^2\rangle}{\langle\tau\rangle}\right)^2 \sim t^2 \\
\langle x^6(t)\rangle &= t\frac{\langle\tau^6\rangle}{\langle\tau\rangle} + 15\left(\frac{t}{\langle\tau\rangle}\right)\langle\tau^2\rangle\langle\tau^4\rangle + 15\left(t\frac{\langle\tau^2\rangle}{\langle\tau\rangle}\right)^3 \sim t^3 \\
&\vdots
\end{aligned}$$

Looking at the moments above we can see that, depending on the ratio t/T, two different regimes come into play. When $t/T \gg 1$ (asymptotic regime) the most important term in the above sums comes from the contribution of the form

$$\langle x^q(t)\rangle \sim \left(t\frac{\langle\tau^2\rangle}{\langle\tau\rangle}\right)^{q/2} \sim t^{q/2}$$

and so the moments scaling is completely standard for every even $q > 0$. On the other hand when $t/T \ll 1$, the q–order moments $\langle x^q\rangle$ are dominated by $N\langle\tau\rangle$, the largest term in T, giving

$$\langle x^q(t)\rangle \sim t\frac{\langle\tau^q\rangle}{\langle\tau\rangle}$$

Using the same matching argument applied for the case of the comb–lattice at the cross–over time $t = T$ and remembering Eq. (4.20), we finally obtain for the case $t/T \ll 1$

$$\langle x^q(T)\rangle \sim T^{q\nu(q)} \sim T\frac{\langle\tau^q\rangle}{\langle\tau\rangle}$$

from which it is possible to calculate the values of the exponent $q\nu(q)$

$$\begin{aligned}
q\nu(q) &= \frac{q}{2},\ q = 2,4,6,\cdots \quad g \in [1,2); \\
q\nu(q) &= q + 2 - g,\ q = 2,4,6,\cdots \quad g \in [2,3); \\
q\nu(q) &= q/2,\ q = 2, \quad g \in [3,4); \\
q\nu(q) &= q + 2 - g,\ q = 4,6,\cdots \quad g \in [3,4); \\
&\vdots
\end{aligned} \tag{4.21}$$

The case characterized by $g \geq 3$ shows the strong anomalous character introduced in the last section. More specifically in this case $q\nu(q)$ is a piece–wise

linear function of q with the property that $2\nu(2) = 1$ (see Fig. 4.8). We can generalize the above result to the odd–order moments by considering the average $\langle |x(t)|^q \rangle \sim t^{q\nu(q)}$ with $(g \in [3,4))$

$$q\nu(q) = \begin{cases} q/2, & q = 1,2 \\ q + 2 - g, & q = 3,4,5,\cdots \end{cases}$$

The last relation suggests a possible form of the probability density, indeed

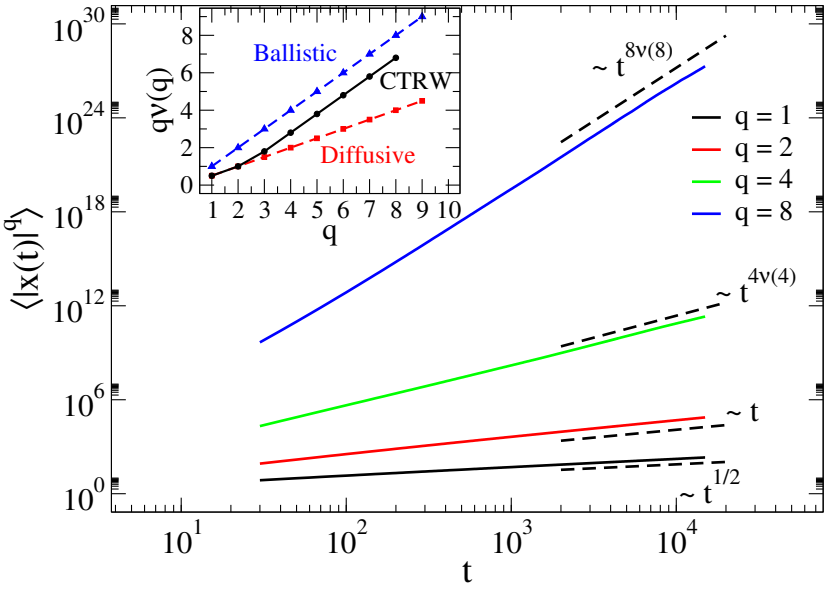

Figure 4.8: $\langle |x(t)|^q \rangle$ $(q = 1,2,4,8)$ *plotted as a function of the time on log–log scale. The picture shows the result obtained by simulating the CTRW process in Eq.* (4.18) *with* $g = 3.2$*; the insets shows the relation* $q\nu(q)$ *vs* q *which underlies the strong anomalous diffusive character of this particular system*

the lowest order moments behave in time as in the case of normal diffusion, thus we expect that the probability density $\mathscr{P}(x,t)$ has a Gaussian–like bulk which scales as $\mathscr{P}(x,t) = t^{-1/2} f(x/t^{1/2})$, in particular there exist a value $c \sim t$ such that the probability density takes the form

$$t^{1/2}\mathscr{P}(x,t) = \begin{cases} f(x/t^{1/2}), & x \leq c \sim t \\ 0, & otherwise \end{cases} \tag{4.22}$$

The suggested form of the probability density is consistent with the q–moments scaling law only if around c, $f(x/t^{1/2})$ assumes the form $f(z) \sim z^{-\alpha}$, that is the tails decay as a power–law behaviour with an exponent α related to g. Let $z^* = x^*/t^{1/2}$ denotes the value of the cross–over between the Gaussian–like bulk and the power–law tails, then we have (for simplicity we consider only

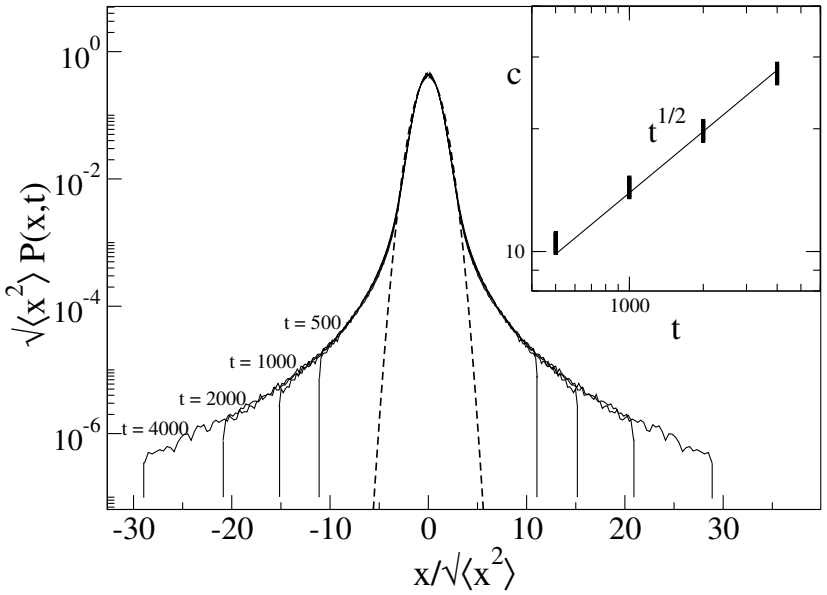

Figure 4.9: *Rescaled probability densities of the CTRW at different times for* $g = 3.2$. *The vertical lines are guide for the eyes to mark the bounded support,* $|x| \leq c(t)$, *of the distributions as assumed in Eq.* (4.22). *The inset shows the scaling* $c(t)/\sqrt{t} \sim t^{1/2}$ *in Eq.* (4.22). *The dashed line represents the Standard Gaussian (see Eq.* (3.2)*)*

the case $x > 0$, being the process symmetrical with respect to the reflection about the origin)

$$\langle x^q(t) \rangle = \int_0^c dx\; x^q \mathscr{P}(x,t) = \\ t^{q/2} \int_0^{z^*} dz\; f(z) + \text{const}\; t^{q/2} \int_{z^*}^{ct^{-1/2}} dz\; z^{q-\alpha} \tag{4.23}$$

The first term of Eq. (4.23) is related with the Gaussian–like bulk and it behaves as $t^{q/2}$; the second one, remembering that $c \sim t$ behaves as $t^{q+\frac{1}{2}-\frac{\alpha}{2}}$. Therefore for small q the dominant contribution comes from the first term, say $\langle x^q(t) \rangle \sim t^{q/2}$, while for large q the leading contribution comes from the second term. The exponent $q + \frac{1}{2} - \frac{\alpha}{2}$ is in agreement with the calculated exponent $q\nu(q)$ only if $\alpha = 2g - 3$, which is the expected behaviour of the probability density tails outside the Gaussian–like bulk. The collapse of the rescaled probability density is shown in Fig. 4.9 together with the standard Gaussian (picture to be adjusted).

The result shown in this section must not be taken as a violation of CLT, indeed within the Gaussian–like bulk the probability density shows the usual scaling and, as we reviewed in Chap. 3 CLT does not grant anything on the nature of the tails. Analogously there is no reason for the high order moments, which receive the main contribution from the tails, to converge to the Gaussian moments. As we stated in the introduction this example exhibits a

peculiar, in some sense still "anomalous", feature, which is highlighted not by the time behaviour of the mean square displacement, rather by the non Gaussian probability density and the higher order moments, suggesting that the remarkable property of standard diffusion, namely $\langle x^2 \rangle \sim t$ is not enough to give information about the possible transport anomalies.

4.4 WALKING ON FRACTAL TREES

The diffusion properties of random walk on graphs and/or within a fractal environment, depend on both the fractal dimension d_f and the spectral dimension d_s [Alexander and Orbach, 1982; ben Avraham and Havlin, 2000], as we discussed in Sec. 4.1.1 and Sec. 4.1.2. Indeed, the relation between spectral and fractal dimension determines the mean square displacement, as reported in Eq. (4.9).

Similarly to the case of CTRW, we can wonder about the behaviour of high–order moments and the possible scaling/collapse of the probability density when we consider a random walk on fractals. In particular, we will focus in the next sections on a class of fractal trees, called Nice Trees of dimension k (NT_k) and some further generalization of them which we will call here Super Nice Trees (SNT).

4.4.1 *Nice Trees of Dimension k*

NT_k are recursive fractal trees such that $d_f = d_s$ apparently implying, according to Eq. (4.9) standard diffusion, with a subsequent Gaussian scaling of the moments and the probability density. They are recursively defined as follows. An origin $\mathcal{O}$ is connected with a site A by a link of length 1: from A the tree splits in k branches of length 2^1 each. The end point of such branches, in turn, split again into k branches of length 2^2 and so on (see Fig. 4.10). Such trees are characterized by the remarkable property that fractal and spectral dimension are the same, as shown in Burioni and Cassi [1994, 1995]; more specifically

$$d_f = d_s(k) = 1 + \frac{\ln k}{\ln 2} \tag{4.24}$$

therefore, despite the nontrivial structure, Eq. (4.9) implies a standard behaviour $\langle x^2(t) \rangle \sim t$ for any value of k, where the distance between two given sites of the tree, say x and y, is defined as the minimum number of links connecting x and y (the path of minimal length connecting x and y is also called in the literature geodesic path [Woess, 2000; Burioni and Cassi, 2005; Philippe and Volchenkov, 2011]). As usual, with $x(t)$ we mean the distance from the origin $\mathcal{O}$ of the graph, to which is associated $x_{\mathcal{O}} = 0$, whereas $(x(t) - x')$ will be the distance at the time t from a fixed node x'.

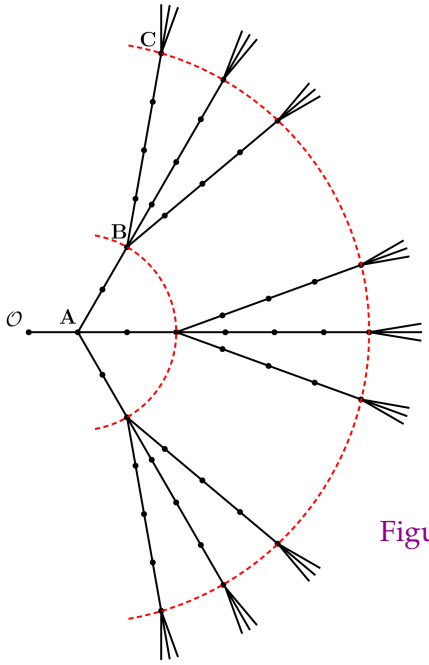

Figure 4.10: *Sketch of the Nice Tree of dimension $k = 3$ together its equivalent model in term of a one dimensional non homogenbeous chain.*

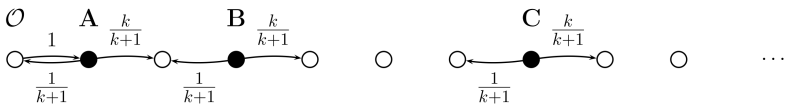

As we learned in the case of CTRW (Sec. 4.3), the linear growth of the MSD with the elapsed time (i.e. $2\nu(2) = 1$) does not grant trivial properties in the probability density scaling, as well as in the behaviour of the higher–order moments.

Each site of the NT_k can be identified with a couple of indices (x, α), indicating respectively the distance from $\mathcal{O}$ and the corresponding branch. Our goal is to study the distribution function $\mathcal{P}_t(x, \alpha)$, that is the probability to find at time t a walker at distance x from $\mathcal{O}$ and on the branch α. A useful quantity in the following reasoning will be the distance from the origin of the branching points, in particular if we associate to the origin the value $x_{\mathcal{O}} = 0$, the branching points will be at the distances

$$x = 2^n - 1, \quad n \in \mathbb{N} \tag{4.25}$$

which clearly is a relation independents from α, due to the geometrical characteristics of NT_k trees. For example, with reference to Fig. 4.10, all the branching points along the red dashed lines are at the same distance from $\mathcal{O}$, thus

using Eq. (4.25) we have three branching points at distance $x_B = 2^2 - 1 = 3$ from $\mathcal{O}$, nine branching points at distance $x_C = 2^3 - 1 = 7$ from $\mathcal{O}$ and so on.

If a walker is not on a branching point, say if its distance x from the origin is such that $x(t) \neq 2^n - 1$, then it will decrease or increase $x(t)$ by one with probability $1/2$, performing a standard random walk; on the other hand, when $x(t) = 2^n - 1$, a walker will increase its distance from the origin by one with probability $k/(k+1)$, choosing independently another branch and thus proceeding on the tree; otherwise it decreases its distance from the origin by one with probability $1/(k+1)$, coming back on the starting branch. Due to the fact that the probability to jump on new branch does not depend on the branch itself, the random variables $x(t)$ and $\alpha(t)$ are independent, so we can write $\mathcal{P}_t(x,\alpha) = \mathscr{P}_t(x)\mathcal{Z}_t(\alpha)$ and focus on the marginal probability distribution

$$\mathscr{P}_t(x) = \sum_{\alpha} \mathcal{P}_t(x,\alpha)$$

Practically the marginal probability is related to the random walk on a simple one dimensional chain with a perfect reflecting boundary condition at $x_{\mathcal{O}} = 0$ and a series of inhomogeneities points, which are at distances $x = 2^n - 1$ from the origin of the line and such that the transition between two neighbours sites can be taken as (see the chain model in Fig. 4.10)

$$\begin{cases} \mathscr{W}(0 \to 1) & = 1 \\ \mathscr{W}(1 \to 0) & = \frac{1}{2} \\ \mathscr{W}(x \to x+1) & = \frac{k}{k+1}, \text{ if } x = 2^n - 1 \\ \mathscr{W}(x \to x-1) & = \frac{1}{k+1}, \text{ if } x = 2^n - 1 \\ \mathscr{W}(x \to x \pm 1) & = \frac{1}{2}, \text{ otherwise} \end{cases} \tag{4.26}$$

The reduction of the problem to a one–dimensional random walk is not surprising and is essentially the same technique applied, for example, to the case of the Cayley Tree in Redner [2001]. Using Eq. (4.26) the probability density as well as the moments–behaviour with the elapsed time can be computed by iterating numerically the master equation

$$\mathscr{P}_{t+1}(x) = \sum_{m} \mathscr{P}_t(m)\mathscr{W}(m \to x) \tag{4.27}$$

Fig. 4.11 shows the result obtained directly by using the master equation for the case $k = 2$ and considering the initial condition

$$\mathscr{P}_0(x) = \frac{1}{2}(\delta_{x,0} + \delta_{x,1})$$

In particular it is shown the moments behaviour $\langle x^q \rangle \sim t^{q/2}$ ($q \leq 8$), which is in agreement, at least up to order eighth, with the Gaussian scaling, namely

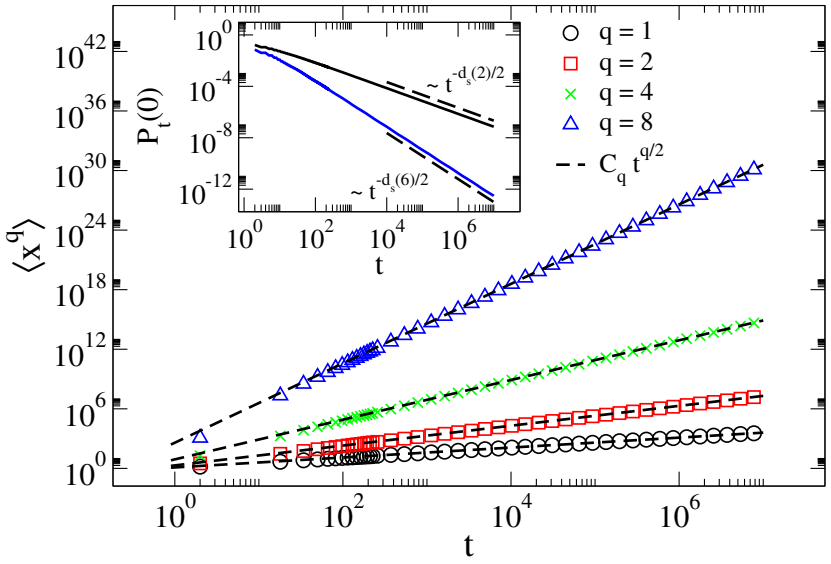

Figure 4.11: *Log–log plot of* $\langle (x_t - x_0)^q \rangle$ *vs time* ($q = 1, 2, 4, 8$, *coloured symbols*) *together with the theoretical prediction in Eq.* (4.29)*;the inset shows the return probability in* t *steps to the origin,* $P_t(\mathcal{O})$ *(see Eq.* (4.8)*), both for* $k = 2$ *(black line) and* $k = 6$ *(blue line), respectively associated to a spectral dimension* $d_s(2) = 2$ *and* $d_s(6) \approx 3.6$.

$\langle x^q \rangle \sim t^{q/2}$; the inset shows the probability to reach the origin of the graph in t steps, $\mathscr{P}_t(\mathcal{O})$, as a function of the time and for two different values of the Tree dimension, namely $k = 2, 6$, giving respectively (see Eq. (4.24)) $d_s = 2$ and $d_s \approx 3.6$; $\mathscr{P}_t(\mathcal{O})$ approaches zero asymptotically in time as a power law, respectively with the exponent $d_s(2)/2$ and $d_s(6)/2$, as predicted in Burioni and Cassi [1994, 1995].

Dashed black lines in the main panel of Fig. 4.11 are plotted by calculating the time behaviour of the moments with a "coarse–grained" approximation of the probability distribution; more specifically, the approximation to the probability distribution can be written as

$$F_t(x) = \frac{2}{\Gamma(d_s/2)(2t)^{d_s/2}} x^{d_s - 1} \, \mathrm{e}^{-x^2/2t} \tag{4.28}$$

which well interpolates the exact numerical result.

The expression (4.28) is a generalization of the radial Gaussian distribution to the case of, generally fractional, spectral dimension $d_s(k)$ and it can be explained by the following argument. Let $\tilde{P}_t \sim \exp(-x^2/2t)$ be the probability density at time t of an unbiased diffusion process defined on a semi–infinite one dimensional line with a perfect reflecting boundary condition in zero. Between two branch points of the NT_k trees we know that the walk is a standard random walk, namely $x(t)$ increase or decrease by one with probability $1/2$; thus at large scales ($x \gg 1$) it is possible to approximate the probability distribution as the product $F_t(x) \propto N_x \tilde{P}_t(x)$, N_x being the number of sites at the

same distance from the tree origin, which can be seen also as the number of independent branches at a given distance x on which a walker can performs the standard random walk; introducing the quantity $n(x)$ defined as the number of branching points between $\mathcal{O}$ and x along a minimal–length path on the tree, we can write $N_x = k^{n(x)}$; an estimation of $n(x)$ can be obtained by observing that the branching points are only those points located at distances given by Eq. (4.25), whose inversion leads to $n(x) = \lfloor \ln x + 1/\ln 2 \rfloor$, which gives $n(x) \approx \ln(x+1)/\ln 2$ at distance x. Now, using the explicit expression for the spectral dimension reported in Eq. (4.24) follows the result $N_x \approx x^{d_x - 1}$, namely

$$F_t(x) \propto x^{d_s - 1}\, \mathrm{e}^{-x^2/2t}$$

which, after normalization, yields the expression (4.28).

The approximate time behaviour of the moments can be computed by using Eq. (4.28) in the usual way

$$\langle x^q(t) \rangle \approx \int_0^\infty dx\; F_t(x) x^q = \quad C_q t^{q/2} \tag{4.29}$$

$$C_q = 2^{q/2} \frac{\Gamma\left(\frac{q+d_s}{2}\right)}{\Gamma\left(\frac{d_s}{2}\right)}$$

whose agreement with numerical moments is really striking (see Fig. 4.11) considering that there are no free parameters. Comparison between the simulated probability density and the approximated one is shown in Fig. 4.12 for the case $k = 2$. Observe that, after rescaling the probability density as $x \to x/\sqrt{\langle x^2 \rangle}$ and $\mathscr{P}_t(x) \to \langle x^2 \rangle \mathscr{P}_t(x)$, namely by using the usual scaling of a Gaussian process, the probability density at different times fully collapses on a single curve; the dashed black line shows the approximation in Eq. (4.28) rescaled at the same way, while the inset shows the probability density for $k = 6$ (black circles) together with the approximated density (red dashed line), emphasizing that the approximated solution which we have found works well for every k .

As a final remark we can conclude this section noting that, despite the geometrical complexity of NT_k trees, the large scale statistical properties of the random walk on this graphs remains Gaussian–like. It is possible to qualitatively understand such behaviour by considering that, if a walker starts from the origin and performs always a step forward on the tree, that is, if its distance from the origin always increases by one, after t steps we will have

$$x(t) = t \approx 2^n - 1$$

with n the number of branching points encountered by the walker during its motion. Inverting the last relation we see that

$$n(t) \sim \ln t$$

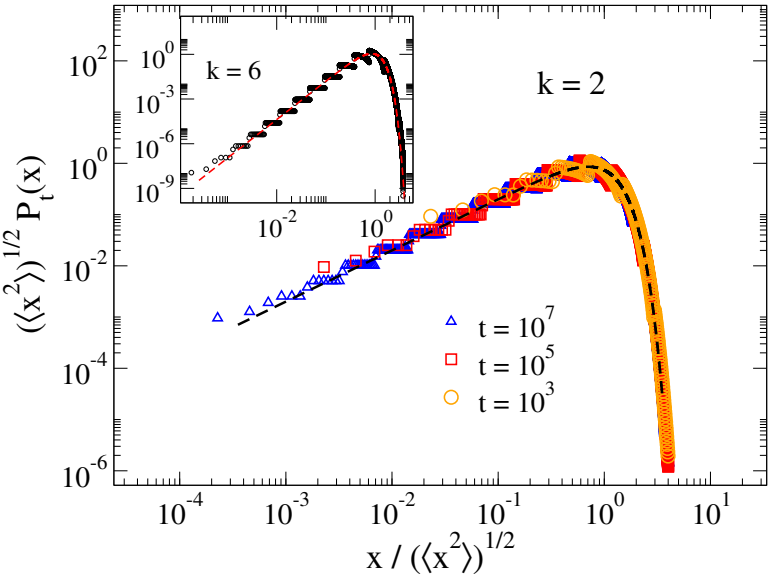

Figure 4.12: *Log–log plot of the rescaled probability density obtained by iterating Eq.* (4.27) *at different times (coloured symbols) and taking* $k = 2$*; the black dashed line represents the "coarse–grained" approximation in Eq.* (4.28)*. Inset shows the same result for* $t = 10^7$ *(black circles) and* $k = 6$ *together the approximation in Eq.* (4.28) *(red dashed line)*

from which follows that the number of branching points visited by a walker during its motion can not grow more faster than $\ln(t)$. Thus, the percentage of time spent by a walker on the branching points will be at most of the order

$$\ln t / t$$

which goes to zero as $t \to \infty$. This means that asymptotically in time a walker will perform a random walk far from the branching points, that is, it will performs a standard random walk.

4.4.2 *Super Nice Trees*

The structure of the NT_k graphs can be easily modified to generate an example of random walk which exhibits standard scaling of all the moments without having a Gaussian probability distribution. For this purpose we change the NT_k structure by defining a new type of tree, which we dub SNT (Super Nice Tree). SNT (see the up panel of Fig. 4.13) can be recursively defined as an NT_k, but at every branching point $x = 2^n - 1$ ($n = 1, 2, 3, \cdots$) the tree splits in k^n branches.

As the previous case, we can refer again to a random walk on the simple one–dimensional line, characterized by well known inhomogeneities in which the jump probabilities change according to the equivalent model showed in the bottom region of Fig. 4.13. In particular we can directly simulate the

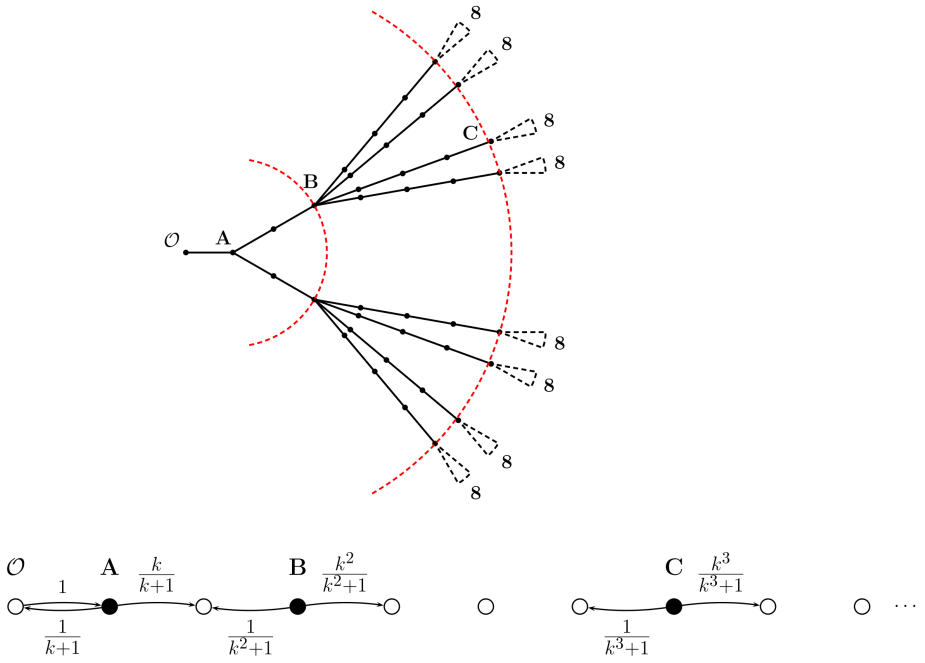

Figure 4.13: *Super Nice Tree and its equivalent model in terms of a one dimensional chain*

probability distribution and the time behaviour of the q–order moments ($q \in \mathbb{N}$) by iterating Eq. (4.27) with the transition matrix given by ($n \in \mathbb{N}$)

$$\begin{cases} \mathscr{W}(0 \to 1) & = 1 \\ \mathscr{W}(1 \to 0) & = \frac{1}{2} \\ \mathscr{W}(x \to x+1) & = \frac{k^n}{k^n+1}, \text{ if } x = 2^n - 1 \\ \mathscr{W}(x \to x-1) & = \frac{1}{k^n+1}, \text{ if } x = 2^n - 1 \\ \mathscr{W}(x \to x \pm 1) & = \frac{1}{2}, \text{ otherwise} \end{cases}$$

Numerical simulations show how, also in this case, the moments behaviour is in agreement with the normal scaling (i.e. $\langle x^q \rangle \sim t^{q/2}$), however the probability distribution is not a Gaussian, see Fig. 4.14

The failure of the scaling $x \to x/\sqrt{\langle x^2 \rangle}$ and $\mathscr{P}_t(x) \to \sqrt{\langle x^2 \rangle}\mathscr{P}_t(x)$ and the corresponding ordinary property $q\nu(q) = q/2$ of the moments, suggest that there should exists a cross–over between two different scaling behaviors separated by a particular value $\tilde{z}$, such that

$$\mathscr{P}_t(x) = \begin{cases} h_t(x), & \frac{x}{\sqrt{t}} \leq \tilde{z} \\ \frac{1}{\sqrt{t}} f\left(\frac{x}{\sqrt{t}}\right), & \frac{x}{\sqrt{t}} \geq \tilde{z} \end{cases}$$

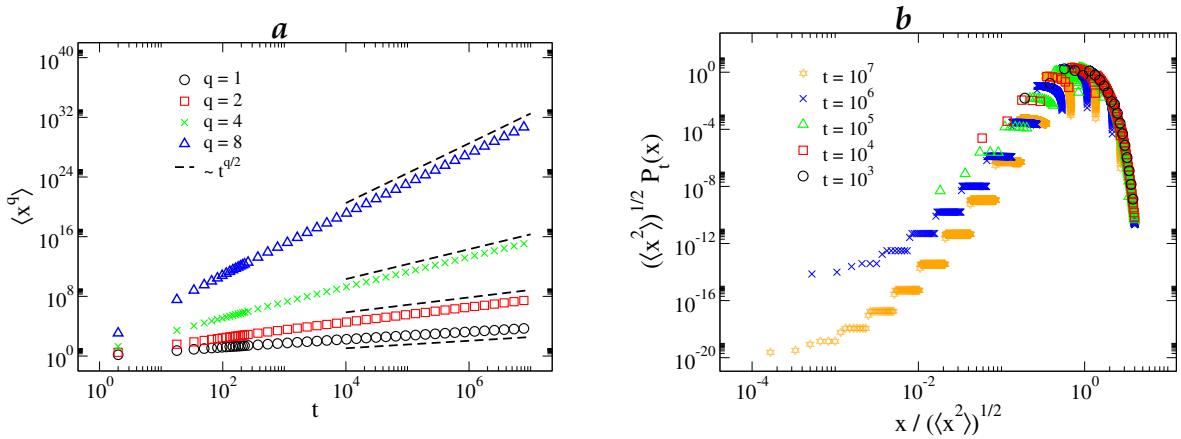

Figure 4.14: ***(a)*** *Time behaviour of the q–order moments ($q = 1, 2, 4, 8$) obtained by simulating a random walk on the structure SNT derived from the NT_2 tree (dashed black lines are proportional to $t^{q/2}$);* ***(b)*** *log–log plot of the rescaled numerical probability densities at different times (coloured symbols); observe how, on small scales, the standard scaling fails, thus highlighting the non Gaussian nature of the process, also if the moments scale in agreement with a Gaussian distribution.*

The above assumption implies that the moments read

$$\begin{aligned} \langle x^q(t) \rangle &= \int_0^{\sqrt{t}\tilde{z}} dx\; x^q h_t(x) + \int_{\sqrt{t}\tilde{z}}^{\infty} dx\; \frac{x^q}{t^{1/2}} f\left(\frac{x}{t^{1/2}}\right) = \\ &= \int_0^{\sqrt{t}\tilde{z}} dx\; x^q h_t(x) + A_q t^{q/2} \end{aligned} \tag{4.30}$$

with $A_q = \int_{\tilde{z}}^{\infty} dz\; z^q f(z)$ a constant depending on q only. The numerical time behaviour of the q–order moments is consistent with the expression in Eq. (4.30) only if the first integral grows slowly than $t^{q/2}$.

4.5 ENTROPIC BREAKING OF THE GENERALIZED FDR

The NT_k trees and the comb–lattice studied in the last sections, enable us to build a more realistic model of diffusion in an highly ramified structures. In particular we can replace the teeth in the simple comb–lattice by an NT_k in the y, z plane (as we performed for the case of the kebab–lattice and the antenna–lattice, see Sec. 4.1.2).

The resulting structure is, as usual, characterized by a main transport direction together with lateral dead–ends, where the particles can be temporarily trapped before to come back on the backbone.

For simplicity, we analyze the case of the NT_2 tree, used to construct the comb teeth, taking an unitary distance between two neighbors teeth. We will call "NT_2–comb" the resulting lattice. In particular, we recall that the spectral dimension for the NT_2 tree (see Eq. (4.24)) is given by $d_s = 2$, which

is the same spectral dimension of the kebab–lattice considered in Sec. 4.1.2 (see Fig. 4.5 **(a)**).

Unlike the comb–like structures studied in Sec. 4.1.2, the NT_2–comb can be used as a toy model useful to point out the qualitative properties related to all those situations in which there is a highly ramified lateral dispersion.

In order to simulate the random walk on the NT_2–comb, we consider the transition matrix in Eq. (4.2) to take into account the jumps along the backbone. The Eq. (4.26) gives the jumping frequencies along the transversal direction, once we interchange x with y and generalize to the case of negative values of y. Practically, every sidebranch, can be considered as a one–dimensional chain, characterized by an infinite number of inhomogeneities situated at $y^* = \pm(2^n - 1)$ ($n \in \mathbb{N}$) from the backbone (i.e. $y = 0$), as discussed in Sec. 4.4.1. In addition, we used $N = 10^6$ particles and an unitary time step.

The mean square displacement does not introduce formal variations respect to the case with $d_s = 2$ treated in Sec. 4.1.2, see Fig. 4.15 **(inset)** compared to Fig. 4.6 **(a)**.

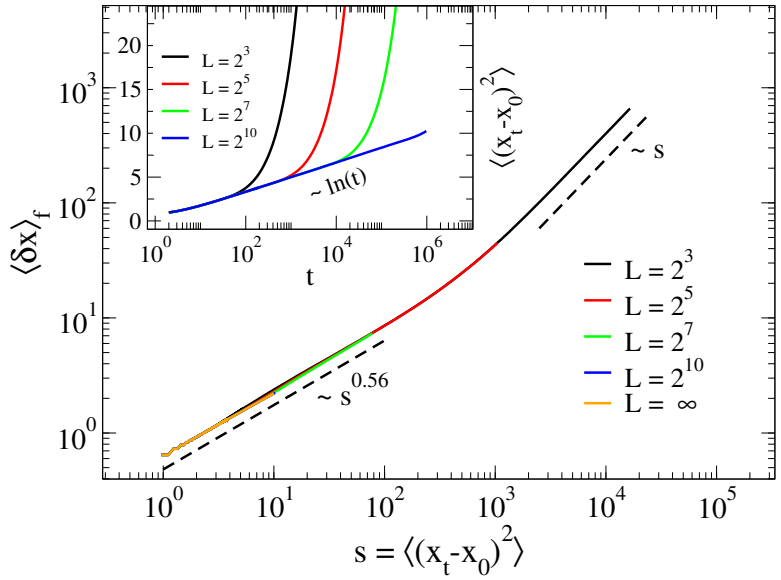

Figure 4.15: *Mean square displacement on log–log scale* ***(inset)*** *and fluctuation dissipation relation* ***(main panel)*** *for the generalized comb–lattice whose teeth are given by NT_2 graphs ($d_s(2) = 2$). Similarly to the case related to the kebab–lattice analyzed in Sec. 4.1.2, the mean square displacement has a pre–asymptotic time behaviour proportional to $\ln(t)$ (see inset); however in this case the FDR (see main panel) is broken, because the branching of the lateral structures acts as an external drift along the transversal direction.*

A different scenario comes into play if we look at the FDR relation when an external bias along the backbone is applied. Contrary to the cases analyzed in Sec. 4.1.2, the geometrical structure of the lateral dead–ends of the

NT_2–comb, introduces a sort of an external drift along the transversal direction, which is due to the inhomogeneities in the jumping probabilities when a walker reaches a branching point y^*. More specifically the unbalance in the transversal direction can be written as

$$\Delta p_y^+ = \left(\frac{k}{k+1} - \frac{1}{2}\right)\delta_{y,y^*}$$

$$\Delta p_y^- = \left(\frac{1}{2} - \frac{1}{k+1}\right)\delta_{y,y^*}$$

thus giving a pure "entropic field" acting on the increasing direction of the lateral structures given by

$$f_y = \Delta p_y^+ + \Delta p_y^- = \frac{k-1}{k+1}\delta_{y,y^*}$$

This entropic field is responsible for the breakdown of the FDR, see the main panel of Fig. 4.15. This is an explicit example in which the geometry has an hard influence on the process. In particular, our result in this section shows how the FDR is more sensitive to the geometrical structure (compare the kebab–lattice with the NT_2–comb) rather than the details of the dynamics, compare Fig. 4.15 **(inset)** with Fig. 4.6 **(a)**. Moreover, we recover another time the manifestation of an entropic–like potential, which is a recurrent topic in this work.

4.6 SUMMARY AND REMARKS

In this chapter we analyzed some discrete random walks on branched structures and an example of CTRW.

Our work was focused on both the asymptotic and the pre–asymptotic properties of such walks. In particular, many of the analyzed systems, show a regime of anomalous transport. Moreover, we also showed that generalized FDRs hold true during the anomalous regime. On the contrary, the "NT_2–comb" considered in Sec. 4.5, clearly shows an entropic breakdown of the generalized FDR at short times, suggesting that FDRs are more sensitive to the geometrical environment rather than to the details of the dynamics.

We analyzed, in contrast to those examples showing anomalous diffusion, a series of situations characterized by a standard scaling of the MSD, however with a non Gaussian probability density. In particular, we investigated an example of CTRW in Sec. 4.3 and the discrete random walk on a highly branched structure (SNT trees) in Sec. 4.4.2. These examples are simple realization of "hidden" anomalies. Indeed, despite the fact that $\langle x^2\rangle \sim t$, the probability density is not Gaussian, suggesting that the exponent ν, frequently used to characterized the anomalous transport via the relation $\langle x^2\rangle \sim t^{2\nu}$ ($2\nu \neq 1$), is not enough to well identify the process. A final remark on this point can be

useful in order to better clarify the role of the anomaly in the diffusive, apparently normal, regime of the random walk when the probability density is not Gaussian. We will discuss here the case of the random walk on the SNT trees studied in Sec. 4.4.2.

The large scale properties of the probability density (see Fig. 4.14 **(b)**) shows the typical scaling expected under the CLT hypothesis (see Chap. 3). This implies that the CLT is not actually violated and, for this reason, we can observe a standard scaling of the q–order moments with the time. However, on small scales, CLT does not hold true. This anomaly reflects on all those problems related to a possible "target–hitting" mechanism on small scales, leading to an *Anomalous Target Searching* (ATS), also under a standard dynamical regime.

5

ANALYTICAL AND NUMERICAL RESULTS ON CONTINUOUS CHANNELS

"Don't Panic !"

Adams [1979]

The entropic diffusive transport within non homogeneous channels [Constantini and Marchesoni, 1999; Reguera and Rubí, 2001; Reguera et al., 2006; Burada et al., 2007, 2008, 2009, 2010; Borromeo and Marchesoni, 2010] is one of the most fascinating example of dynamics influenced by the non trivial geometry of the surrounding environment. As we reviewed in more details in Chap. 1, many implications are related to the constrained diffusion, for example, the separation of DNA fragments moving in narrow channels [Han and Craighead, 2000; Heng et al., 2004] or the emergence of a pre–asymptotic subdiffusive transport [Santamaria et al., 2006] in a spiny dendrite. This retardation is due to a transient trapping of molecules within dendritic spines.

In this chapter we focus on the investigation of the properties of diffusive motion within two–dimensional periodic channels. We will consider the asymptotic as well as the pre–asymptotic regime using both analytical and numerical techniques.

The most common theoretical approach is embodied in the Fick–Jacobs [Jacobs, 1967] approximation and its generalizations [Burada et al., 2009]. The validity of the FJ (Fick–Jacobs) description in the unbiased [Burada et al., 2009, 2007; Marchesoni and Savel'ev, 2009] and biased [Marchesoni, 2010; Borromeo and Marchesoni, 2010] case was extensively studied (see also Chap. 2). In particular, one of the main question related to the unbiased diffusion in the asymptotic regime is the estimation of the effective diffusion coefficient D_{eff} along the longitudinal direction, as a function of the external geometrical parameters [Burada et al., 2009]. It controls the rapidity of the mass spreading, thus affecting, for example, the ability of the particles to hit some target regions on large time and length scales and consequently suggesting a possible engineering of nano–devices in order to get some desirable dynamical property. We derive a simple analytical estimation of D_{eff} without using the FJ approximation, comparing our result with the already known approximations and with numerical data produced by performing Brownian dynamics. More-

over we will also discuss the limits of our approach by taking into account different types of channel geometries.

The asymptotic mobility represents another interesting dynamical property [Borromeo and Marchesoni, 2005, 2010; Marchesoni, 2010; Ghosh et al., 2012b,a] which naturally comes into play when we consider the case of biased diffusion (see also Chap. 2). We will take into account this point by analyzing the effects of the time scales separation between the transversal and longitudinal motion, focusing on both the asymptotic and the pre–asymptotic mobility within the linear response approximation. Few results about the pre–asymptotic properties are already known, most of them are related with the escape problem from a narrow channel into a wide space region [Holcman and Schuss, 2004; Shuss et al., 2007; Dagdug et al., 2007; Holcman and Schuss, 2011]. The emergence of a position dependent microscopic diffusion coefficient was also worked out by analyzing the time scales separation between the transversal and longitudinal motion within the channel [Berezhkovskii and Szabo, 2011]. On the contrary, our work on the pre–asymptotic properties will be focused on the transient behaviour of the longitudinal mean square displacement and the "fate" of the FDR (Fluctuation–Dissipation Relation) before and after the cross–over to the standard diffusion. In particular, we show how it is possible to tune the cross–over time of the dynamics along the transport direction by choosing properly the initial distribution of the particles within the channel.

We refer for our discussion to a particular class of channels, characterized by a well defined transport direction together with transversal dead–ends where the particles can be temporarily trapped before to proceed along the longitudinal direction and consequently contribute to the transport process.

5.1 RECALLING THE DIFFUSION EQUATIONS IN CONFINED SYSTEMS

In this section we recall some of the main results reviewed in Chap. 2. We consider the dynamics of sufficiently diluted passive tracers moving into two–dimensional periodic channels, see Fig. 5.1. The single particle trajectory evolves in time according to the Langevin equation [Langevin, 1908; Zwanzig, 2001], whose form in the overdamped regime (high viscosity) can be expressed as

$$\frac{d\mathbf{r}}{dt} = -\frac{\boldsymbol{\nabla} V(\mathbf{r})}{\eta} + \sqrt{2k_B T \eta}\boldsymbol{\xi}_t \tag{5.1}$$

with η the viscous friction coefficient, k_B the Boltzmann constant , T the thermodynamic temperature and $V(\mathbf{r})$ an external field. The stochastic term $\boldsymbol{\xi}_t$ is chosen as a Gaussian white noise:

$$\langle \xi_t^{(i)} \rangle = 0, \quad \langle \xi_t^{(i)} \xi_{t'}^{(j)} \rangle = \delta_{ij}\delta(t-t') \quad i,j = x,y.$$

$$\omega_{\mathrm{Sm}}(x) = \frac{R}{2} + \mathcal{A}\sin^{\gamma}\left(\frac{2\pi x}{L}\right) \qquad \omega_{\mathrm{Sh}}(x) = \begin{cases} \frac{R}{2}, & 0 \le x \le \frac{L}{4} - \frac{\Delta_\kappa}{2} \\ \frac{2\mathcal{A}+R}{2}, & \frac{L}{4} - \frac{\Delta_\kappa}{2} \le x \le \frac{L}{4} + \frac{\Delta_\kappa}{2} \\ \frac{R}{2}, & \frac{L}{4} + \frac{\Delta_\kappa}{2} \le x \le \frac{L}{2} \end{cases}$$

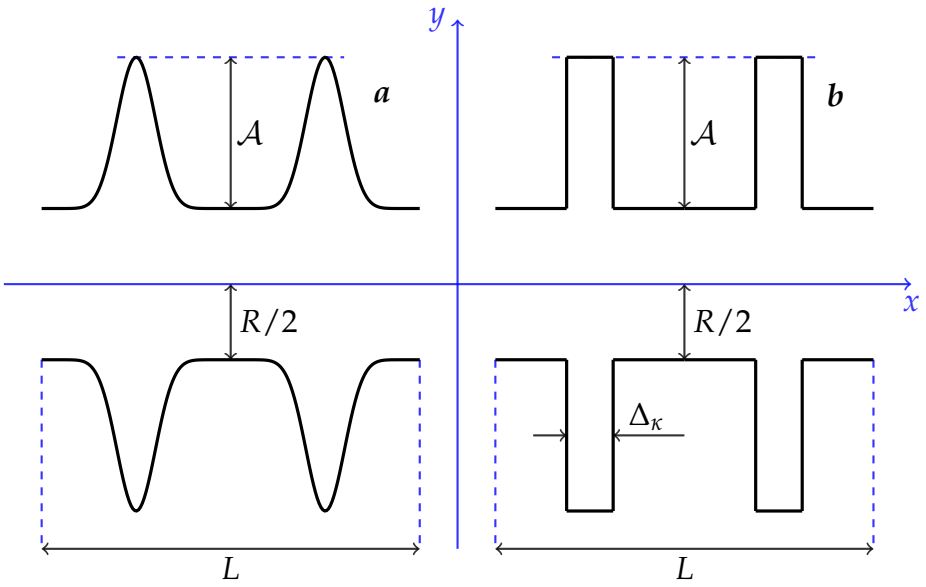

Figure 5.1: *Sketch of the periodic channels considered in this Chapter;* ***(a)*** *Smooth channel (Sm);* ***(b)*** *Sharp channel (Sh)*

The Fokker–Planck equation [Risken, 1989] for the probability density $\mathscr{P}(\mathbf{r}, t)$ (see Chap. 3) related to the stochastic dynamics in Eq. (5.1) can be written as

$$\begin{cases} \partial_t \mathscr{P}(\mathbf{r}, t) + \boldsymbol{\nabla} \cdot \mathbf{J}(\mathbf{r}, t) & = 0 \\ \mathbf{J}(\mathbf{r}, t) & = -\left[\frac{\boldsymbol{\nabla} V(\mathbf{r})}{\gamma} + D_0 \boldsymbol{\nabla}\right] \mathscr{P}(\mathbf{r}, t) \end{cases} \tag{5.2}$$

where $D_0 = k_B T/\eta$ denotes the microscopic diffusion coefficient useful to characterize the particle motion in the free case. Moreover we assume no–flux boundaries:

$$\mathbf{J}(\mathbf{r}, t) \cdot \hat{\mathbf{n}}(\mathbf{r}) = 0, \qquad \mathbf{r} \in \textit{Channel walls} \tag{5.3}$$

with $\hat{\mathbf{n}}(\mathbf{r})$ the local versor outgoing from the channel walls. The problem on the mesoscopic scale is then fully classified by the equations (5.2) and (5.3), however the analytical solution is complicated by the non homogeneous shape of the boundary profile.

In order to simplify the description of the transport properties it is usual to describe the problem in terms of the marginal density [Kalinay and Percus, 2005a, 2006b; Berezhkovskii et al., 2010; Burada et al., 2009] $\mathscr{G}(x, t)$, defined by

$$\mathscr{G}(x, t) = \int_{-\omega(x)}^{+\omega(x)} dy \; \mathscr{P}(x, y, t)$$

where we considered the special case of a symmetric channel respect to the longitudinal axis, described by the boundary profile $\omega(x) > 0$.

The standard approach encloses the information about the non homogeneous boundaries in the generalized FJ equation [Jacobs, 1967; Zwanzig, 1992; Kalinay and Percus, 2006a] given by

$$\frac{\partial \mathscr{G}(x,t)}{\partial t} = \frac{\partial}{\partial x}\left\{\sigma(x)D(x)\frac{\partial}{\partial x}\left[\frac{\mathscr{G}(x,t)}{\sigma(x)}\right]\right\} \tag{5.4}$$

with $\sigma(x)$ the cross–section of the channel taken into account. In the case of a symmetric two–dimensional channel we have $\sigma(x) = 2\omega(x)$. The function $D(x)$ is a microscopic local diffusion coefficient which parametrically depends also from D_0.

The mathematical form of the local diffusion coefficient $D(x)$ is unknown. Zawanzig [Zwanzig, 1992] was the first who perturbatively calculated $D(x)$ under the assumption of small fluctuations from the local equilibrium condition, that is by assuming

$$\mathscr{P}(\mathbf{r},t) = \frac{\mathscr{G}(x,t)}{\sigma(x)} + \delta\mathscr{P}(\mathbf{r},t), \quad \frac{\delta\mathscr{P}(\mathbf{r},t)\sigma(x)}{\mathscr{G}(x,t)} \ll 1$$

He derived for $D(x)$ the expression

$$D_{\mathrm{Zw}}(x) = D_0\left[1 + \frac{1}{12}\left(\frac{d\sigma}{dx}\right)^2\right]^{-1} \tag{5.5}$$

which is valid for a two–dimensional channel.

Before Zwanzig, Fick derived the Eq. (5.4) in the limiting case $\delta\mathscr{P}(\mathbf{r},t) = 0$. In particular he showed that

$$D_{\mathrm{FJ}}(x) = D_0 \tag{5.6}$$

The same result was also explained by Jacobs in his book on diffusive processes [Jacobs, 1967].

Reguera and Rubí (RR) improved the estimation of $D(x)$ proposed by Zwanzig using an heuristic argument [Reguera and Rubí, 2001]. In particular they obtained for the case of a two–dimensional channel the expression

$$D_{\mathrm{RR}}(x) = D_0\left[1 + \frac{1}{4}\left(\frac{d\sigma}{dx}\right)^2\right]^{-1/3} \tag{5.7}$$

Finally, Kalinay and Percus (KP) performed an elegant perturbative treatment to expand $D(x)$ as a linear and non linear combination of terms containing $\sigma(x)$ and its derivatives [Kalinay and Percus, 2005a,b, 2006a,b, 2008].

Neglecting the second and the higher order derivatives of $\sigma(x)$, KP found for $D(x)$ the expression

$$D_{\mathrm{KP}}(x) = D_0 \frac{\arctan\left(\frac{1}{2}\frac{d\sigma(x)}{dx}\right)}{\frac{1}{2}\frac{d\sigma(x)}{dx}} \tag{5.8}$$

which applies in the case of a two–dimensional channel (see Chap. 3)

On large time and length scales, Eq. (5.4) gives a standard diffusive behaviour $\langle (x_t - x_0)^2 \rangle \approx 2D_{\mathrm{eff}}t$. The effective diffusion coefficient, D_{eff}, is given by the Lifson–Jackson (LJ) formula [Lifson and Jackson, 1962]

$$D_{\mathrm{eff}} = \frac{1}{\langle \sigma(x) \rangle \left\langle \frac{1}{D(x)\sigma(x)} \right\rangle} \tag{5.9}$$

where the averages in the denominator have to be understood as

$$\langle f(x) \rangle = \frac{1}{L} \int_{x_0}^{x_0+L} dx\, f(x),$$

being $f(x) = f(x+L)$ whatever periodic function of x

It is interesting to observe that the one–dimensional reduction of the problem can be obtained by writing the Fokker–Planck equation related to the one dimensional Langevin equation given by

$$\frac{dx}{dt} = -\frac{dV(x)}{dx} + \sqrt{2D(x)}\xi_t$$

with the "external" potential

$$V(x) = -k_B T \ln \sigma(x)$$

For this reason $V(x)$ is also called entropic potential: a potential related only to the possible available states in the configuration space.

5.2 ASYMPTOTIC DIFFUSION

Our main goal of this section is a simple analytical expression, useful to estimate the effective diffusion coefficient D_{eff} related to the longitudinal motion; D_{eff} is expected to be lower than its respective value in free space, denoted with D_0 and clearly the slowdown of diffusion is due to the presence of periodically spaced traps, which we dub "humps" (H), related to those regions of the channel such that $|y| > R/2$ (Fig. 5.1). Within the H region the particles spend a certain quantity of time before to come back in the "shaft" (S) region, i.e. $|y| \leq R/2$, and consequently contribute to the transport along the longitudinal direction.

For our discussions we will refer to two types of structures (see Fig. 5.1). Formally, the boundary of the channel in Fig. 5.1 **(a)** will be expressed by the smooth function

$$\omega_{\mathrm{Sm}}(x) = \frac{R}{2} + \mathcal{A}\sin^{\gamma}\left(\frac{2\pi x}{L}\right) \tag{5.10}$$

We will refer hereafter to this channel as the Smooth channel (Sm). The channel boundary in Fig. 5.1 **(b)** is characterized by the sharp profile

$$\omega_{\mathrm{Sh}}(x) = \begin{cases} \frac{R}{2}, & 0 \le x \le \frac{L}{4} - \frac{\Delta_\kappa}{2} \\ \frac{2\mathcal{A}+R}{2}, & \frac{L}{4} - \frac{\Delta_\kappa}{2} \le x \le \frac{L}{4} + \frac{\Delta_\kappa}{2} \\ \frac{R}{2}, & \frac{L}{4} + \frac{\Delta_\kappa}{2} \le x \le \frac{L}{2} \end{cases}; \tag{5.11}$$

and we will refer hereafter to this channel as the Sharp channel (Sh). The period of both channels is equal to $L/2$. More complicated boundaries will be taken into account in Sec. 5.6.

In order to estimate analytically D_{eff} we construct a simple one dimensional Markov chain. We observe that in the long time limit the motion along the transverse direction becomes stationary. Thus the probability $P_H(t)$ to be somewhere in the H region and the probability $P_S(t) = 1 - P_H(t)$ to be somewhere in the S region, are characterized both by a constant value. In particular, by assuming ergodicity we have

$$\lim_{t\to\infty} P_S(t) = P_S^{eq} = \frac{\mu(S)}{\mu(H)+\mu(S)}, \tag{5.12}$$

where $\mu(S)$ and $\mu(H)$ are the surface (measure) of the S region and the H region respectively within a single period of the channel. Practically $P_S(t)$ is the probability that *at the instant* t, $N_S(t)$ particles are within the S region, thus $P_S(t) = N_S(t)/N$, being N the total number of diffusing particle within the channel[1].

Asymptotically, we can treat the motion along the transport direction as a simple random walk on a one–dimensional lattice such that, at every fixed time step δt, a walker on a given site can jump on the right with probability $P_S^{eq}/2$, on the left with probability $P_S^{eq}/2$ or it can remain on the same site with probability P_H^{eq}. By construction, the random walk with non zero P_H^{eq} leads to a reduction of the diffusion coefficient, due to the fact that, at every time step a walker can be trapped on a given site. We expect for this model an asymptotic standard diffusion with an effective diffusion coefficient $D_{\mathrm{eff}} < D_0$, being D_0 the free diffusion coefficient in the limit $P_H^{eq} = 0$. The mean square displacement for this system behaves as

$$\langle x^2 \rangle = 2D_{\mathrm{eff}}t$$

1 Obviously $P_H(t) = (N - N_S(t))/N$

where the asymptotic effective diffusion coefficient can be expressed in the simple form:

$$D_{\text{eff}} = D_0 P_S^{eq} \tag{5.13}$$

If we take into account the Sharp channel in Eq. (5.11), using Eq. (5.12) we have

$$\mu(S) = \frac{RL}{2}, \qquad \mu(H) = 2\mathcal{A}\Delta_\kappa.$$

Thus, using Eq. (5.13), the effective diffusion coefficient for the Sharp channel takes the form

$$\frac{D_{\text{eff}}}{D_0} = \frac{RL}{4\mathcal{A}\Delta_\kappa + RL} \tag{5.14}$$

In the same way, calculating the explicit form of $\mu(S)$ and $\mu(H)$ for the Smooth channel in Eq. (5.10) we obtain the result

$$\frac{D_{\text{eff}}}{D_0} = \frac{\pi R}{2\beta\left(\frac{1}{2}, \frac{\gamma+1}{2}\right)\mathcal{A} + \pi R} \tag{5.15}$$

with $\beta(\cdot,\cdot)$ the Euler beta function.

In order to verify our analytical result in Eq. (5.13) and the particular cases in Eq. (5.14) and E. (5.15) we performed numerical simulations by integrating the overdamped Langevin equation in (5.1) with $V(\mathbf{r}) = 0$, assuming no–flux boundaries. For our simulations we taken $N = 7 \times 10^4$ particles, $D_0 = 1$ and a time step of 0.005. In order to avoid a particle flux outgoing from the channel we used both a rejection method and a numerical routine useful to calculate the reflection at the boundaries. We found that the results was the same. For this reason in the following, we present the simulations performed using the rejection method, which we preferred because it is more fast. In addition we chosen as geometrical parameters for both channels (see Fig. 5.1) $R = 4$, $L = 10$ and $\mathcal{A} = 2^{-1}, 2^2, 2^4, \cdots 2^{14}$; in addition, only for the Smooth channel we fixed $\gamma = 10$ (Eq. (5.10)), while the value of $\Delta_\kappa = 1.23 \approx R/4$ for the Sharp channel (Eq. (5.11)) was fixed to have the numerical value given by the Eq. (5.15) equivalent to the value obtained using Eq. (5.14), in order to compare the results for both channels.

The numerical results are shown in Fig. 5.2. The black circles refer to the Smooth channel, whereas the black squares embodies to the Sharp channel case. The solid black line represents the theoretical estimation given in Eq. (5.14) and Eq. (5.15).

In the case of the Smooth channel it is possible to calculate the value of the effective diffusion coefficient using also the LJ formula given in Eq. (5.9); the dashed coloured lines in Fig. 5.2 show the results of such calculation, where the integrals in Eq. (5.9) was performed numerically.

The LJ formula does not apply for the Sharp Channel, being $\omega_{\text{Sh}}(x)$ not derivable everywhere. In principle the singularities of the Sharp channel can

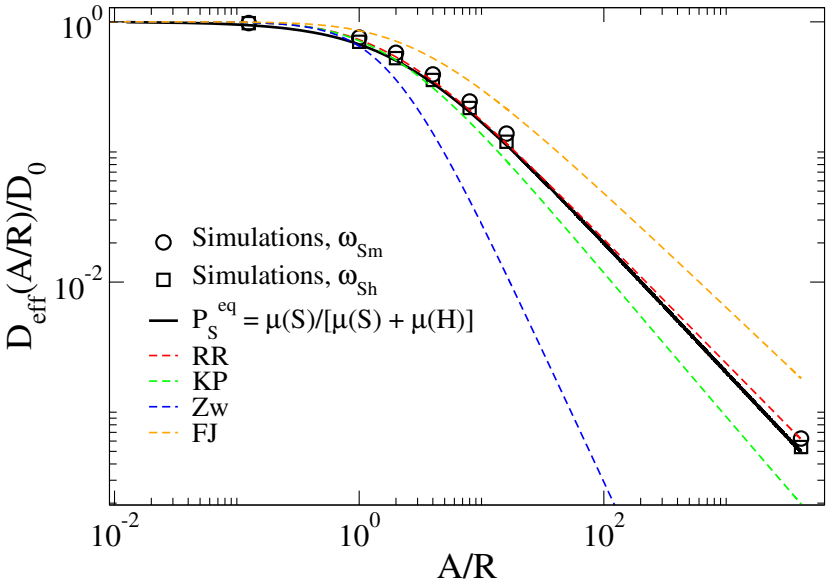

Figure 5.2: *Log–log Plot of the Eq.* (5.14) *and Eq.* (5.15) *(continuum black line) vs* $\mathcal{A}/R$ *together with the simulated data: circles show the case related to the Smooth channel whereas squares represent the case related to the Sharp channel. The simulations are compared to the results obtained for the Smooth channel using Eq.* (5.9) *with* $D_{RR}(x)$ *(red),* $D_{KP}(x)$ *(green),* $D_{Zw}(x)$ *(blue) and* $D_{FJ}(x)$ *(orange) (see Sec. 5.1).*

be treated by expanding $\omega_{\text{Sh}}(x)$ in Fourier series, which is differentiable term by term. However this approach is technically hard and in every case such regularization procedure does not work if $\omega_{\text{Sh}}(x)$ is a multivalued function of x, as we will discuss in Sec. 5.6. Moreover, almost all the calculation of the microscopic diffusion coefficient $D(x)$, are related with perturbative treatments, implying that the greater is the perturbation of a given channel from the flat cylindrical geometry, the greater will be the error introduced by a perturbative approach. Obviously it is possible to work out higher order terms in the perturbative series, for example the series calculated by KP (see Eq. (2.36)), however such calculations, typically, are not simple to perform. Another approach which can be more useful than the FJ approximation in the case of the Sharp channel is based on the boundary homogenization [Berezhkovskii et al., 2006, 2009, 2010; Makhnovskiia et al., 2010], see also Chap. 2. Berezhkovskii and co–workers performed a calculation of the effective diffusion coefficient for the Sharp Channel, however as the authors explain, their result is valid only when $2\Delta_\kappa \geq 2A + R$, which is not the case taken in account here.

Our approach, which is a different elaboration of the result previously suggested by Dagdug et al. [2007], well reproduces the simulated data, however also this simple picture can not work in every cases, as we will try to critical explain in Sec. 5.6.

5.3 TRANSIENT MSD AND FDR: RECOVERING THE COMB LATTICE

In this section we show the relation between the comb–lattice studied in the previous chapter and the asymptotic result discussed in the last section. Actually, the qualitative equivalence between the geometry of the comb–lattice (see Fig. 4.1) and the channels considered in this section, can be used to generalize the results found in Sec. 4.1, to the present case of diffusion in periodic channels.

In order to write the equation for the transient MSD and the effective diffusion coefficient we briefly recall our results about the calculations performed on the comb–lattice in Sec. 4.1.

The longitudinal MSD for the comb lattice with finite length sidebranches and unitary space and time increments, satisfies the relation (see Eq. (4.4))

$$\frac{\langle (x_N - x_0)^2 \rangle}{2N} = F_{\mathrm{B}}(N)$$

being $F_B(N)$ the mean percentage of time (frequency) which a given walker spends in the backbone during the time "interval" $[0, N]$ ($F_{\mathrm{B}}(N)$ was called μ_t in Eq. (4.4)).

We assume that the last relation holds true also for the diffusion within the periodic channels taken into account in the last section (see Fig. 5.1), provided that it must be compared with the numerical results (see the following sections). When we consider the above equation for the continuous case within a time interval $[0, t]$, contrary to the discrete case, such relation must be verified instantaneously, independently by the length of the interval $[0, t]$. In particular, for small intervals, we have $\langle (x_t - x_0)^2 \rangle / t \approx d\langle (x_t - x_0)^2 \rangle / dt$ and we get the generalized form

$$\frac{1}{2D_0} \frac{d\langle (x_t - x_0)^2 \rangle}{dt} = P_{\mathrm{S}}(t) \tag{5.16}$$

with $P_S(t)$ the *instantaneous* probability to be somewhere in the Shaft region. The Eq. (5.16) was firstly used, without presenting a derivation, by Dagdug et al. [2007] in order to study the escape problem from a narrow channel into a wide one. Our "derivation" is obviously informal. Moreover, Eq. (5.16) cannot be extended to arbitrary periodic channels, as we will discuss in Sec. 5.6.

Similarly to the case relative to the MSD, we can generalize the relation in Eq. (4.6), obtained for the random walk performed on the comb–lattice with a non vanishing external drift f along the backbone. The equation for the mean drift $\langle \delta x_N \rangle_f$ is

$$\frac{\langle \delta x_N \rangle_f}{fN} = F_{\mathrm{B}}(N)$$

with $F_B(N)$ the same as in the case with $f = 0$. The generalized transient form of the above equation for the continuous case, at least within the linear response approximation, is give by

$$\frac{1}{fv_0}\frac{d\langle \delta x_t\rangle_f}{dt} = P_S(t) \tag{5.17}$$

where we introduced the free mobility

$$v_0 = \frac{D_0}{k_B T}$$

An immediate consequence of the relations in Eq. (5.16) and Eq. (5.17) is the validity at any time of the FDR in the linear response approximation. We recall that when there are not geometrical constraints on the particle motion, the Einstein FDR reads

$$\frac{\langle \delta x_t\rangle_f}{\langle (x_t - x_0)^2\rangle_0} = \frac{f}{2k_B T}$$

where $\langle \delta x_t\rangle_f = \langle (x_t - x_0)\rangle_f - \langle (x_t - x_0)\rangle_0$, being $\langle \cdots \rangle_\phi$ the average over the particle ensemble calculated with ($\phi = f$) or without ($\phi = 0$) considering the influence of the external field $\mathbf{F} = f\hat{\mathbf{x}}$; k_B is the Boltzmann constant and T the absolute thermodynamic temperature. In the present case of diffusion within periodic channels, due to the transient behaviour in Eq. (5.16) and Eq. (5.17), we have

$$\frac{\langle \delta x_t\rangle_f}{\langle (x_t - x_0)^2\rangle_0} = \frac{\frac{fD_0}{k_B T}\int_0^t dz\ P_S(z)}{2D_0\int_0^t dz\ P_S(z)} = \frac{f}{2k_B T} \tag{5.18}$$

implying that the FDR forgets completely the geometry of the channels, being it contained in $P_S(t)$. Individually, both the transient MSD and FDR depend on the geometry and (as we explain in the next section) by the initial particle distribution, however, their ratio is characterized by a perfect magnification, as we just discussed for the comb–lattice.

The asymptotic limit for the MSD and the mean drift are given by

$$\langle (x_t - x_0)^2\rangle \approx P_S^{eq} D_0 t = D_{\text{eff}} t$$

$$\langle \delta x_t\rangle_f \approx P_S^{eq} f v_0 t = f v_{\text{eff}} t$$

where $D_{\text{eff}} = D_0 P_S^{eq}$ and $v_{\text{eff}} = D_{\text{eff}}/k_B T$ can be calculated using Eq. (5.12).

The asymptotic formula for the mean drift can be also obtained in another way, using a "small" f expansion of the non linear mobility. In Chap. 2 we reviewed the results about the non linear mobility $v(f)$ in the asymptotic

regime [Burada et al., 2007; Borromeo and Marchesoni, 2010; Ghosh et al., 2012a,b]. In order to make the exposition clear we summarize here the result

$$v(f) = \frac{L(1 - \mathrm{e}^{-\beta f L})}{f \int_0^L dx\, \mathrm{e}^{-\beta U(x)} \int_{x_0}^{x_0+L} dx'\, \frac{\mathrm{e}^{\beta U(x')}}{D(x')}}$$

$$\xrightarrow[f\to 0]{} \frac{D_{\mathrm{eff}}^{(\mathrm{FJ})}}{k_{\mathrm{B}} T}$$

with $D_{\mathrm{eff}}^{(\mathrm{FJ})}$ given by the LJ [Lifson and Jackson, 1962] formula in Eq. (5.9) and $U(x) = -fx - k_{\mathrm{B}} T \ln \sigma(x)$. Asymptotically in time, we thus find the same expression for the mean drift behaviour. Moreover, with reference to Fig. 5.2, we see that the FJ estimation of the effective diffusion coefficient using $D_{RR}(x)$ (see Eq. (5.7)), is in agreement with our estimation of $D_{\mathrm{eff}} = D_0 P_S^{eq}$. From this, we can conclude that the two approaches give approximately the same results, whereas other estimations of $D_{\mathrm{eff}}^{(LJ)}$ using $D_{\mathrm{Zw}}(x)$ (Eq. (5.5)), $D_{\mathrm{FJ}}(x)$ (Eq. (5.6)) or $D_{KP}(x)$ (Eq. (5.8)) can be discarded, at lest for the present study, being them not in agreement with the simulating data.

We finish the section by stressing that the key quantity for the pre–asymptotic transport is the probability $P_S(t)$. We will show in the next section how it is possible to find such quantity, starting from a simple kinetic model, whereas in Sec. 5.5 we present a numerical verification of the Eq. (5.18). Finally in Sec. 5.6 we will discuss the limits and benefits of the present approach.

5.4 PRE–ASYMPTOTIC PROPERTIES.

The study of the pre–asymptotic regime is important in order to have informations about the trapping process of the H region. Indeed the transient trapping of molecules within the H region can induce a pre–asymptotic regime characterized by a time behaviour of the mean square displacement slower than the standard diffusive one. As a consequence we expect that there exists a cross–over time τ_x between the asymptotic and pre–asymptotic motion. We found that τ_x can be tuned by taking a different initial particle distribution within the channel, so $\tau_x(\mathbf{r}_0)$ is a function of the initial particle position, being $\mathbf{r}_0$ a short notation to write the initial position of all the particles. More specifically we considered three types of initial conditions: an initial distribution with the particles uniformly distributed in one period of the S region, $\mathbf{r}_0 \in S$, another one with the particles uniformly distributed in one period of the H region, $\mathbf{r}_0 \in H$, and finally an initial condition with the particles uniformly distributed within one period of the whole surface of the channel, $\mathbf{r}_0 \in (S \cup H)$.

When the local equilibrium assumption is fulfilled (i.e. $|d\omega(x)/dx| \ll 1$, see Sec. 2.4), we have $\tau_x \gg \tau_y$, being τ_y the typical relaxation time related to the transversal motion. However, when strong fluctuations from the local equilibrium condition occur, we can have also the opposite case: $\tau_y \gg \tau_x$. In this situation, the pre–asymptotic transversal motion has a strong influence on the pre–asymptotic properties of the longitudinal one.

The Fig. 5.3 shows the longitudinal MSD on the log–log scale for the different initial distributions defined above. In particular, the case with $\mathcal{A} = 2^6$ is shown specialized for the Brownian dynamics performed within the Sharp channel shown in Fig. 5.1 **(b)** (the inset shows the same result for $\mathcal{A} = 2^3$), emphasizing the strong dependence of the dynamics by the initial condition during the pre–asymptotic motion. The details of the simulations are reported in Sec. 5.2, while in Sec. 5.6 we will discuss why we considered the Sharp channel, rather than the Smooth one. squares symbols in Fig. 5.3 represent the MSD when $\mathbf{r}_0 \in H$, triangles are associated to $\mathbf{r}_0 \in \left(S \cup H\right)$ and circles are relative to the case $\mathbf{r}_0 \in S$; the meaning of the coloured dashed lines will be clear immediately.

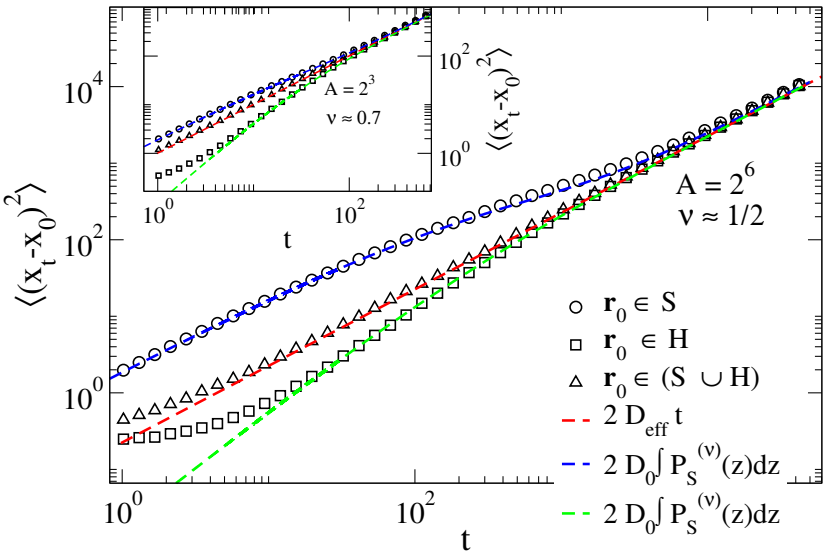

Figure 5.3: *Log–log plot of $\langle (\Delta x_t)^2 \rangle$ as a function of the time for $\mathcal{A} = 2^6$ and three different initial conditions:* ***(squares)*** $\mathbf{r}_0 \in H$; ***(triangles)*** $\mathbf{r}_0 \in (H \cup S)$; ***(circles)*** $\mathbf{r}_0 \in S$. *The inset shows the same result for $\mathcal{A} = 2^3$ while the coloured dashed lines represent the model explained in Eq. (5.21)*

It is possible to qualitatively understand the analytical form of $\langle (\Delta x_t)^2 \rangle$ as a function of the elapsed time, given the initial condition. The result is strongly influenced by the transverse motion and, in order to highlight this point we will use the relation found in the last section

$$\langle (\Delta x_t)^2 \rangle = 2D_0 \int_0^t dz \; P_S(z) \tag{5.19}$$

Before to show the results for the transient mean square displacement, we emphasize that Eq. (5.19) has meaning only if the S and H regions can be unambiguously identified, as we will discuss in more details in Sec. 5.6. When this distinction of the channel in two main areas applies, we can perform a coarse–graining description of the process in terms of a two state kinetic model. More specifically, we introduce the "S state", characterized by the probability $P_S(t)$ and the "H state", to which is associated the probability $P_H(t) = 1 - P_S(t)$. In addition, $k_S(t)$ and $k_H(t)$ are the transition rates between these two states. The kinetic equation which rules the evolution of the probability $P_S(t)$ is thus given by

$$\frac{dP_S(t)}{dt} = -k_S(t)P_S(t) + \Big(1 - P_S(t)\Big)k_H(t) \tag{5.20}$$

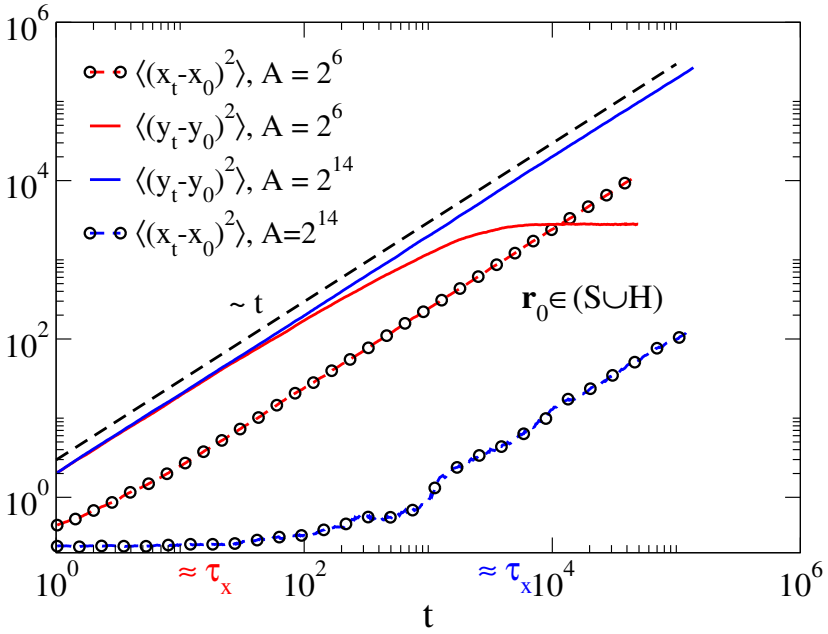

Figure 5.4: *Log–log plot of the transversal mean square displacement $\langle(y_t - y_0)^2\rangle$ (continuum blue and red lines) as a function of the time. It is well evident that in this case $\tau_x \ll \tau_y$ (see the dashed blue and red lines), thus for $\tau_x \lesssim t \ll \tau_y$, $\langle(\Delta y_t)^2\rangle \sim t$, supporting the derivation of the Eq. (5.21).*

The motion along the longitudinal direction can not modify the transitions between the S and H states. Thus, such transitions, will be related only to the velocity in the variations of the transversal process. So Before the equilibration of the transversal motion, we can reasonably assume

$$k_R(t) \sim \frac{d}{dt}\sqrt{\langle(y_t - y_0)^2\rangle}, \qquad R = S, H$$

At this point we take into account separately two main situations, say $\mathcal{A} \to \infty$ and $\mathcal{A} \to 0$.

- $\mathcal{A} \to \infty$
  When $\mathcal{A} \to \infty$ in Eq. (5.10) or Eq. (5.11), strong fluctuations from the local equilibrium assumption can take place, leading to the time scales separation $\tau_x \ll \tau_y$, see Fig. 5.4. In this limiting case, as it is shown in Fig. 5.4, for $\tau_x \lesssim t \ll \tau_y$ we have $\langle(\Delta y_t)^2\rangle \sim t$, which implies $k_R(t) \sim t^{-1/2}$. So integrating Eq. (5.20) we get the solution

$$P_S(t) = P_S(0) \exp\left[-\left(\frac{t}{\tau_0}\right)^{1/2}\right] + \frac{D_{\text{eff}}}{D_0}\left\{1 - \exp\left[-\left(\frac{t}{\tau_0}\right)^{1/2}\right]\right\} \quad (5.21)$$

  where τ_0 is a phenomenological parameter and, in agreement with Eq. (5.13), we substituted P_S^{eq} with D_{eff}/D_0 in the second term. The phenomenological function (5.21) can be used to calculate the time behaviour $\langle(\Delta x_t)^2\rangle$ applying Eq. (5.19). The result is shown in Fig. 5.3**(main panel)**. The blue dashed line is the result of the integration of Eq. (5.21) taking $P_S(0) = 1$, that is, $\mathbf{r}_0 \in S$. When the particles start in the H region we have $P_S(0) = 0$ and the integration of Eq. (5.21) leads to the dashed green line showed in Fig. 5.3. Finally, when $P_S(0) = P_S^{eq}$, that is $\mathbf{r}_0 \in (S \cup H)$, the first and the third term of the Eq. (5.21) cancel out and we should have directly a standard diffusive behaviour, characterized by the diffusion coefficient D_{eff}, as shown by the red dashed line. The agreement is satisfactory considering that the Eq. (5.21) follows from a simple argument, based on reasonable assumptions, however not rigorous. The free parameter τ_0 has to be adjusted with a fit procedure, for example, comparing Eq. (5.21) directly with the numerical behaviour of $P_S(t)$, in particular, for $\mathcal{A} = 2^6$ it is found that $\tau_0 \approx 35$.

- $\mathcal{A} \to 0$
  The opposite regime is given by the case with $\mathcal{A}$ comparable with all the other geometrical parameters. In this case we found that it is possible to generalize Eq. (5.21) with the more general function (see Fig. 5.3 **(inset)**)

$$P_S^{(\nu)}(t) = P_S(0) \exp\left[-\left(\frac{t}{\tau_0}\right)^{\nu}\right] + \frac{D_{\text{eff}}}{D_0}\left\{1 - \exp\left[-\left(\frac{t}{\tau_0}\right)^{\nu}\right]\right\}$$

  where ν is another fit parameter. For example, when $\mathcal{A} = 2^3$ we found that $\tau_0 \approx 18$ and $\nu \approx 0.7$.

5.5 PRE–ASYMPTOTIC RESPONSE TO AN EXTERNAL FIELD

We now focus on the transport problem in a two–dimensional periodic channel considering a non vanishing external longitudinal field $\mathbf{F} = f\hat{\mathbf{x}}$ in the linear response regime, that is, when $fL/k_BT \ll 2$ (recall that the period of the Sharp channel and the Smooth channel is $L/2$).

We just analyzed the FDR in Chap. 4, taking into account some branched structures. It is natural to wonder if the the FDR holds true both in the asymptotic and the pre–asymptotic regime for the present case of diffusion within periodic channels. According to our reasoning in Sec. 5.3 and the Eq. (5.18) we expect that, at least within the linear response approximation, the FDR does not depend on the geometry of the considered channels.

Here we present the comparison between the results obtained performing Brownian dynamics within the Sharp Channel and the analytical result in Eq. (5.18), which, in dimensionless units (see Chap. 2) reads[2]

$$\frac{\langle \delta x_t \rangle_f}{\langle (x_t - x_0)^2 \rangle_0} = \frac{f}{2}, \qquad \text{with } f \to f = \frac{fL}{k_B T}, \quad x \to x = \frac{x}{L} \tag{5.22}$$

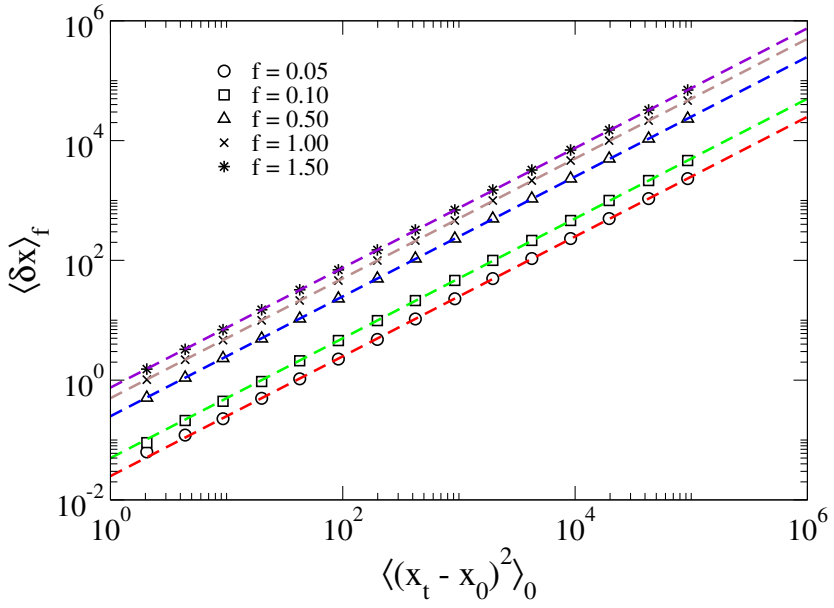

Figure 5.5: *Log–log plot of $\langle \delta x_t \rangle_f$ vs $\langle (x_t - x_0)^2 \rangle_0$ (black symbols); the coloured dashed lines represent the theoretical relation in Eq. (5.22). Numerical results (black symbols) are the same for every $\mathcal{A}$ and are independent from the initial particle distribution within the channel. Here is the case of the Sharp channel (see Eq. (5.11)), however the result is exactly the same if we take as boundary $\omega_{Sm}(x)$ (see Eq. (5.10)).*

We performed numerical simulations taking as external field the values $f = 0.05, 0.1, 0.5, 1.0, 1.5$. The result is plotted in Fig. 5.5. Coloured dashed lines represent Eq. (5.22) and symbols are the numerical results, for every value of $\mathcal{A}$ (see Fig. 5.1) and every initial particle distribution within the channel, showing a perfect magnification between the MSD and the mean drift, as predicted by Eq. (5.18). Thus, despite the fact that individually $\langle \delta x_t \rangle_f$ and $\langle (x_t - x_0)^2 \rangle_0$ depend on both the geometry and the initial particle distribution,

2 The Same result is obtained for the Smooth Channel.

their ratio, at least for small f, forgets completely the confined environment and the way to "relax" and "fluctuate" appears exactly as in the free case, also if the local equilibrium condition is strongly broken.

5.6 DISCUSSION.

In this section we present a discussion on our previous results. We start by analyzing the limits of the approach used to derive the effective diffusion coefficient in Sec. 5.2. To this end it is interesting to compare the previous results with other kind of geometries, as shown in Fig. 5.6.

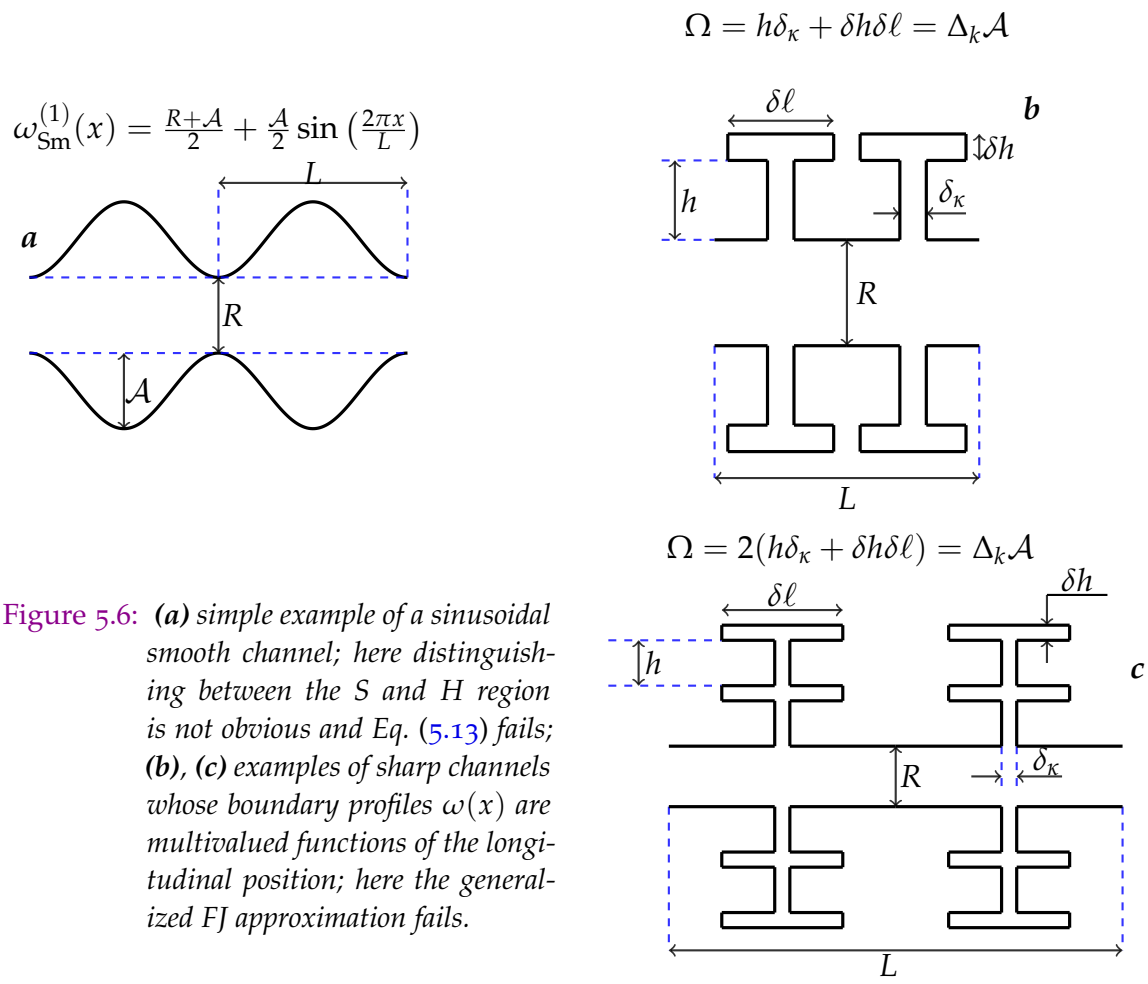

Figure 5.6: ***(a)*** *simple example of a sinusoidal smooth channel; here distinguishing between the S and H region is not obvious and Eq. (5.13) fails;* ***(b)***, ***(c)*** *examples of sharp channels whose boundary profiles $\omega(x)$ are multivalued functions of the longitudinal position; here the generalized FJ approximation fails.*

The derivation of the effective diffusion coefficient proposed in Sec. 5.2, beyond the saturation assumption on the probability $P_S(t)$ and the ergodic hypothesis, is linked to another assumption, which is not less important, namely the subdivision of the channel in two main areas. We dubbed such regions of the channel the "Shaft" region (S), characterized by $|y| \leq R/2$, and the Hump region (H), characterized by $|y| > R/2$ (see Fig. 5.1). Actually, this distinction is exact only for the Sharp channel, whose boundary profile is given by $\omega_{\text{Sh}}(x)$ in Eq. (5.11). For the case of the Smooth Channel, characterized by the boundary profile $\omega_{\text{Sm}}(x)$ we see that, when $\gamma \gg 1$ (see Eq. (5.10)), there is all a region of the channel well approximated by the constant $R/2$, so we can still speak about the S and the H regions. On the contrary, when we take $\gamma = 1$, that is, if we consider the boundary profile

$$\omega^{(1)}_{\text{Sm}}(x) = \frac{R + \mathcal{A}}{2} + \mathcal{A} \sin\left(\frac{2\pi x}{L}\right)$$

the subdivision in two main region S and H is not so obvious and the agreement with Eq. (5.13) will be less better, see Fig. 5.7 **(b)**. The term $\mathcal{A}/2$ in the last equation was added to avoid an overlap of the boundary profile with the longitudinal axis, as shown in Fig. 5.6 **(a)**.

The possibility to distinguish between two main regions of the channel is at the heart of our approach which fails when this particular picture does not apply. Obviously, the same limitations are valid also for the transient MSD and FDR formulas given, respectively, in Eq. (5.16) ans Eq. (5.17). Another problem with our approach concerns the estimation of P_S^{eq} "via ergodic hypothesis". Indeed in those cases characterized by a vanishing measure of the Shaft region, say $\mu(S) = 0$ we would have, simply by applying Eq. (5.12), $D_{\text{eff}} = 0$, which is clearly a wrong result. An example is provided by the Sharp Channel in Fig. 5.1 **(b)** if we take $\Delta_\kappa = L/2$, studied by Borromeo and Marchesoni [2010].

Despite the limitations of our approach, we want now emphasize the benefits. If we can unambiguously subdivide the channel in the regions S and H, the Eq. (5.13), being it based only on the evaluation of the measure of the H region and the S region, should be stable, asymptotically in time, also if we deform the H region; for example, if we consider structures like those in Fig. 5.6 **(b)** and **(c)**.

It is possible to check the stability of Eq. (5.13) by performing numerical simulations of the Eq. (5.1) with $V(\mathbf{r}) = 0$ in such "spiny–like" structures. Let be Ω the surface area of the Hump region of the channels shown in Fig. 5.6 **(b)** and **(c)**. The set up of the geometrical parameters is made up only by fixing, as in Sec. 5.2, the area of the Hump region:

$$\Omega = \mu(H)$$

with $\mu(H)$ the measure of the H region of both the Sharp channel and the Smooth Channel. In addition we used $R = 4$ and $L = 10$.

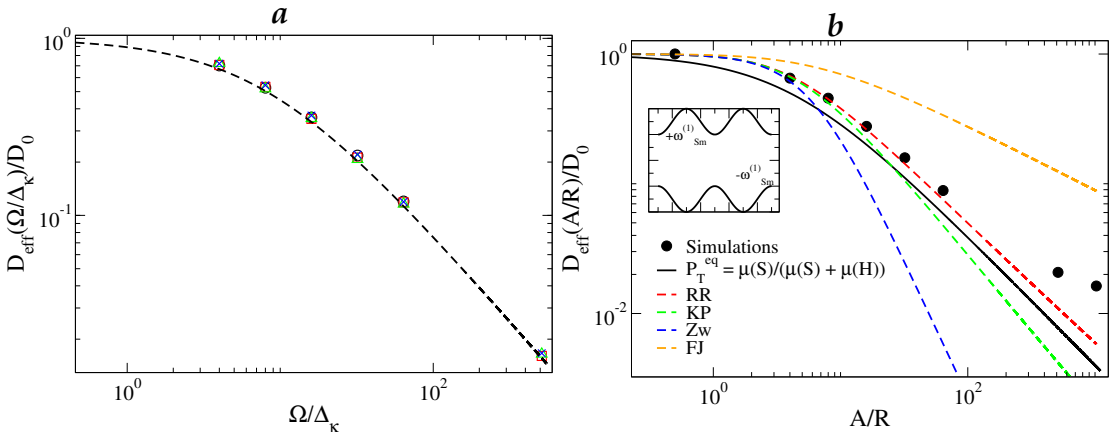

Figure 5.7: ***(a)*** *Log–log plot of the Eq. (5.13) (black dashed line) vs Ω/Δ_κ, specialized for the structures depicted in Fig. 5.6 (b) and (c) together with the simulated data (coloured symbols);* ***(b)*** *log–log plot of the Eq. (5.13) (black continuum line) specialized for the structure in Fig. 5.6 (a) together with the simulated data (black circles) and the results obtained using the generalized FJ approach (coloured dashed lines).*

We performed simulations for $\delta_\kappa \approx R/4$ and $\delta_\kappa = R/2$ (see Fig. 5.6 **(b)** and **(c)**). The results are shown in Fig. 5.7 **(a)** and once again we can observe a good agreement with Eq. (5.13) for the case of the spiny–like structures. On the other hand, as explained above, the agreement becomes less better when the net subdivision of the channel in two main regions fails.

Our results on the pre–asymptotic regime come from a numerical and semi–analytical approach, using as a "guide–line", our results on branched structures discussed in Chap. 4. In particular we found that the longitudinal cross–over time τ_x between the asymptotic and pre–asymptotic motion can be opportunely tuned by choosing properly the initial particle distribution within the channel. With reference to Fig. 5.3, observe that taking all the particles distributed uniformly within the region $\Big(S \cup H\Big)$, the resulting diffusion appears, after a very small transient, immediately standard, namely the MSD increases linearly with the time, as it is highlighted by the triangles in Fig. 5.3 together with the theoretical prediction $\langle (x_t - x_0)^2 \rangle \approx 2D_{\text{eff}}t$ (dashed red line). It is astonishing the fact that also for $\mathcal{A} = 2^6$, for a strong perturbation of the flat cylindrical geometry, the diffusive behaviour is soon established if the particles are initially uniformly distributed within all the entire surface of one period of the channel. In particular from Fig. 5.3 we see that $\tau_x(\mathbf{r}_0 \in S) \gtrsim \tau_x(\mathbf{r}_0 \in H) \equiv \tau_x^{(+)}$, however $\tau_x^{(+)} \gg \tau_x\Big(\mathbf{r}_0 \in (S \cup H)\Big)$. This particular behaviour has enormous consequences on the pre–asymptotic efficiency of the process. Indeed before $\tau_x^{(+)}$ the averaged space covered along the longitudinal direction is such that

$$\langle (x_t - x_0)^2 \rangle_{\mathbf{r}_0 \in H} < \langle (x_t - x_0)^2 \rangle_{\mathbf{r}_0 \in S \cup H} < \langle (x_t - x_0)^2 \rangle_{\mathbf{r}_0 \in S}$$

implying a faster or slower hitting of far regions of the channel with respect to the initial condition in the pre–asymptotic regime. As a consequence, all those processes related to a "target–hitting" mechanism on the time scale $t \ll \tau_x^{(+)}$, are drastically influenced by the pre–asymptotic motion. In particular, the condition $\mathbf{r}_0 \in H$ ensures a localization around the initial condition for $t \lesssim \tau_x^{(+)}$, whereas when $\mathbf{r}_0 \in S$ there is a faster mass spreading within the channel. The "middle way" is characterized by $\mathbf{r}_0 \in (S \cup H)$, resulting almost immediately in a standard diffusive behaviour, so transporting the particles, also when $t \ll \tau_x^{(+)}$, across various periods of the channel, both within the S region and the H region.

6

CONCLUSIONS

"Do! Or do not! There is no try."

Yoda, Star Wars–Episode V

In this work we have discussed some effects on diffusive processes which can be induced by the presence of geometrical constraints. We have considered, as examples of complex geometrical environment, both channels with non homogeneous boundaries and fractal structures. Such environments with an high degree of geometrical complexity are frequently encountered in Nature, for instance in the living cells [Stanley and Meakin, 1988; Bressloff and Newby, 2013]. Moreover, the diffusion in complex frameworks is relevant to recent experiments and applications of nanotechnology [Lebedev et al., 2008; Bancaud et al., 2009; Lieberman-Aiden et al., 2009]. From a theoretical point of view such problems constitute the test–bed for modeling and computational approaches where the thermodynamic limit or the central limit theorem cannot be invoked, in principle, as applicable.

For the case of diffusion on branched structures (see Chap. 4), we shown that the Fluctuation Dissipation Relation (FDR), at least within the linear response approximation, are more sensitive to the geometry, rather than to the details of the dynamics. The striking case is provided by the comb where the teeth are square–lattice plaquettes (see Sec. 4.1.2) and the NT_2–comb (see Sec. 4.5), characterized both by $d_s = 2$ and $\langle (\Delta x_t)^2 \rangle \sim \ln(t)$. However, the generalized FDR is broken at short times in the NT_2–comb case, in particular during the pre–asymptotic regime.

We have also studied some examples of non Gaussian "standard" diffusion. In particular, we showed that also when the CLT holds true on large scale (see the SNT case, Sec. 4.4.2), the non Gaussian scaling at short length scales introduces interesting anomalies, especially if we look at the time behaviour of the hitting probability.

Our results on diffusion within two–dimensional periodic channels, suggest that a control on the geometry of a given channel offers the possibility to tune the diffusion properties along the transport direction in the long time limit. In order to enhance or decrease the diffusion of particles flowing into

a nanoscale channel, it is crucial to know the dependence of the effective diffusion constant D_{eff} on the geometrical properties of the channel. As we reviewed in Chap. 2, there are several attempts and approximation in the literature able to capture the different aspects of such dependence. To reinforce the already existing approximations for D_{eff}, we proposed another approach to estimate analytically D_{eff}, essentially by identifying the asymptotic trapping probability within the lateral dead–ends, as a measure of the trapping region.

We have also analyzed the transient regime before standard diffusion takes place. This pre–asymptotic regime is more complicated and its properties are not universal. It depends crucially both on the channel geometry and the initial particle distribution within the channel. In particular, we found that the cross–over time τ_x on which the longitudinal diffusion becomes standard can be increased by two- or three-order of magnitude by simply changing the system preparation.

A possible further development of this work would amount to considering channels with irregular boundaries. More specifically, three main situations could be taken into account:

- the boundary profile can be written as the sum of two components $\omega(x) = \omega_p(x) + \omega_n(x)$ where $\omega_p(x) = \omega_p(x + L)$ is the periodic part and $\omega_n(x)$ represents a random perturbation with a finite correlation length. This case embodies the situation of quenched disordered boundary Obviously, the effective diffusion coefficient $\mathcal{D}_{\text{eff}}$ becomes a random variable as it depends on specific the realization of the disorder. Also in this case, by using the same mapping procedure explained in Chap. 2, it is possible to derive the effective one–dimensional Fokker–Planck equation. Assuming again the local equilibrium condition, $|d\omega/dx| \ll 1$, the equation is another time in the form of the Fick-Jacobs equation (Eq. (5.4) with $D(x) = D_0$). In this simple limit, using a multiscale analysis similar to the one described in Chap. 2, it is possible to show that the effective diffusion coefficient takes on the expression

$$\mathcal{D}_{\text{eff}} = D_{\text{eff}}\, \mathrm{e}^{-\langle \mathcal{V}_n^2 \rangle}$$

being $\mathcal{V}_n(x)$ the entropic field related to the random perturbation ω_n in dimensionless units. The average $\langle \mathcal{V}_n^2 \rangle$ is given by

$$\langle \mathcal{V}_n^2 \rangle = \frac{1}{L} \int_0^L dx\ \mathcal{V}_n^2(x)$$

and represents the averaged of the entropic field over a unitary cell of the channel, whereas D_{eff} is the effective diffusion coefficient without the disorder (Sec. 2.5)

An interesting development of the theory can be done by investigating the asymptotic diffusion when the local equilibrium condition does not hold true. Two possibilities can be taken into account:

- The external boundaries is a smooth regular function of the time, $\omega(x,t) = \omega(x+L,t)$, with all the time and space derivatives well defined for every order. In this case, invoking again the condition $|d\omega/dx| \ll 1$ and repeating the mapping procedure explained in Chap. 2 we obtain the equation

$$\frac{\partial \mathscr{G}(x,t)}{\partial t} = \frac{\partial}{\partial x}\left\{\sigma(x) D_0 \frac{\partial}{\partial x}\left[\frac{\mathscr{G}(x,t)}{\sigma(x)}\right]\right\} + \frac{d\omega(x,t)}{dt}\mathscr{G}(x,t)$$

- The boundary is of the form

$$\omega(x,t) = \omega(x,t) + \omega_n(x,t)$$

with $\omega_n(x,t)$ an explicit additive dynamical disorder.

In principle, the explicit or induced time dependence ($d\omega(x,t)/dt$)) can lead to resonances, once the geometrical parameters are opportunely chosen or can drive some bias along the longitudinal direction, thus "activating" the process.

All the situations described above are the natural perspectives of our work, in the hope of contributing to shed some light on the complicated and fascinating puzzle named *Transport on the Mesoscale*.

BIBLIOGRAPHY

D. N. Adams. *"The Ultimate Hitchhiker's Guide to the Galaxy"*. The Random House Publishing Group, 1979.

W. J. Adams. *"The Life and Times of the Central Limt Theorem."*. American Mathematical Society, 2009.

S. Alexander and R. L. Orbach. "*Density of states on fractals : ⟨⟨ fractons ⟩⟩*". *J. Phys. (Paris) Lett.*, **43**:625–631, 1982.

K. H. Andersen, P. Castiglione, A. Mazzino, and A. Vulpiani. "*Simple stochastic models showing strong anomalous diffusion*". *The Eur. Phys. Journal B - Condensed Matter and Complex Systems*, **18**:447–452, 2000.

R. Araya, V. Nikolenko, K. B. Eisenthal, and R. Yuste. ""*Sodium channels amplify spine potentials*". *PNAS*, **104**:12347, 2007.

V. E. Arkhincheev. "*Diffusion on random comb structure: effective medium approximation*". *Physica A: Statistical Mechanics and its Applications*, **307**:131–141, 2002.

V. E. Arkhincheev. "*Unified continuum description for sub–diffusion random walks on multi–dimensional comb model*". *Physica A: Statistical Mechanics and its Applications*, **389**:1–6, 2010.

R. D. Astumian and P. Hänggi. "*Brownian Motors*". *Phys. Today*, **55**:33, 2002.

R. Baluscu. "*V–Langevin Equations, Continuous Time Random Walks and Fractional Diffusion.*". *arXiv*, 0704.2517v1, 2006. URL http://arxiv.org/abs/0704.2517.

A. Bancaud, S. Huet, N. Daigle, J. Mozziconacci, J. Beaudouin, and J. Ellenberg. "*Molecular crowding affects diffusion and binding of nuclear proteins in heterochromatin and reveals the fractal organization of chromatin.*". *EMBO J.*, **28**: 3785, 2009.

E. Barkai and V. N. Fleurov. "*Generalized Einstein relation: A stochastic modeling approach*". *Physical Review E*, **58**:1296–1310, 1998.

E. Barkai, R. Metzler, and J. Klafter. "*From continuous time random walks to the fractional Fokker–Planck equation*". *Phys. Rev. E*, **61**:132, 2000.

P. Barthelemy, J. Bertolotti, and D. S. Wiersma. "*A Lévy flight for light*". *Nature*, **453**:495, 2008.

D. ben Avraham and S. Havlin. *"Diffusion and reaction in Fractals and disordered systems"*. Cambridge university press, 2000.

O. Bénichou, C. Chevalier, B. Meyer, and R. Voituriez. "*Facilitated Diffusion of Proteins on Chromatin*". *Phys. Rev. Lett.*, **106**:038102, 2011.

A. Berezhkovskii and A. Szabo. "*Time scale separation leads to position–dependent diffusion along a slow coordinate*". *J. Chem. Phys.*, **135**:074108, 2011.

A. M. Berezhkovskii, Y. A. Makhnovskii, M. I. Monine, V. Yu. Zitserman, and S. Y. Shvartsman. "*Boundary homogenization for trapping by patchy surfaces*". *J. Chem. Phys.*, **121**:11390, 2004.

A. M. Berezhkovskii, M. I. Monine, C. B. Muratov, and S. Y. Shvartsman. "*Homogenization of boundary conditions for surfaces with regular arrays of traps*". *J. Chem. Phys.*, **124**:036103, 2006.

A. M. Berezhkovskii, A. V. Barzykin, and V.Yu. Zitsermanc. "*One–dimmensional description of diffusion in a tube of abruptly changing diameter: Boundary homogenization based approach*". *J. Chem. Phys.*, **131**:224110, 2009.

A. M. Berezhkovskii, M. A. Pustovoit, and S. M. Bezrukov. "*Diffusion in a tube of varying cross section: Numerical study of reduction to effective one–dimensional description.*". *Chem. Phys.*, **367**:110, 2010.

H. C. Berg. *"Random Walks in Biology"*. Princeton University Press, 1983.

H. C. Berg and E. D. Purcell. "*Physics of Chemoreceptions*". *Biophys. J.*, **20**:193, 1977.

H. J. Berg and T. E. J. Behrens. *"Diffusion MRI: from quantitative measurament to in–vivo neuroanatomy"*. Academic Press, 2009.

S. M. Block. "*Making light work with optical tweezers*". *Nature*, **360**:493, 1992.

G. Boffetta and A. Vulpiani. *"Probabilità in Fisica."*. Springer, 2012.

M. Borromeo and F. Marchesoni. "*Noise–assisted transport on symmetric periodic substrates*". *Chaos*, **15**:026110, 2005.

M. Borromeo and F Marchesoni. "*Particle transport in a two–dimensional septate channel*". *Chemical Physics*, **375**:536, 2010.

Jean-P. Bouchaud and A. Georges. *Anomalous diffusion in disordered media: Statistical mechanisms, models and physical applications*". *Physics Reports*, **195**:127–293, 1990.

P. C. Bressloff and B. A. Earnshaw. "*Diffusion–trapping model of receptor trafficking in dendrites*". *Phys. Rev. E*, **75**:041915, 2007.

P. C. Bressloff and J. M. Newby. "*Stochastic models of intracellular transport*". *Rev. Mod. Phys.*, **85**:135–196, 2013.

R. Brown. "*A Brief Acoount of Microscopical Observations made in the Months of June, July, and August, 1827, on the Particles contained in the Pollen of Plants; and on the General Existence of active Molecules in Orgnanic and Inorganic Boidies*". *Philosophical Magazine*, **4**:161, 1827.

P. S. Burada, G. Schmid, D. Reguera, J. M. Rubí, and P. Hänggi. "*Biased diffusion in confined media: Test of the Fick–Jacobs approximation and validity criteria*". *Phys. Rev. E*, **75**:051111, 2007.

P. S. Burada, G. Schmid, P. Talkner, P. Hänggi, D. Reguera, and J. M. Rubí. "*Entropic particles transport in periodic channels*". *BioSystems*, **93**:16, 2008.

P. S. Burada, P. Hänggi, F. Marchesoni, G. Schmid, and P. Talkner. "*Diffusion in confined geometries*". *ChemPhysChem*, **10**:45–54, 2009.

P. S. Burada, G. Schmid, Y. Li, and P. Hänggi. "*Controlling diffusive transport in confined geometries*". *Acta Physica Polonica B*, **41**:935, 2010.

R. Burioni and D. Cassi. "*Fractals without anomalous diffusion*". *Phys. Rev. E*, **49**: R1785–R1787, 1994.

R. Burioni and D. Cassi. "*Spectral dimension of fractal trees*". *Phys. Rev. E*, **51**: 2865–2869, 1995.

R. Burioni and D. Cassi. "*Random walks on graphs: ideas, techniques and results*". *J. Phys. A: Math. Gen*, 38:R45, 2005.

G. Caldarelli and A. Vespignani. *"Large Scale Structure and Dynamics of Complex Networks."*. World Scientific, 2007.

E. F. Casassa and G. C. Berry. "*Angular distribution of intensity of rayleigh scattering from comblike branched molecules*". *J. Poly. Sci. Part A–2*, **4**:881, 1966.

D. Cassi and S. Regina. "*Random walks on kebab lattices: logarithmic diffusion on ordered structures*". *Mod. Phys. Lett. B*, **9**:601–606, 1995.

P. Castiglione, A. Mazzino, P. Muratore-Ginanneschi, and A. Vulpiani. "*On strong anomalous diffusion*". *Physica D: Nonlinear Phenomena*, **134**:75–93, 1999.

M. Cencini, F. Cecconi, and A. Vulpiani. *"Chaos, From Simple Models to Complex Systems"*, volume **17**. Series on Advances in Statistical Mechanics, World Scientific, 2010.

S. Chandrasekhar. "*Stochastic Problems in Physics and Astronomy*". *Rev. Mod. Phys.*, **15**:1–89, 1943.

A. V. Chechkin and R. Klages. "*Fluctuation relations for anomalous dynamics*". *J. of Stat. Mech.: Theory and Experiment*, 2009:L03002, 2009.

A. V. Chechkin, F. Lenz, and R. Klages. "*Normal and Anomalous Fluctuation Relations for Gaussian Stochastic Dynamics*". *J. of Stat. Mech.: Theory and Experiment*, 2012:L11001, 2012a.

A. V. Chechkin, F. Lenz, and R. Klages. "*Normal and anomalous fluctuation relations for Gaussian stochastic dynamics*". *J. of Stat. Mech.: Theory and Experiment*, 2012:L11001, 2012b.

A. J. Chorin and O. H. Hald. *"Stochastic Tools in Mathematics and Science."*. Second Edition, Springer, 2009.

T. C. Choy. *"Effective Medium Theory: Principles and Applications"*. Claredon,Oxford, 1999.

G. Constantini and F. Marchesoni. "*Threshold diffusion in a tilted washboard potential*". *Europhys. Lett.*, **48**:491, 1999.

J. Crank. *"The Mathematics of Diffusion"*. Clarendon Press, 1975.

L. Dagdug, A. M. Berezhkovskii, Y. A. Makhnovskii, and V. Yu. Zitserman. "*Transient diffusion in a tube with dead ends*". *J. Chem. Phys.*, **127**:224712, 2007.

E. De Schutter and P. Smolen. *"Calcium dynamics in large neuronal models."*. In Methods in Neuronal Modeling, C. Koch and I. Segev, eds. (Cambridge, MA: MIT Press), 1998.

P. A. M. Dirac. *"Quantum Mechanics."*. Oxford University Press, Fourth Edition, 1958.

J. F. Douglas, J. Roovers, and K. F. Freed. "*Characterization of branching architecture through "universal" ratios of polymer solution properties*". *Macromolecules*, **23**:4168, 1990.

D. A. Doyle, J. M. Cabral, R. A. Pfuetzner, A. Kuo, J. M. Gulbis, S. L. Cohen, B. T. Chait, and R. MacKinnon. "*The Structure of the Potassium Channel: Molecular Basis of K+ Conduction and Selectivity*". *Science*, **280**:69, 1998.

A. Einstein. "*über die von der molekularkinetischen theorie der wärme geforderte bewegung von in ruhenden flüssigkeiten suspendierten teilchen*". *Annalen der Physik*, **322**:549–560, 1905.

C. P. Fall. *"Computational Cell Biology"*. Springer, 2002.

W. Feller. "*The fundamental limit theorems in probability*". *Bull. Amer. Math. Soc.*, **51**:800, 1945.

W. Feller. *"An Introduction to Probability Theory and Its Applications"*, volume **1**. John Wiley and Sons, 1968.

W. Feller. *"An Introduction to Probability Theory and its Applications."*, volume **2**. Wiley, Second Edition, 1971.

R. P. Feynmann, R. B. Leighton, and S. Matthew. *"The Feynmann lectures on Physics"*, volume **I**. Addison–Wesley Publishing Group, 1977.

J. C. Fiala and K. M. Harris. *"Dentrite structure. In: Dendrites"*. Oxford University Press, 1999.

A. Fick. "*Ueber Diffusion*". *Annalen der Physik*, **170**:59–86, 1855.

H. Fisher. *"A History of the Central Limt Theorem."*. Springer, 2010.

G. Forte, R. Burioni, F. Cecconi, and A. Vulpiani. "*Anomalous diffusion and response in branched systems: a simple analysis*". *J. Phys.: Cond. Mat.*, **25**:465106, 2013a.

G. Forte, F. Cecconi, and A. Vulpiani. "*Non–Anomalous Diffusion is not always Gaussian*". *submitted to EPJ B.*, , 2013b.

T. Franosch, M. Grimm, M. Belushkin, F. M. Mor, G. Foffi, L. Forrò, and S. Jeney. "*Resonances arising from hydrodynamic memory in Brownian motion*". *Nature*, **478**:85, 2011.

E. Frey and K. Kroy. "*Brownian motion: a paradigm of soft matter and biological physics*". *Annalen der Physik*, **14**:20–50, 2005.

F. R. Gantmakher. *"Lecture Notes in Analytical Mechanics."*. Mir Publishers, 1970.

C. W. Gardiner. *"Handbook of Stochastic Methods"*. Springer, 1985.

C. W. Gardiner. *"Stochastic Methods"*. Springer, 2009.

Y. Gefen, A. Aharony, and S. Alexander. "*Anomalous Diffusion on Percolating Clusters*". *Phys. Rev. Lett.*, **50**:77, 1983.

P. K. Ghosh, P. Hänggi, F. Marchesoni, S. Martens, F. Nori, L. Schimansky-G., and G. Schmid. "*Driven Brownian transport through arrays of symmetric obstacles*". *Physical Review E*, **85**:011101, 2012a.

P. K. Ghosh, P. Hänggi, F. Marchesoni, F. Nori, and G. Schmid. "*Brownian transport in corrugated channels with inertia*". *Physical Review E*, **86**:021112, 2012b.

I. Goldhirsch and Y. Gefen. "*Analytic method for calculating properties of random walks on networks*". *Phys. Rev. A*, **33**:2583–2594, 1986.

H. Goldstein, C. P. Poole, and J. L. Safko. *"Classical Mechanics."*. Pearson New International Edition, 1950.

I. Goychuk and P. Hänggi. "*The role of conformational di usion in ion channel gating*". *Physica A*, **325**:9, 2003.

G. Gradenigo, A. Sarracino, D. Villamaina, and A. Vulpiani. *Einstein relation in superdiffusive systems*". *J. of Stat. Mech.: Theory and Experiment*, 2012:L06001, 2012.

T. Graham. "*On the Law od the Diffusion of Gases.*". *Philos. Mag. and J. of Sci.*, **2**: 175, 1833.

K. Hahn and J. Kärger. "*Molecular Dynamics Simulation of Single–File Systems*". *J. of Phy. Chem.*, **100**:316, 1996.

K. Hahn, J. Kärger, and V. Kukla. "*Single–File Diffusion Observation*". *Phys. Rev. Lett.*, **76**:2762, 1996.

O. H. Hald. "*Approximation of Wiener integrals*". *J. Comput. Phys.*, **69**:460, 1987.

J. Han and H. G. Craighead. "*Separation of Long DNA Molecules in a Microfabricated Entropic Trap Array*". *Science*, **288**:1026, 2000.

P. Hänggi and F. Marchesoni. "*100 years of Brownian motion*". *Chaos*, **15**:26101, 2005.

P. Hänggi and F. Marchesoni. "*Artificial Brownian motors: Controlling transport on the nanoscale*". *Reviews of Modern Physics*, **81**:387, 2009.

P. Hänggi, F. Marchesoni, and F. Nori. "*Brownian motors*". *Annalen der Physik*, **14**:51–70, 2005.

S. Havlin and D. ben Avraham. "*Diffusion in disordered media*". *Adv. Phy.*, **51**: 187, 2002.

C. P. Haynes and A. P. Roberts. "*Continuum diffusion on networks: Trees with hyperbranched trunks and fractal branches*". *Phys. Rev. E*, **79**:031111, 2009.

J. B. Heng, C. Ho, T. Kim, R. Timp, A. Aksimentiev, Y. V. Grinkova, S. Sligar, K. Schulten, and G. Timp. "*Sizing DNA Using a Nanometer–Diameter Pore*". *Biophys. J.*, **87**:2905, 2004.

B. Hille. "*Ionic channels in excitable membranes. Current problems and biophysical approaches*". *Biophys. J.*, **22**:283, 1978.

B. Hille. *"Ion Channels of Excitable Membranes"*. Sinauer Associates, Inc., 1992.

A. Hodgkin and A. Huxley. "*Action potentials recorded from inside a nerve fibre*". *J. Physiol. (Lond.)*, **144**:710, 1939.

A. Hodgkin and A. Huxley. "*A quantitative description of membrane current and its application to conduction and excitation in nerve.*". *J. Physiol. (Lond.)*, **117**:500, 1952.

D. Holcman and Z. Schuss. "*Escape Through a Small Opening: Receptor Trafficking in a Synaptic Membrane*". *J. of Stat. Phys.*, **117**:975, 2004. ISSN 0022-4715.

D. Holcman and Z. Schuss. "*Diffusion laws in dendritic spines*". *J. of Math. Neuro.*, **1**:1, 2011.

J. Hrabe, S. Hrabětová, and K. Segethz. "*A Model of Effective Diffusion and Tortuosity in the Extracellular Space of the Brain*". *Biophys. J.*, **87**:1606, 2004.

R. Huang, I. Chavez, K. M. Taute, B. Lukič, S. Jeney, M. G. Raizen, and E. D. Florin. "*Direct observation of the full transition from ballistic to diffusive Brownian motion in a liquid*". *Nat. Phys.*, **7**:576, 2011.

B. D. Hughes. *"Random Walks and Random Environments."*, volume **1**. Oxford (Clarendon Press), 1995.

A. F. Huxley and R. M. Simmons. "*Proposed mechanism of force generation in striated muscle* ". *Nature*, **233**:533, 1971.

T. Inn. *"Electronic Quantum Transport in Mesoscopic Semiconductor Structures"*. Springer Tracts in Modern Physics, 2004.

K. Itô and H. McKean. *"Diffusion Processes and Their Sample Paths"*. Springer–Verlag, Berlin, 1974.

C. Itzykson and J. M. Drouffe. *"From Brownian motion to renormalization and lattice gauge theory"*, volume **I**. Cambridge University Press, 1989.

J. D. Jackson. "*CLassical Electrodynamics*". *Nature*, **233**:533, 1971.

M. H. Jacobs. *"Diffusion Processes"*. Springer, 1967.

Y. N. Jan and L. Y. Jan. "*Branching out: mechanisms of dendritic arborization*". *Nat. Rev. Neuros.*, **11**:316, 2010.

R. S. Johnson. *"Singular Perturbation Theory"*. Springer, 2005.

P. Kalinay and J. K. Percus. "*Projection of 2D diffusion in a narrow channel onto the longitudinal dimension*". *J. Chem. Phys.*, **122**:204701, 2005a.

P. Kalinay and J. K. Percus. "*Extended Fick–Jacobs equation: Variational approach*". *Phys. Rev. E*, **72**:061203, 2005b.

P. Kalinay and J. K. Percus. "*Corrections to the Fick–Jacobs equations*". *Phys. Rev. E*, **74**:041203, 2006a.

P. Kalinay and J. K. Percus. "*Exact dimensional reduction of linear dynamics*". *J. Stat. Phys.*, **123**:1059, 2006b.

P. Kalinay and J. K. Percus. "*Approximation of the generalized Fick–Jacobs equation*". *Phys. Rev. E*, **78**:021103, 2008.

J. Kärger and D. M. Ruthven. *"Diffusion in zeolites and other microporous solids."*. Willey and Sons, 1992.

V. M. Kenkre, E. W. Montroll, and M. F. Shlesinger. Generalized master equations for continuous–time random walks. *J. of Stat. Phys.*, **9**:45, 1973.

J. Klafter and R. Silbey. "*Derivation of the Continuous–Time Random–Walk Equation*". *Phys. Rev. Lett.*, **44**:55, 1980.

J. Klafter, A. Blumen, and M. F. Shlesinger. "*Stochastic pathway to anomalous diffusion*". *Phys. Rev. A*, **35**:3081, 1987.

J. Klafter, M. F. Shlesinger, and G. Zumofen. "*Beyond Brownian Motion*". *Physics Today*, **49**:33, 1996.

R. Klages, G. Radons, and I. M. Sokolov. *"Anomalous transport."*. Wiley–VCH, 2008.

P. E. Kloeden and E. Platen. *"Numerical Solutions of Stochastic Differential Equations."*. Second Edition, Springer, 1995.

R. Kubo. "*Statistical–Mechanical Theory of Irreversible Processes. I. General Theory and Simple Applications to Magnetic and Conduction Problems.*". *J. Phys. Soc. Jpn.*, **12**:570, 1957.

R. Kubo, M. Toda, and N. Hashitsume. "*Statistical Mechanics of Linear Response*". *Statistical Physics II*, pages 146–202, 1991.

K. J. Laidler. *"Chemical Kinetics"*. Third Edition, Harper and Row, 1987.

P. Langevin. "*On the Theory of Brownian Motion*". *C. R. Acad. Sci. (Paris)*, **146**: 530, 1908.

R. B. Laughlin, D. Pines, J. Schmalian, B. P. Stojković, and P. Wolynes. "*The middle way*". *PNAS*, **97**:32, 2000.

D. V. Lebedev, M. V. Filatov, A.I. Kuklin, A. Kh. Islamov, J. Stellbrink, R. A. Pantina, Yu. Yu Denisov, B. P. Toperverg, and V. V. Isaev-Ivanov. "*Structural hierarchy of chromatin in chicken erythrocyte nuclei based on small–angle neutron scattering: Fractal nature of the large–scale chromatin organization*". *Crystallogr. Rep.*, **53**:110, 2008.

T. Li, S. Kheifets, D. Medellin, and M. G. Raizen. "*Measurement of the Instantaneous Velocity of a Brownian Particle*". *Science*, **328**:1673, 2010.

E. Lieberman-Aiden, N. L. van Berkum, L. Williams, M. Imakaev, T. Ragoczy, A. Telling, I. Amit, B. R. Lajoie, P. J. Sabo, M. O. Dorschner, R. Sandstrom, B. Bernstein, M. A. Bender, M. Groudine, A. Gnirke, J. Stamatoyannopoulos, L. A. Mirny, E. S. Lander, and J. Dekker. "*Comprehensive mapping of long-range interactions reveals folding principles of the human genome.*". *Science*, **326**: 289, 2009.

S. Lifson and J. L. Jackson. "*On the Self–Diffusion of Ions in a Polyelectrolyte Solution*". *J. Chem. Phys.*, **36**:2410, 1962.

Y. A. Makhnovskii, A. M. Berezhkovskii, and V. Y. Zitserman. "*Homogenization of boundary conditions on surfaces randomly covered by patches of different sizes and shapes*". *J. Chem. Phys.*, **124**:036103, 2006.

Yu. A. Makhnovskiia, A. M. Berezhkovskii, and V.Yu. Zitsermanc. "*Diffusion in a tube with alternating diameter*". *Chem. Phys.*, **367**:110, 2010.

B. Mandelbrot. *"The Fractal Geometry of Nature"*. W. H.Freeman and Company, 1983.

B. Mandelbrot. *"Fractals and the art of roughness."*. TED Conferences (2010), 2010. URL http://www.ted.com/talks/lang/en/benoit_mandelbrot_fractals_the_art_of_roughness.html.

F. Marchesoni. "*Mobility in periodic channels formed by cilindrical cavities*". *J. Chem. Phys.*, **132**:166101, 2010.

F. Marchesoni and S. Savel'ev. "*Rectification currents in two–dimensional artificial channels*". *Phys. Rev. E*, **80**:011120, 2009.

F. Marchesoni and A. Taloni. "*Subdiffusion and Long–Time Anticorrelations in a Stochastic Single File*". *Phys. Rev. Lett.*, **97**:106101, 2006.

U. M. B. Marconi, A. Puglisi, L. Rondoni, and A. Vulpiani. "*Fluctuation–dissipation: Response theory in statistical physics*". *Physics reports*, **461**:111–195, 2008.

S. Martens, G. Schmid, L. Schimansky-Geier, and P. Hänggi. *"Entropic particle transport: Higher–order corrections to the Fick–Jacobs diffusion equation"*. *Phys. Rev. E*, **83**:051135, 2011.

S. Matthias and F. Müller. *"Asymmetric pores in a silicon membrane acting as massively parallel brownian ratchets"*. *Nature*, **424**:53, 2003.

R. Metzler and J. Klafter. *"The random walk's guide to anomalous diffusion: a fractional dynamics approach"*. *Physics Reports*, **339**:1–77, 2000.

K. K. Mon and J. K.. Percus. *"Molecular dynamics simulation of anomalous self–diffusion for single–file fluids"*. *J. Chem. Phys.*, **119**:3343, 2003.

E. W. Montroll and G. H. Weiss. *"Random Walks on Lattices. II"*. *J. Math. Phys.*, **6**:167, 1965.

T. Nakayama, K. Yakubo, and R. L. Orbach. *"Dynamical properties of fractal networks: Scaling, numerical simulations, and physical realizations"*. *Rev. Mod. Phys.*, **66**:381, 1994.

T. J. Ngo-Anh, B. L. Bloodgood, M. Lin, B. L. Sabatini, J. Maylie, and J. P. Adelman. *"SK channels and NMDA receptors form a Ca^{2+}–mediated feedback loop in dendritic spines"*. *Nat. Neurosci.*, **8**:642, 2005.

R. C. O'Reilly and Y. Munakata. *"Computational Explorations in Cognitive Neuroscience"*. Massachusetts Institute of Technology, 2000.

R. E. Oswald, G. L. Millhauser, and A. A. Carter. *"Diffusion model in ion channel gating"*. *Biophys. J.*, **59**:1136, 1991.

A. Papagiannopoulos, T. A. Waigh, T. Hardingham, and M. Heinrich. *"Solution Structure and Dynamics of Cartilage Aggrecan"*. *Biomacromolecules*, **7**:2162, 2006.

J. P. Perrin. *"Les Atomes."*. Alcan, Paris, 1913.

B. Philippe and D. Volchenkov. *"Random Walks and Diffusions on Graphs and Databases"*. Springer, 2011.

I. Podlubny. *"Fractional differential equations."*. Academic press, 1999.

H. Poincaré. *"Science and Hypothesis."*. Dover Publications (Ne York), English version, 1952.

A. Pope. *"An Essay on Man. Moral Essays and Satires."*. Reprinted version, CASSELL and COMPANY, Limited: London, Paris and Melbourne (1891), 1734. URL http://www.gutenberg.org/ebooks/2428.

A. Pramukkul, and P. Svenkeson, P. Grigolini, M. Bologna, and B. West. "*Complexity and the Fractional Calculus.*". *Advances in Mathematical Physics*, **2013**:1, 2013.

Yu. V. Prokhorov and V. Statulevičius. *"Limit Theorems of Probability Theory"*. Springer, 1991.

E. Ramón-Moliner. *"The morphology of dendrites. In: The Structure and Function of Nervous Tissue"*, volume I. Academic Press, 1968.

S. Ramón y Cajal. *"Histology of the Nervous System of Man and Vertebrates."*. Oxford Univ Press, 1995.

S. Redner. *"A guide to first–passage processes"*. Cambridge University Press, 2001.

D. Reguera and J. M. Rubí. "*Kinetic equations for diffusion in the presence of entropic barriers*". *Phys. Rev. E*, **64**:061106, 2001.

D. Reguera, G. Schmid, P. S. Burada, J. M. Rubí, P. Reimann, and P. Hänggi. "*Entropic Transport: Kinetics, Scaling, and Control Mechanisms*". *Phys. Rev. Lett.*, **96**:130603, 2006.

P. Reimann, C. Van den Broeck, H. Linke, P. Hänggi, J. M. Rubi, and A. Pérez-Madrid. "*Giant Acceleration of Free Diffusion by Use of Tilted Periodic Potentials*". *Phys. Rev. Lett.*, **87**:010602, 2001.

H. Risken. *"The Fokker–Planck Equation"*. Springer, 1989.

R. Roque-Malherbe. *"Adsorption and Diffusion in Nanoporous Materials"*. CRC Press, Taylor and Francis Group, 2005.

C. Sachs, M. Hildebrand, S. Völkening, J. Wintterlin, and G. Ertl. "*Spatiotemporal Self–Organization in a Surface Reaction: From the Atomic to the Mesoscopic Scale*". *Science*, **293**:1635, 2001.

M. S. P. Sansom, F. G. Ball, C. J. Kerry, R. McGee, R. L. Ramsey, and P. N. R. Usherwood. "*Markov, fractal, diffusion, and related models of ion channel gating*". *Biophys. J.*, **56**:1229, 1989.

F. Santamaria, S. Wils, E. De Schutter, and J. G. Augustine. "*Anomalous Diffusion in Purkinje Cell Dendrites Caused by Spines* ". *Neuron*, **52**:635, 2006.

G. J. Schütz, H. Schindler, and T. Schmidt. "*Single–molecule microscopy on model membranes reveals anomalous diffusion*". *Biophys. J.*, **73**:1073, 1997.

E. K. Scott and L. Luo. "*How do dendrites take their shape?*". *Nat. Neur.*, **4**:359, 2001.

P. N. Sen. "*Diffusion and tissue microstructure*". *J. of Phys.: Cond. Matt.*, **16**:S5213, 2004.

M. F. Shlesinger, M. G. Zaslavsky, and J. Klafter. "*Strange Kinetics*". *Nature*, **363**:31–37, 1993.

Z. Shuss, A. Singer, and D. Holcman. "*The narrow escape problem for diffusion in cellular microdomains*". *PNAS*, **104**:16098, 2007.

M. Smoluchowski. "*Zur kinetischen theorie der brownschen molekularbewegung und der suspensionen*". *Ann. der Phys.*, **21**:756, 1906.

T. H. Solomon, E. R. Weeks, and H. L. Swinney. "*Observation of anomalous diffusion and Lévy flights in a two-dimensional rotating flow*". *Phys. Rev. Lett.*, **71**:3975, 1993.

H. E. Stanley and P. Meakin. "*Multifractal phenomena in physics and chemestry*". *Nature*, **335**:405–409, 1988.

S. Stuart and M. Spruston, N. and. Häusser. *"Dendrites"*. Oxford University Press, 1999.

S. Tarafdar, A. Franz, C. Schulzky, and K. H. Hoffmann. "*Modelling porous structures by repeated Sierpinski carpets*". *Physica A*, **292**:1, 2001.

K. Thulasiraman and M. N. S. Swamy. *"Graphs:Theory and Algorithms."*. John Wiley and Sons, 1992.

S. Torquato. *"Random Eterogeneous Materials"*. Springer, 2002.

D. Villamaina, A. Puglisi, and A. Vulpiani. "*The fluctuation–dissipation relation in sub–diffusive systems: the case of granular single–file diffusion*". *J. of Stat. Mech.: Theory and Experiment*, 2008:L10001, 2008.

D. Villamaina, A. Sarracino, G. Gradenigo, A. Puglisi, and A. Vulpiani. "*On anomalous diffusion and the out of equilibrium response function in one-dimensional models*". *J. of Stat. Mech.: Theory and Experiment*, 2011:L01002, 2011.

T. A. Waigh and A. Papagiannopoulos. "*Biological and Biomimetic Comb Polyelectrolytes*". *Polymers*, **2**:57, 2010.

G. H. Weiss. *"Aspects and applications of random walks"*. Amsterdam NL, 1994.

G. H. Weiss and S. Havlin. "*Some properties of a random walk on a comb structure*". *Physica A*, **134**:474–482, 1986.

N. Wiener. *"Nonlinear Problems in Random Theory"*. MIT Press,Cambridge, MA, 1958.

W. Woess. *"Random Walks on Infinite Graphs and Groups"*. Cambridge University Press, 2000.

I. Y. Wong, M. L. Gardel, D. R. Reichman, E. R. Weeks, M. T. Valentine, A. R. Bausch, and D. A. Weitz. "*Anomalous Diffusion Probes Microstructure Dynamics of Entangled F–Actin Networks*". *Phys. Rev. Lett.*, **92**:178101, 2004.

A. L. Yakimiv. *"Probabilistic Applications of Tauberian Theorems."*. VSP (Leiden–Boston), 2005.

R. Yuste and W. Denk. "*Dendritic spines as basic functional units of neuronal integration*". *PNAS*, **375**:682, 1995.

G. Zumofen and J. Klafter. "*Scale–invariant motion in intermittent chaotic systems*". *Phys. Rev. E*, **47**:851, 1993.

R. Zwanzig. "*Diffusion–controlled ligand binding to spheres partially covered by receptors: an effective medium treatment.*". *PNAS*, **87**:5856, 1990.

R. Zwanzig. "*Diffusion Past and Antropy Barrier*". *J. Phys. Chem.*, **96**:3926, 1992.

R. Zwanzig. *"Nonequilibrium Statistical Mechanics"*. Oxford University Press, 2001.

R. Zwanzig and A. Szabo. "*Time dependent rate of diffusion–influenced ligand binding to receptors on cell surfaces*". *Biophys. J.*, **60**:671, 1991.